Synthesis of Metal Bis(Terpyridine)-DNA Complexes for Use Towards the Assembly of Cubic Lattices

Author: Sui Shen

Boston College

The Graduate School of Arts and Sciences

Department of Chemistry

SYNTHESIS OF METAL BIS(TERPYRIDINE)-DNA COMPLEXES FOR USE TOWARDS THE ASSEMBLY OF CUBIC LATTICES

a thesis

by

SUI SHEN

Submitted in partial fulfilment of the requirements

for the degree of

Master of Science

July 2010

ABSTRACT

Synthesis of Metal Bis(Terpyridine)-DNA Complexes for Use Towards the Assembly of Cubic Lattices

Sui Shen

Department of Chemistry, Boston College

There are two major goals for my project. The first is to create and characterize metal-ligand-DNA complexes that could be synthesized using traditional organic methods followed by solid phase techniques. The second is to demonstrate that these complexes with complementary DNA sequences could self-assemble into higher-ordered structures.

In order to generate supramolecular DNA-metal structures such as cubic lattices, it is necessary to create an octahedral metal-ligand center tethering six DNA arms as a building block. The Iron/Ru (II) bis(2,2':6',2''terpyridine) derivatives were chosen because: (i) the complex is well known to present octahedral geometry; (ii) the coordination is very stable; and (iii) while previous work required the solid-phase synthesis of six DNA arms simultaneously—an inefficient process—by using terpyridine ligands we need only extend three arms at once. Thus, several terpyridine-linker compounds were synthesized via two different routes. A DNA 14mer

was synthesized afterwards by “Reverse Coupling Protocol” on a solid phase synthesizer and the terpyridine was connected to it followed by elongation of the rest two DNA arms. The DNA-terpyridine complexes were evaluated by stepwise hybridization tests and gel electrophoresis with or without the assistance of radio labeling. In addition, the assembly of metal with the terpyridine-DNA complex was also characterized by adding different metal ions such as Iron (II) and Ru (II) to the complex. Various buffer conditions were applied in constructing those conjugates in order to help forming branched DNA-ligand-metal complexes with higher molecular weight.

Chapter 1: Introduction

1.1 DNA, its discovery, properties and synthesis

1.1.1 The discovery of DNA

1.1.2 Properties of DNA structure and driving force of DNA duplex formation

1.1.3 Solid Phase DNA synthesis

1.2 Self-assembly and supramolecular chemistry

1.2.1 Introduction

1.2.2 Coordination chemistry

Introduction

Terpyridine coordination chemistry-Formation, Geometry and Characterization

1.2.3 DNA based self-assembly

Hydrogen bonding and self-assembly

Self-assembled DNA nanostructures and applications

Chapter 1: Introduction

1.1 DNA, its discovery, properties and synthesis

DNA was first discovered and isolated by biologist Dr. Friedrich Miescher in 1869. His research was published in 1871 and at that time, was not at first apparent significant. It gradually became one of the major interests in science after Albrecht Kossel conducted research on its chemical structure. In 1919, Dr. Phoebus Levene[1] identified the sugar, base and phosphate subunits of DNA and suggested that DNA consisted of a string of nucleotide linked together through phosphate groups. The identification of DNA was continued by William Astbury who produced the first X-ray pattern of DNA in 1937, which showed the existence of regular structure and base stacking. The most important X-ray diffraction image of DNA provided by Rosalind Franklin and Raymond Gosling in 1953 suggested that DNA was a double helix and able to adopt different conformations depending on the relative humidity and the counterion present[2-4]. In the mean time, Chargaff and his colleagues proved that the ratio of A to T and G to C is always 1:1 regardless of base composition.

The work done by Franklin, Chargaff, Gulland[5] and other scientists yielded critical experimental data that enabled Watson and Crick to discover the structure of DNA[6,7]. Watson and Crick proposed that base pairs of adenine with thymine (A-T) and guanine with cytosine (G-C) were

formed by hydrogen-bonding. This explained Chargaff and Gullands' data. These base pairs are stacked like rolled coins at 3.4Å distance as shown by Astbury and Wilkins' X-ray data, and 36^{o} between adjacent base-pairs in the right handed rotation pattern produced a double helix with ten base pairs per turn. In addition, from Furberg's structure of cytidine[8], they were able to build up the model of the helix in which bases located along the helix axis and sugar-phosphate backbones with antiparallel orientation along the periphery. This discovery answered many questions, created new challenges, and led to an explosion of new areas of biochemistry and genetics. The essence of it, in other words, was to reveal DNA at an atomic level.

1.1.2 Properties of DNA structure and driving force of DNA duplex formation

The basic units of DNA are nucleotides. There are three parts in a nucleotide (Shown in **Figure 1.1a**): a sugar, a phosphate group and a heterocyclic base. The common heterocyclic bases found in DNA belong to two groups: purines (adenine and guanine) and pyrimidines (cytosine and thymine). **Figure 1.1b** shows the structure of the four bases.

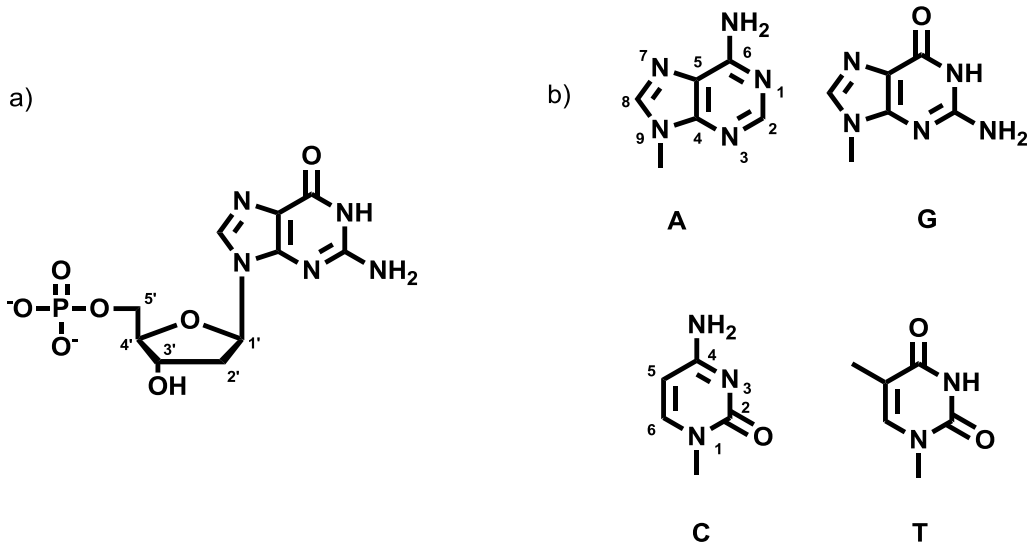

Figure 1.1. a) A nucleotide (dGMP) is shown. The numbering scheme for the deoxyribose is indicated. b) The four bases A, G, C and T. A and C illustrate the numbering system for the purines and pyrimidines

The two single strands in a DNA double helix are connected by complementary base pairing between hydrogen bond donor and acceptor groups present on the bases. The common base pairs are shown in **Figure 1.2**. Two hydrogen bonds are found in A-T base pair and three are found in G-C base pair.

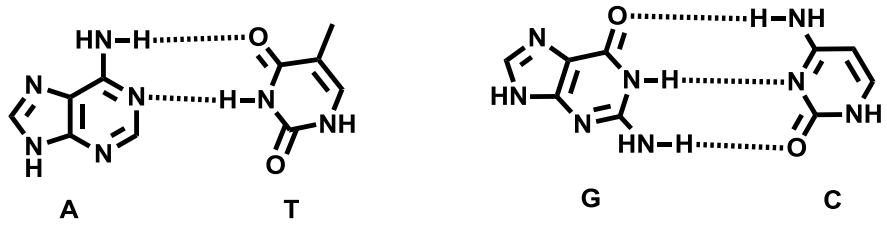

Figure 1.2. A:T and G:C base pairs

There are many structural features related to the properties of bases, nucleosides and nucleotides. First, bases are planar. They have keto and amino forms due to electron resonance. The amino groups are coplanar with the heterocycles. Second, sugar puckers ($C_{2'}$-endo and $C_{3'}$-endo) exist in nucleotides (**Figure 1.3**). The reason is that the system tends to avoid eclipsed conformation and thus reduce its energy by puckering. Third, there are two orientations about the glycosyl $C_{1'}$-N bond-s*yn* and *anti*, which is defined by torsion angle χ (**Figure 1.4**). In the *syn* conformation, the heterocyclic base moiety is projected toward the sugar and in the *anti* conformation, the direction is opposite.

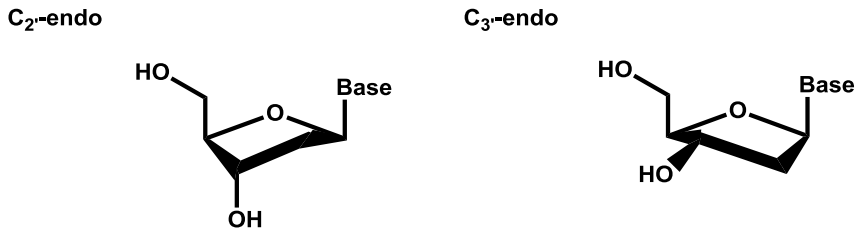

Figure 1.3. Illustration of $C_{2'}$-endo and $C_{3'}$-endo configuration

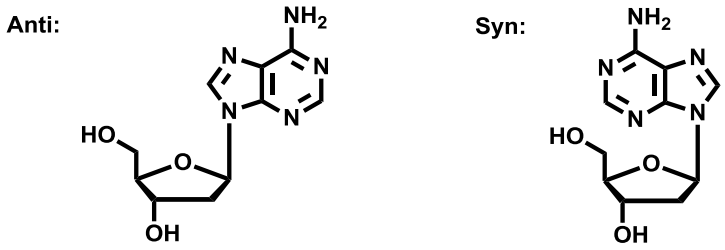

Figure 1.4. *syn* and *anti* configuration

DNA has a number of helical forms, which was caused by different conditions such as salt concentration, humidity and nucleotide composition. The most common ones are A-form and B-form illustrated in **Figure 1.5**. B-form naturally existing in organisms can be transformed to A-form by reducing the humidity.

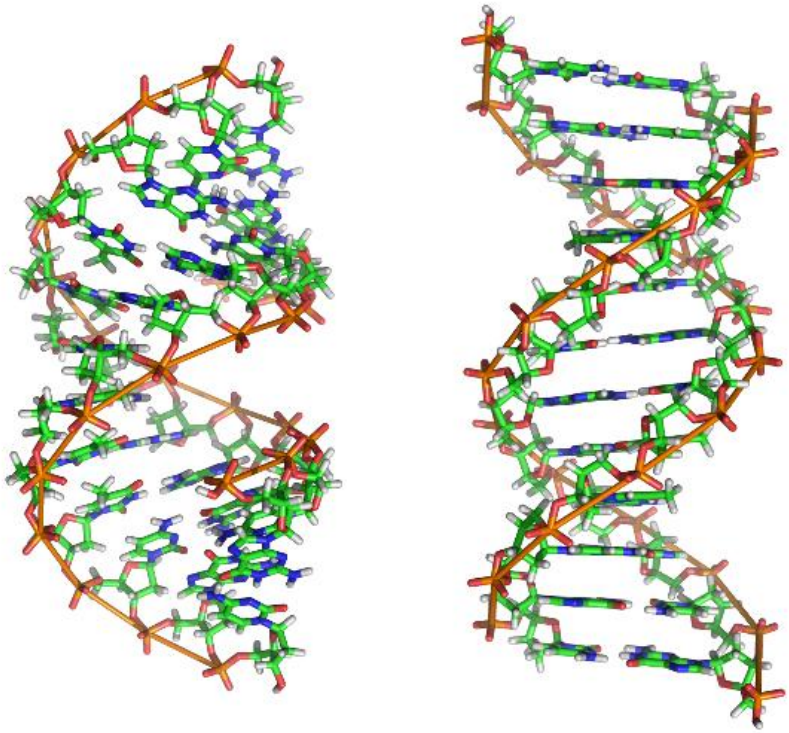

Figure 1.5. Left: A-form helix; Right: B-form helix. Picture adapted from Saenger[9]

The major structural differences between A-form and B-form helix are: 1. The sugar adopts a $C_{3'}$-endo configuration in A-form while it is $C_{2'}$-endo in B-form helix. The difference makes the distance between sugar and phosphate shorter in A-form than in B-form. As a result, A-form helix has 11-12 nucleotides and B-form helix only has 9 nucleotides. 2. A-form DNA has a very

deep and narrow major groove and a shallow wide minor groove, while the depths of major and minor grooves in B-form DNA are almost identical and the width of major groove is greater than the minor groove. 3. The displacement of base pairs away from the helix axis (D) is very different for A-form and B-form. A-form has a D value of 4.5Å and B-form has a D value of only 0.2Å. Indeed, there are other helix configurations such as Z-form and C-form. However, those structures can hardly be seen in nature because they depend highly on the sequences of the DNA and environmental factors.

The major driving forces for DNA duplex formation are hydrogen bonding and base stacking. Hydrogen bonds are electrostatic in character and can be written as X—H ··· Y, where X and Y are highly electronegative atoms such as N, O or S. In order to form stable base pairs, at least two hydrogen bonds have to be formed. In addition, it is important that base pairs in any sequence should fit into the helix without distortion, in other words, the distance between $C_{1'}$ is essentially the same for different base pairs, and only Watson-Crick base pairs A—T and G—C can meet the requirement.

Stacking between bases is another factor of duplex formation. Base stacking arises from dipole-induced dipole interactions and the overlap of permanent dipole moments. Hydrophobic interactions which are energy favorable also contribute to the stacking. In a DNA helix, C=O and

NH_2 groups superimpose over the π electronic system of the adjacent base to provide a π-π stacking pattern. It is noticeable that base stacking formation is additive, diffusion controlled and stabilized by weak interactions.

DNA duplex stability can also be affected by couterions and salt concentration. The phosphate backbone of DNA is negatively charged. Repulsion between two backbones destabilizes double helix formation. The addition of positive charged counterions, for example, Mg^{2+} and Na^{+}, could reduce the charge-charge repulsion.

1.1.3 Solid Phase DNA synthesis

The principle of solid phase synthesis was developed by Bruce Merrifield in the 1950s and 1960s[10]. This technique was initially applied to the synthesis of polypeptides. Soon after this invention, the method was used to synthesize oligonucleotides[11] and has been developed extensively. Nowdays, the synthesis of short and medium size DNA sequences is a relatively simple exercise. The significant advantages of solid phase synthesis over solution synthesis are the following:

- Oligonucleotide can be assembled quickly;

- All reactions can be driven to completion due to the large excess amount of reagents;
- The automatic cycle not only avoids contamination and potential product loss, but also reduces laborious purification;
- The yield is high (over 98.5% on each coupling step).

Most of synthetic oligonucleotides are prepared by solid phase phosphoramidite techniques. The most popular solid support is controlled pore glass (CPG), which is made up of porous borosilicate glass beads. All phosphoramidite monomers have necessary protecting groups (**Figure 1.6**) and are stable under argon.

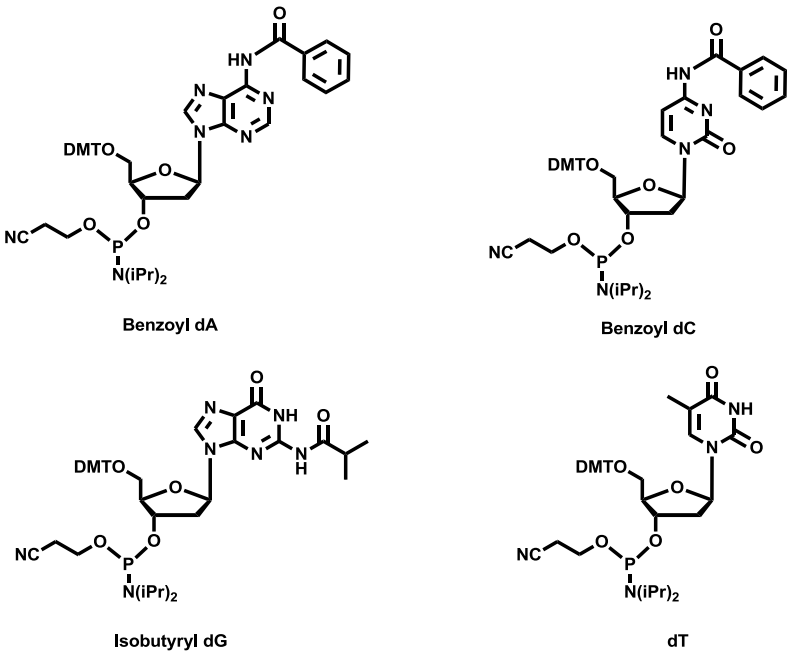

Figure 1.6. Standard protected phosphoramidites

The synthesis of oligonucleotides is performed in the 3’ to 5’ direction on the synthesizer instead of 5’-3’ in enzymatic synthesis due to the better reactivity of the primary 5’-hydroxyl group. It is also noticeable that 5’-3’synthesis is also achievable by using commercially available reverse phosphoramidites. Both conventional and reverse phosphoramidites are shown in **Figure 1.7**.

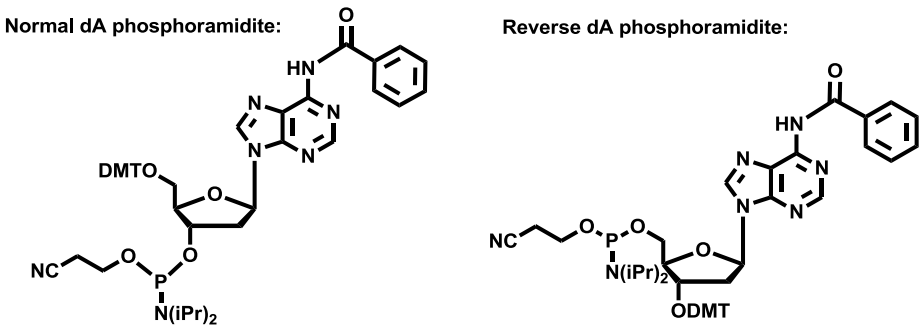

Figure 1.7. Normal and reverse phosphoramidites

The synthesis cycle is shown in **Figure 1.8**. The DMT group is cleaved from the 5’-hydroxyl of the existing oligonucleotide by treating with 3% trichloroacetic acid (TCA) in DCM. The free hydroxyl attacks the phosphoramidite of new nucleotide in the coupling step with the help of tetrazole to provide the N+1 product. The unreacted free hydroxyls are capped by acetyl group in order to prevent unwanted elongation. This step is extremely important because if capping is not preformed, a complex mixture of truncated sequences would make further purification very difficult. An oxidation step by using I_2/H_2O solution is followed in order to yield a more stable phosphate triester. The cycle continues until the desired sequence is achieved. Once the synthesis

is complete, the solid support is treated with aqueous ammonia solution at 55^{o}C for 8hrs. This process enables the deprotection of exocyclic base and phosphorus protecting groups and breaks the succinyl ester linkage in order to release the oligonucleotide from the solid support. The product is dried and purified by HPLC. It is important to leave the DMT groups on the oligonucleotide in order to get a better separation on the HPLC. Further steps include DMT deprotection, desalting and gel electrophoresis.

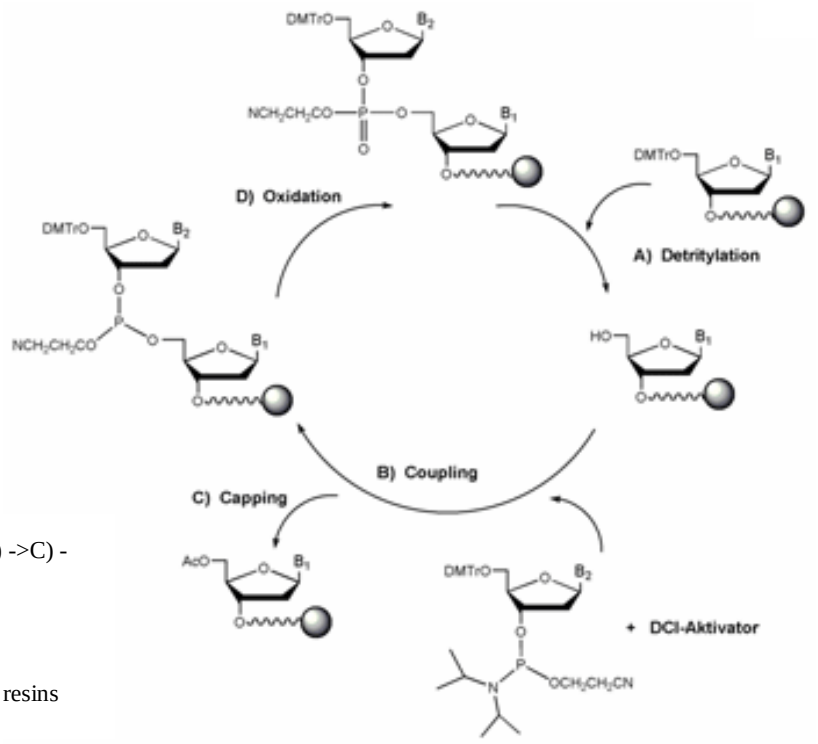

Oligonucleotide synthesis: A) ->B) ->C) ->D)
The complete cycle ends up with deprotection and removal from the resins

Figure 1.8. Oligonucleotide synthesis cycle (picture adapted from Eurofins MWG Operons)

1.2 Self-assembly and supramolecular chemistry

1.2.1 Introduction

Supramolecular chemistry has become a major field in today's research community since 1987. Nobel Laureate J.M. Lehn described the concept[12] as "chemistry beyond the molecule". The organized entities of higher complexity that result from the association of two or more chemical species held together by intermolecular forces. Self recognition and self assembly processes that represent the basic components in supramolecular chemistry-interactions are mainly non-covalent such as Van de Waals, hydrogen-bonding and coordination. The most well-known example is the DNA duplex.

The nature of supramolecular chemistry requires self-assembly as the synthesis protocol. Self-assembly offers many advantages over traditional multi-step synthesis. First, it is very time-consuming and complicated to synthesize macromolecules via multi-step synthesis processes; the overall yield is inevitably low due to the losses in each step. However, self-assembly, in most cases, is one step reaction. And the so called "building blocks" designed to self-assemble are relatively small and thus much easier to be synthesized by a stepwise synthesis process. Second, self-assembly of the monomers happens spontaneously through non-covalent interactions such as hydrogen bonding and Van de Waals which are kinetically labile. This characteristic enables self-repair and finally results in relatively defect-free and thermodynamically stable assemblies

that display high structural integrity[19]. Indeed, nature has been choosing this approach of non-covalent interactions for the construction of genetic code, virus, cells, and organs. For example, hydrogen bonding and base stacking interactions provide the very basic integrity and stable structures of DNA/RNA; Protein-protein networks constructed by non-covalent bonds in virions of rhinovirus are essential to protect their nucleic acids. In conclusion, the strategy of weak interaction is nature's expression of the most economical structural solution to a given set of conditions[19,20,21].

1.2.2 Coordination chemistry

Introduction

One of the most significant interactions in supramolecular chemistry is metal-ligand coordination. Metal centers can adopt a number of geometries such as hexahedron or octahedron and can form defined structures by linking with ligands. Among many advantages of coordination chemistry, a variety of ligands and metal center selection could provide a wide array of structures—from two dimensions to three dimensions. A good application is called directional-bonding approach, which was first developed by Stang. The most important feature of this method is the great

directionality offered by metal-ligand coordinative bonding compared to weak electrostatic and π- π stacking interactions[19]. In addition, the range of coordinative bond energies is about 10-30 kcal/mol per interaction, which is of intermediate strength relative to non-covalent bonds (H-bond, ~1-8 kcal/mol) and covalent bonds (C-C, 83 kcal/mol). This makes the selection of either a kinetic product or a thermodynamic product depend on the ligands, reaction condition and metal identity. Other major self-assembly pathways driven by coordination chemistry include the symmetry interaction approach developed by Lehn[22] and coworkers and the weak-link approach designed by Mirkin[23-26].

Terpyridine coordination chemistry-Formation, Geometry and Characterization

2,2':6',2"-terpyridine has three nitrogen atoms and can act as a tridentate ligand[13,14]. The advantage of the terpyridine ligand is the strength of the metal-ligand coordination ability. With many transition metals in low oxidation states, a bis-terpyridine-metal complex is formed with a distorted octahedral coordination at the metal center. The stability of such kinds of complexes can be explained by the strong metal-ligand(d-π*) back donation. In order to get symmetrical $[M(terpyridine)_2]^{2+}$ complexes, the ligand is treated with specific metal ions such as Fe(II), Zn(II), Cu(II) and Ru(II) in a 2:1 (ligand:metal) ratio (**Figure 1.9a**). In addition, unsymmetrical bisterpyridine-metal complex can be achieved by a two step procedure (**Figure 1.9b**). Ru(III)

and Os(III) are generally used in this strategy. The metal(III)-terpyridine 1:1 complex is purified and subsequently reduced *in situ* to form the bisterpyridine complexes.

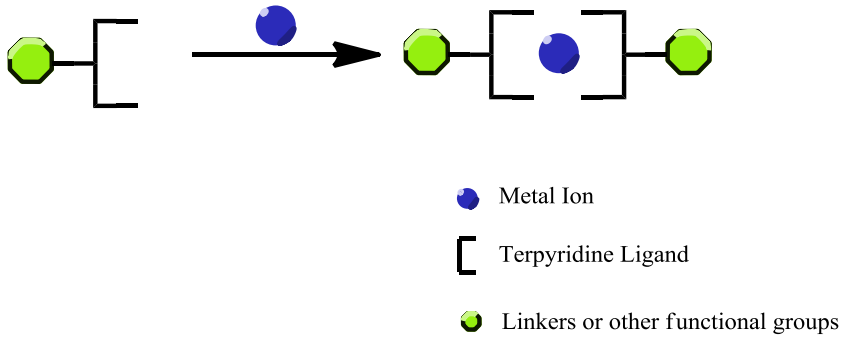

Figure 1.9a. Schematic representation of the formation of symmetrical bisterpyridine complexes

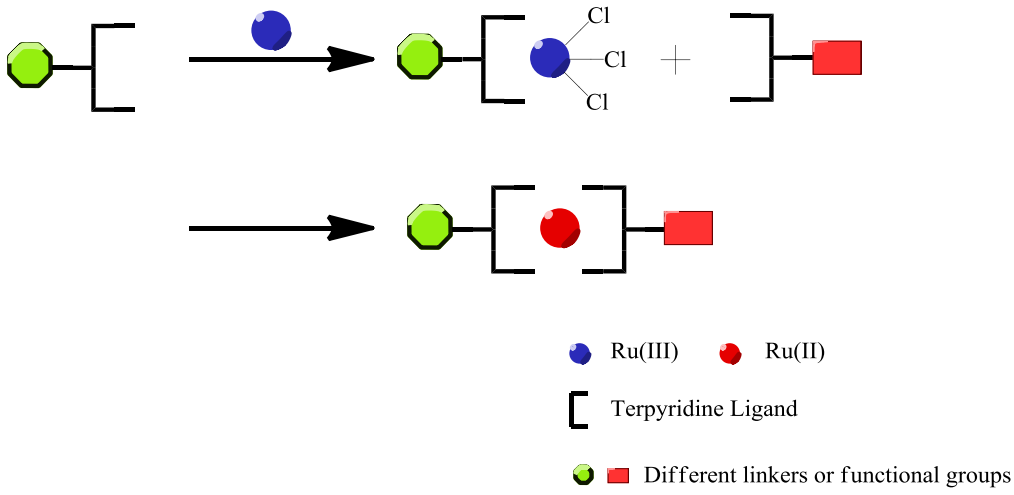

Figure 1.9b. Schematic representation of the formation of unsymmetrical bisterpyridine complexes

The UV-Vis spectra of such complexes show strong characteristic metal-ligand charge transfer (MLCT) bands (**Figure 1.10**). The absorption is in the visible region with intense color, for example, red for Ru(II) and purple for Fe(II). A distinct peak can be detected for Fe(II)

complexes, however, only a shoulder band can be observed for Ru(II) ones[15]. Other tools for analysis of bisterpyridine metal complexes include MALDI-TOF[16,17,18], ^{1}H-NMR[27-29] and X-ray crystallography.

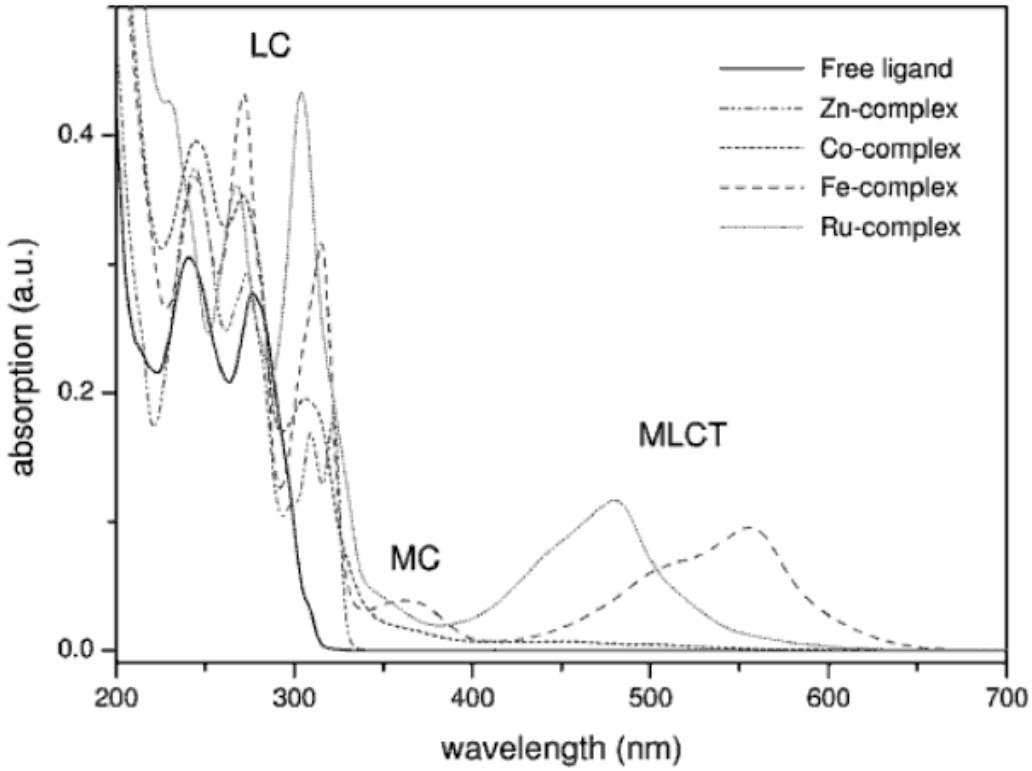

Figure 1.10. UV-Vis spectra of metal-terpyridine complexes, figure adopted from Schubert[15]

1.2.3 DNA based self-assembly

Hydrogen bonding and self-assembly

The research on supramolecular chemistry we have discussed so far is mainly based on coordination bonding between ligands and metal centers. The design of the ligands as well as the

selection of metal sources is very important in order to aid in forming the shape of the assembly. However, as we mentioned above, building blocks can be selected or designed to have hydrogen bond donor and acceptor groups positioned in a good way that the shape and composition of an assembly can be dictated. This strategy is greatly used by nature, for instance, the assembly of phospholipid bilayers, the intermolecular folding of tRNA[30], and the formation of DNA double helix. In many cases, it is true that the association of two biologically active molecules goes through a complicated pathway, however, it is quite simple and beautiful that two DNA single strands self-assemble to a duplex stabilized by Watson-Crick base pairing. In addition, the combined helix is quite robust towards many different conditions with a persistence length of around 50nm[31]. Furthermore, the mature solid phase techniques, PCR, enzymatic *in vivo* synthesis and the computer assisted DNA architecture design software make the construction of supramolecular assemblies by oligonucleotides possible and interesting.

Self-assembled DNA nanostructures and applications

A great amount of work has been done in the realm of DNA nanostructures since the 1980s due to the popularization of PC and the solid phase synthesis technique. One of the most notable scientists in the field of DNA nanotechnology is Nadrian Seeman, whose work is published as reviews in many journals[31,32,33]. His first attempt was to make branched junctions, which was

applied to building up cubes (**Figure 1.11**) and even more complicated structures, such as knots or Borromean rings through sticky ends method. However, further investigation showed that such kinds of branched junction are not rigid enough to construct supramolecular assemblies. Thus, he started to focus on the application of DNA "double crossover" molecules. They consist of two four-arms branches attached at two adjacent arms. The two dimensional arrays made by DX molecules have been used for the construction of nanomechanical device. The device is controlled by the transformation from the Z-form to the B-form of DNA[34] (**Figure 1.12**).

a)

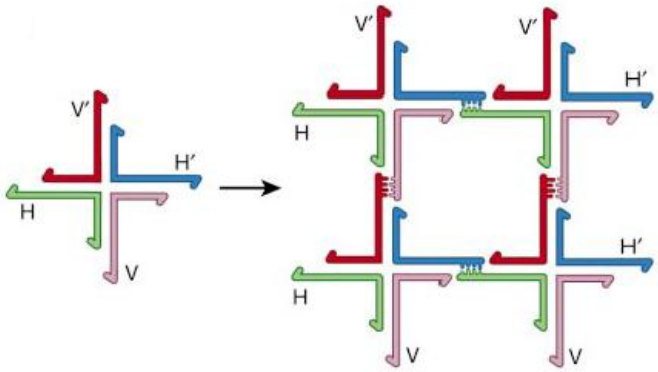

b)

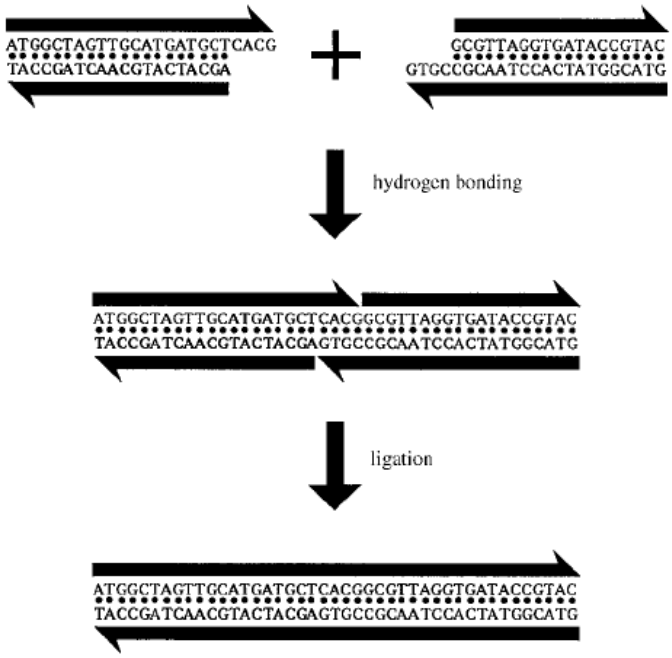

Figure 1.11. a) DNA branched junctions formed through sticky ends; b) sticky ended cohesion and ligation (enzymatic catalysis). Adapted from Seeman[31,32].

a)

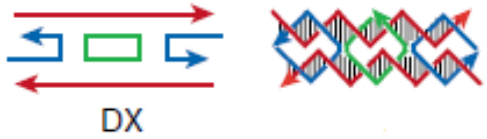

b)

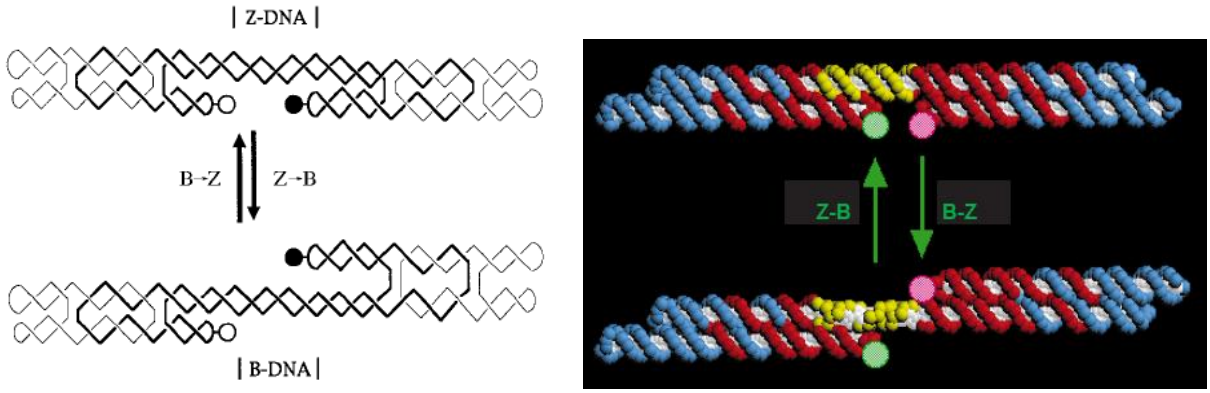

Figure 1.12. a) DNA double crossover molecules (DX). b) Left, schematic figure of a nanomechanical device based on B-Z transition of DNA. Right, cartoon of the B-Z transition. The device consisted of two DX molecules (red and blue) flanking with a central 20bp proto-Z-DNA (yellow) with a B-form conformation. Fluorophores were labeled by pink and green. The transformation was detected by FRET. Adapted from Seeman[32,34].

The experiments above show DNA nanostructures constructed solely of nucleic acids. It is notable that others have utilized nanoparticle-based hubs tethering DNA strands as building blocks that can self-assemble into higher-ordered structures[35,36]. Mirkin and coworkers functionalized gold (Au) particles with complementary DNA regions that could result in different colloidal crystal formations (**Figure 1.13**)[37].They demonstrated that DNA can be used

to control the crystallization of nanoparticle –oligonucleotide conjugates to the extent that different DNA sequences guide the assembly of the same kind of inorganic nanoparticle into different crystalline states[37]. Another example is that DNA has been used as "scaffold" for the organization of nanoparticles. Niemeyer and coworkers utilized ssDNA as a scaffold to direct biotin-functionalized Au nanoparticles through the use of DNA-STV conjugates[38].

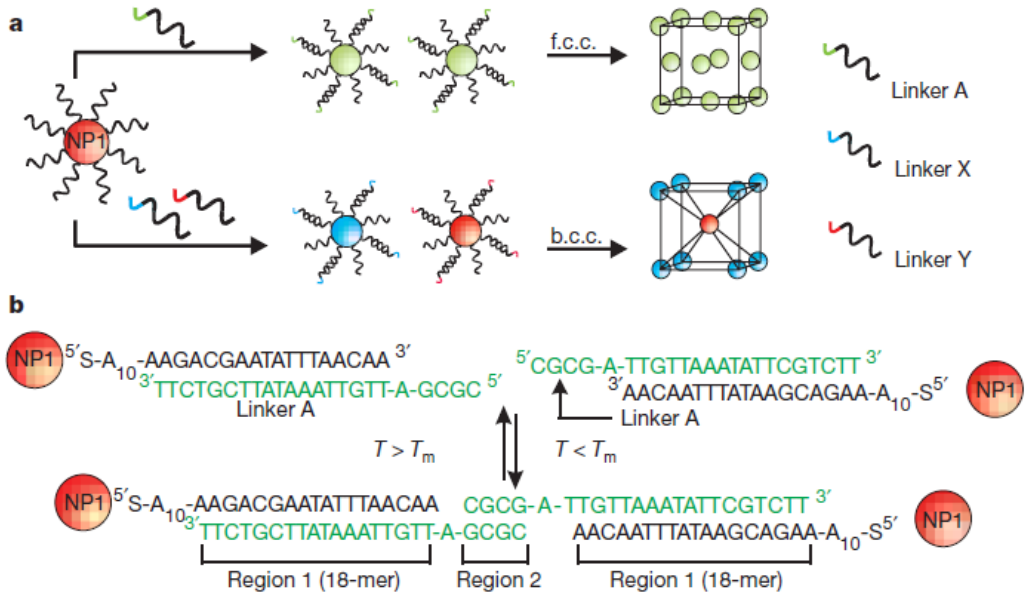

Figure 1.13. a) Different crystalline states created by the self-assembly of Au-linker-DNA with different oligonucleotide sequences. 2) Single component assembly system (f.c.c) where Au nanoparticles are assembled using one DNA sequence—Linker A. Adapted from Mirkin[37].

One of the most exciting areas in DNA nanotechnology is the so called "DNA origami", which is developed by Paul Rothermund using the "bottom-up" methodology. DNA origami is the nanoscale folding of DNA to create arbitrary two and three dimensional shapes. The specificity

of the interactions between complementary base pairs makes DNA a useful construction material through design of its sequences. The self-assembly involves the folding of a long single strand of viral DNA aided by multiple smaller "staple" strands. These shorter strands bind the longer in various places, resulting in various two dimensional shapes and even higher ordered three dimensional structures[38,39]. As a famous application, Kurt V. Gothelf et al.[40] extended the DNA origami method into three dimensions by creating a $42 \times 36 \times 36$ nm^3 DNA box that could be opened in the presence of an external DNA "key". The structure and shape of the DNA box was determined by AFM, SAXS and Cryo-TEM. The specific "open and close" event of the lid is characterized by FRET (**Figure 1.14**).

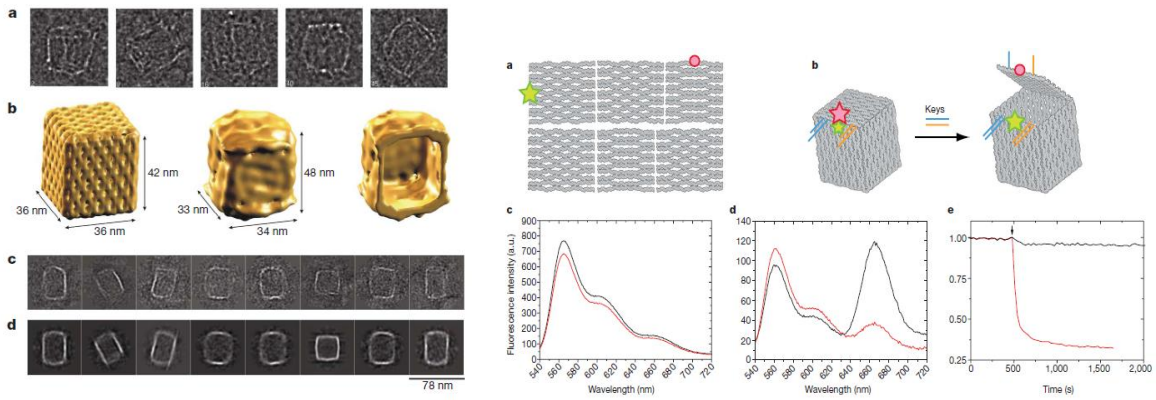

Figure 1.14. Left: Characterization of DNA origami box by cryo-TEM and SAXS. Right: Programmed opening of the box lid. Adapted from Gothelf[40].

Bottom-up self-assembly methods are considered promising alternatives that offer inexpensive, parallel synthesis of nanostructures under relatively mild conditions. These nano devices may have many interesting applications such as logic sensor, nanocargos or even nano computers.

1.2.4 DNA-metal conjugates formed by coordination and hydrogen bond

From previous chapters, we know that coordination chemistry between metal and ligands will result in the formation of discrete geometries and stable structures. In addition, it is also clear that hydrogen bonding, especially in DNA/RNA, can be used with ease in generation of self-assembly building blocks due to the accuracy and predictability. Both methods proved to be powerful in building up supramolecular structures with different key points. As a result, both could be utilized in the synthesis of building blocks that could lead to defined 2D or even 3D structures. Metal center could provide the geometry for the metal-DNA conjugate, while DNA tethered to the metal-ligand complex can be used as arms/bricks to construct the scaffold. The charge-charge repulsion among the DNA strands may further reinforce the specified geometry. Kristen Stewart in Prof. McLaughlin's lab has synthesized two-dimensional linear arrays by using a ruthenium (II) bis(terpyridine) derivative as the metal center tethered with synthetic oliogonucleotides (**Figure 1.15**).

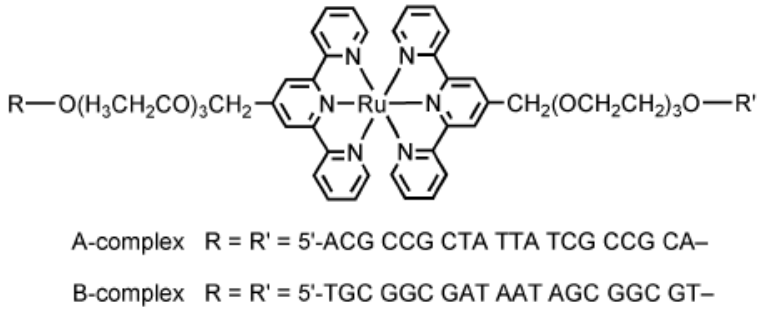

Figure 1.15. The Ru (II) bis(terpyridine) monomer[41]

In order to form a three-dimensional lattice, at least four DNA arms are required around the metal hub. A four-arm hub was designed with a Ni (II) cyclam center in order to provide a tetrahedral structure. Although the cyclam itself is cyclic in nature, Ni (II) was added to help the overall lattice organization. Just like in the example above, a linker between DNA and metal-cyclam hub is necessary to better address the four arms and minimize steric effects. Building block and hybridization test are shown in **Figure 1.16**[42]. Tethering DNA sequences to octahedral metal centers was also characterized by Kristen, and ruthenium (II) tris(bipyridine) was chosen because 1) the monomer is well known to present octahedral geometry; 2) it is stable to ligand exchange reaction. However, the coupling of DNA-ligand complex with Ru (II) was not successful under ambient temperature. Alternative route such as constructing the octahedral ligand-metal center first followed by DNA synthesis was also disfavored by the low yield of synthesizing five DNA sequences concurrently (**Figure 1.17**). In order to build up highly ordered, crystalline-like lattices, further investigations based on various ligands and metal centers are

necessary. Once such conjugates form, techniques such as XRD, TEM and SEM can be applied to determine their 3D structures.

a)

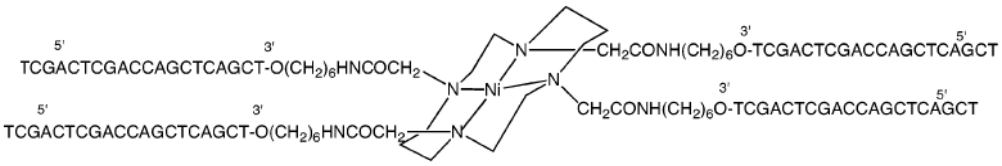

b)

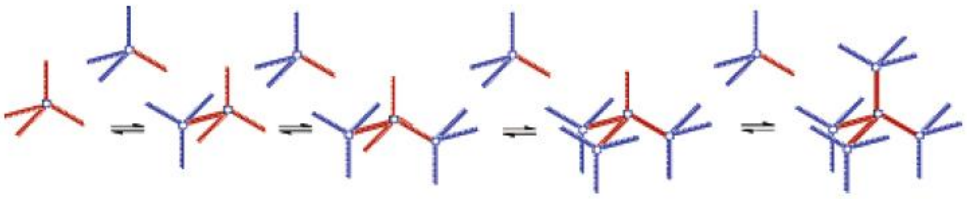

Figure 1.16. a) The Ni (II) cyclam-DNA conjugate; b) The hybridization equilibrium between cyclam-DNA conjugate with four identical arms and cyclam-DNA conjugate with one complementary strand attached. Adapted from Kristen Stewart[42].

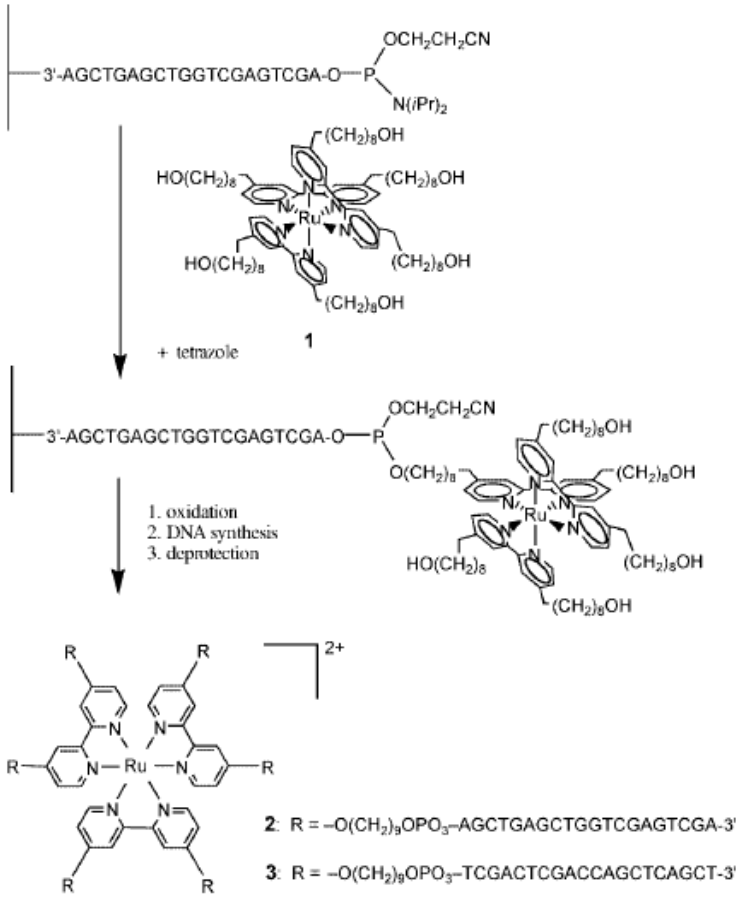

Figure 1.17. Solid phase synthesis of DNA-$[Ru(bipyridine)_3]^{2+}$ building block. Adapted from Kristen Stewart[43].

1.3. Applications for metal-ligand-DNA assembly

One of the original thoughts of building up DNA lattice based on metal-ligand-DNA building blocks was to use it as scaffold for the assembly of multicomponent DNA-protein complexes. These complexes such as TFIID-TATA box are of importance in biological systems, for example, the initiation of eukaryotic transcription. The most accurate structure information is provided by

X-ray diffraction patterns of single crystals. Although this method works fine with proteins, it can hardly be applied to DNA-protein complexes. Although examples of protein-DNA complex crystal structures exist, there is no real picture of the crystal structure of multiprotein-DNA complexes. However, DNA lattice could provide the approach in doing such kinds of discovery. The reason is very simple: DNA lattice itself is a highly ordered structure, which is very similar to a crystal. This characteristic could help the formation of crystal-like DNA-protein complexes upon ordered, self-assembled binding event. Another application is to use DNA-ligand-metal assembly as encapsulation material. The pore size in DNA-metal lattice varies based on different sequences of the DNA arms—from several nm^2 to hundreds nm^2. Such pores could be used to carry nanoscale particles. In addition, metal complex-DNA assemblies could provide controlled release of encapsulated agents, such as nano devices or therapeutics. Other applications include ELISA solid support, nano device and so on.

1.4 Project goals

There are two primary goals of this project:

1. To develop and characterized metal-ligand-DNA conjugates that can be synthesized by using a combination of organic and solid-phase syntheses techniques;
2. To prove that those complexes have the possibility of forming higher ordered structures.

The major system we examined is Ru (II)/Fe (II)-terpyridine-DNA complexes.

1.5 References

1) Levene. P. *J. Bio. Chem.* **1919**, *40*, 415-424.

2) Franklin, R.E.; Gosling, R.G. *Acta. Crystallogr.* **1953**, *6*, 675-678.

3) Franklin, R.E.; Gosling, R.G. *Acta. Crystallogr.* **1953**, *6*, 673-677.

4) Franklin, R.E.; Gosling, R.G. *Nature* **1953**, *172*, 675-678.

5) J.M. Gulland *Cold Spring Harbor Symp. Quant. Biol.* **1947**, *12*, 95-103.

6) Watson, J.D.; Crick, F.H.C. *Nature* **1953**, *171*, 737-738.

7) Crick, F.H.C.; Watson, J.D. *Proc. Roy. Soc. (London) Ser. A.* **1954**, *223*, 80-96.

8) Furberg, S. *Acta. Crystallogr.* **1951**, *3*, 325-331.

9) Saenger, W. *Principles of Nucleic Acid Structure*; Springer-Verlag: New York, **1894.**

10) Merrifield, B. *J. Am. Chem. Soc.* **1963**, *85*, 2149-2154.

11) R. L. Letsinger, J. L. Finnan, G. A. Heavner, W. B. Lunsford, *J. Am. Chem. Soc.* **1975**, *97*, 3278

12) George R. Newkome, Ralf Güther, Charles N. Moorefield, Francesca Cardullo, Luis Echegoyen, Eduardo Pérez-Cordero, Heinrich Luftmann, *Angew. Chem.* **1995**, *24*, 2023-2026.

13) W.R.McWhinnie, J.D.Miller, *Adv. Inorg. Chem. Radiochem.* **1969**, *12*, 135-215.

14) E.C. Constable, *Adv. Inorg. Chem. Radiochem.* **1986**, *30*, 69-121.

15) Ulrich S. Schubert, Harald Hofmeier and George R. Newkome, *Modern Terpyridine Chemistry*, Wiley-VCH Verlag GmbH & Co. KGaA, Weinheim

16) M. A. R Meier, B. G. G. Lohmeijer, U. S. Schubert*, J. Mass Spectrom.* **2003**, *38*, 510-516

17) M. Karas, M.Glückmann, J. Schäfer, *J. Mass Spectrom.* **2000**, *35*, 1-12

18) U.S. Schubert, C. Eschbaumer, *Polym. Prepr.* **2000**, *41*, 676-677

19) Stefan Leininger, Bogdan Olenyuk, and Peter J. Stang, *Chem. Rev.* **2000,** *100,* 853-908

20) (a) Haeckel, E. *Challenger Monograph;* Georg Reimer: Berlin, 1887. (b) Haeckel, E. *Zoology* **1887**, *18*, 1803.

21) Ercolani, G. *J. Phys. Chem. B* **1998**, *102*, 5699.

22) Ruben, M.; Breuning, E; Gisselbrecht, J. P.; Lehn, J-M. *Angew. Chem. Int. Ed.* **2000**, *39*, 4139-4142.

23) Holliday, B. J.; Mirkin. C. A. *Angew. Chem. Int. Ed.* **2001**, *40*, 2022-2043.

24) Liu, X.; Eisernberg, A. H.; Stern, C. L.; Mirkin, C. A. *Inorg. Chem.* **2001**, *40*. 2940-2941.

25) Holliday, B. J.; Farrell, J. R.; Mirkin, C. A.; Lam, K. C.; Reingold, A. L. *J. Am. Chem. Soc.* **1999**,121, 6316-6317.

26) Farrell, J. R.; Mirkin, C. A.; Liable-Sands, L. M.; Reingold, A. L. *J. Am. Chem. Soc.* **1998**,120, 11834-11835.

27) I. Bertini, C.Luchinat, *Coord. Chem. Rev.*, **1996**, *150*, 1-292.

28) H. S. Chow, E. C. Constalbe, C. E. Housecroft, K. J. Kulicke, Y. Tao, *Dalton Trans.* **2005**, 236-237.

29) H. Hofmeier, Ph. D. thesis, Eindhoven University of Technology, **2004.**

30) Whitesides, G. M.; Mathias, J. P.; Seto, C. T. *Science* **1991**, *254*, 1312-1319.

31) Seeman, N.C. *Nature* **2003**, *421*, 427-431.

32) Seeman, N.C. *Angew. Chem. Int. Ed.* **1998**, *37*, 3220-3238.

33) Seeman, N.C. *Biochemistry* **2003**, *42*, 7259-7269.

34) Mao, C.; Sun, W.; Shen, Z.; Seeman, N. C. *Nature* **1999**, *397*, 144-146.

35) Waybright, S. M.; Singleton, C, P.; Wachter, K.; Murphy, C. J.; Bunz, U. H. F. *J. Am. Chem. Soc.* **2001**,123, 1828-1833.

36) Fogleman, E. A.; Yount, W. C.; Xu, J.; Craig, S. L. *Angew. Chem. Int. Ed.* **2002**, *41*, 4026-4028.

37) Sung Yong Park, Abigail K. R. Lytton-Jean, Byeongdu Lee, Steven Weigand, George C. Schatz & Chad A. Mirkin, *Nature* **2008**, *451*, 553-556.

38) P.W.K. Rothemund, "Folding DNA to create nanoscale shapes and patterns" *Nature* **2006**, *(440)* 297–302.

39) Wikipedia, http://en.wikipedia.org/wiki/DNA_origami

40) Andersen ES, Dong M, Nielsen MM, Jahn K, Subramani R, Mamdouh W, Golas MM, Sander B, Stark H, Oliveira CL, Pedersen JS, Birkedal V, Besenbacher F, Gothelf KV, Kjems J., *Nature.* **2009**, *459(7243):*73-6.

41) Niemeyer, C. M.; Sano, T.; Smith, C. L.; Cantor, C. R. *Nucleic Acids Res.* **1994**, *22*, 5530-5539.

42) Stewart, K. M.; McLaughlin, L. W. *J. Am. Chem. Soc.* **2004**,126, 2050-2057.

43) Kristen M. Stewart, Javier Rojo, and Larry W. McLaughlin, *Angew. Chem.* **2004**, *116*, 5932-5935.

Chapter 2: Design and Synthesis of Terpyridine Derivatives

2.1 Introduction

In order to get an ordered 3D DNA cubic matrix, an octahedral structure is necessary for the building block (**Figure 2.1**). To use a terpyiridine-linker-metal complex as the desired structure provider has several advantages: 1. Two terpyridine molecules strongly coordinate with a dielectronic metal anion such as Fe^{2+} or Ru^{2+} and give the octahedral geometry. 2. Linkers tethered to the terpyridine will provide flexibility to the complex to reduce charge-charge repulsion among DNA strands. Here we selected 1,4 butanediol as the linker with one of its hydroxyl group bonded to the terpyridine and the other end protected with DMT. The ether bond linkage is stable enough for further DNA synthesis as proved by previous work done by Kristen Stewart in Mclaughlin's lab[2].

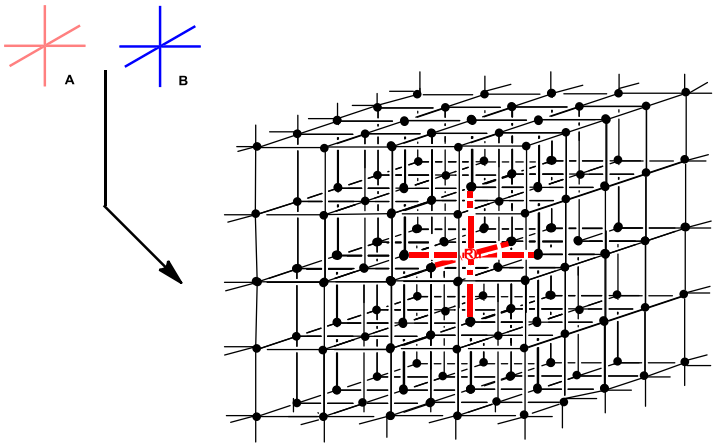

Figure 2.1. 3D DNA lattice formation

2.2 Results and Discussion

2.2.1 Design of the terpyridine hub

The terpyridine ligand is widely used in supermolecular systems. Terprydines are relatively easy to prepare and have greater ability to coordinate with transition metals such as Fe and Ni. Recent reviews and books by Schubert and Hofmeier[3] describe a great number of synthetic routes for terpyridines used in the formation of supermolecular architectures. At an early stage of our research, we used 2,2',6',2''-terpyridine as our starting material and made the desired terpyridine-linker molecule for further DNA synthesis (**Scheme 2.1a**). However, after a while we found another way to achieve our goal-using single pyridine derivatives to form terpyridine compounds via Claisen condensation and pyridone formation reactions (**Scheme 2.1b**). This method has several advantages: a) It is much cheaper to use pyridine as starting material instead of terpyridine; b) It could generate terpyridine with both identical linkers and different linkers; c) It is easier to purify the products from each step.

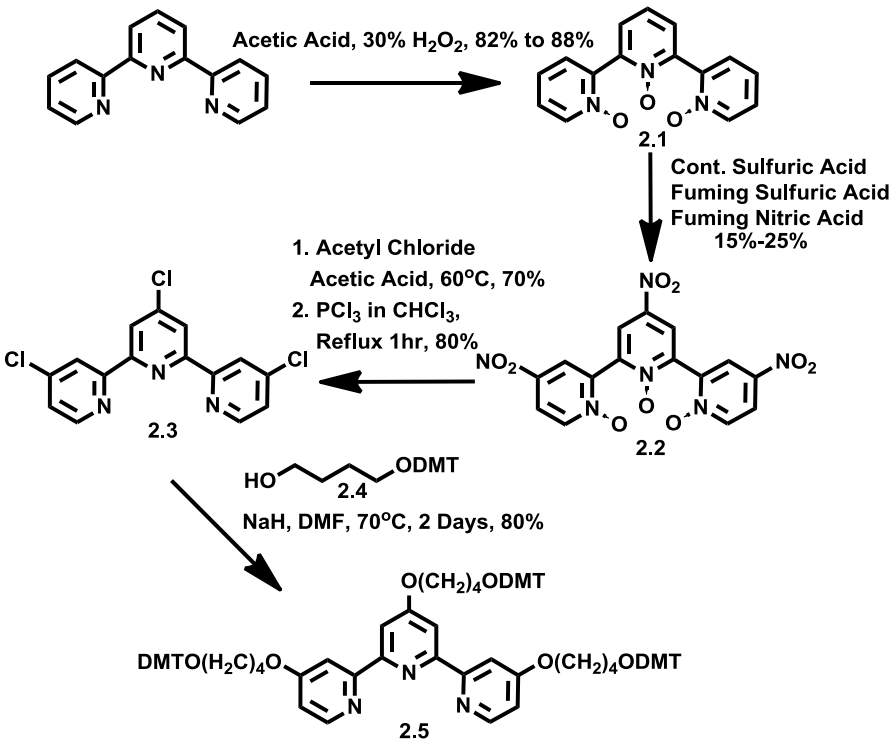

Scheme 2.1a. Terpyridine-linker formation based on 2,2':6',2'' terpyridine[4]

2.2.2 Multiple routes of synthesizing terpyridine-linker compounds

Our first route is shown above. The idea of synthesizing terpyridine 4,4',4''substitutes came from Case's paper[5]. Previous attempts included amide bond and C-C bond formation, which were not very successful. Then we decided to use 1,4 butanediol as the linker to make an ether bond with the terpyridine. The starting material was activated by hydrogen peroxide to become the N-oxide as the first step, and then compound **2.1** was nitrated to become compound **2.2**. After the nitration, chlorine was added, and finally the N-oxide was reduced to give product **2.3**.

Before the linker was coupled to the terpyridine, we had tried the coupling between pyridine derivative and linker and it had a good yield. As a result, we did the same reaction using our precious terpyridine compound with a stronger base and a longer reaction time. The yield of the final step varied from 50% to 70%. Then compound **2.5** was treated with TFA to perform DMT deprotection in order to prepare the terpyridine for DNA synthesis.

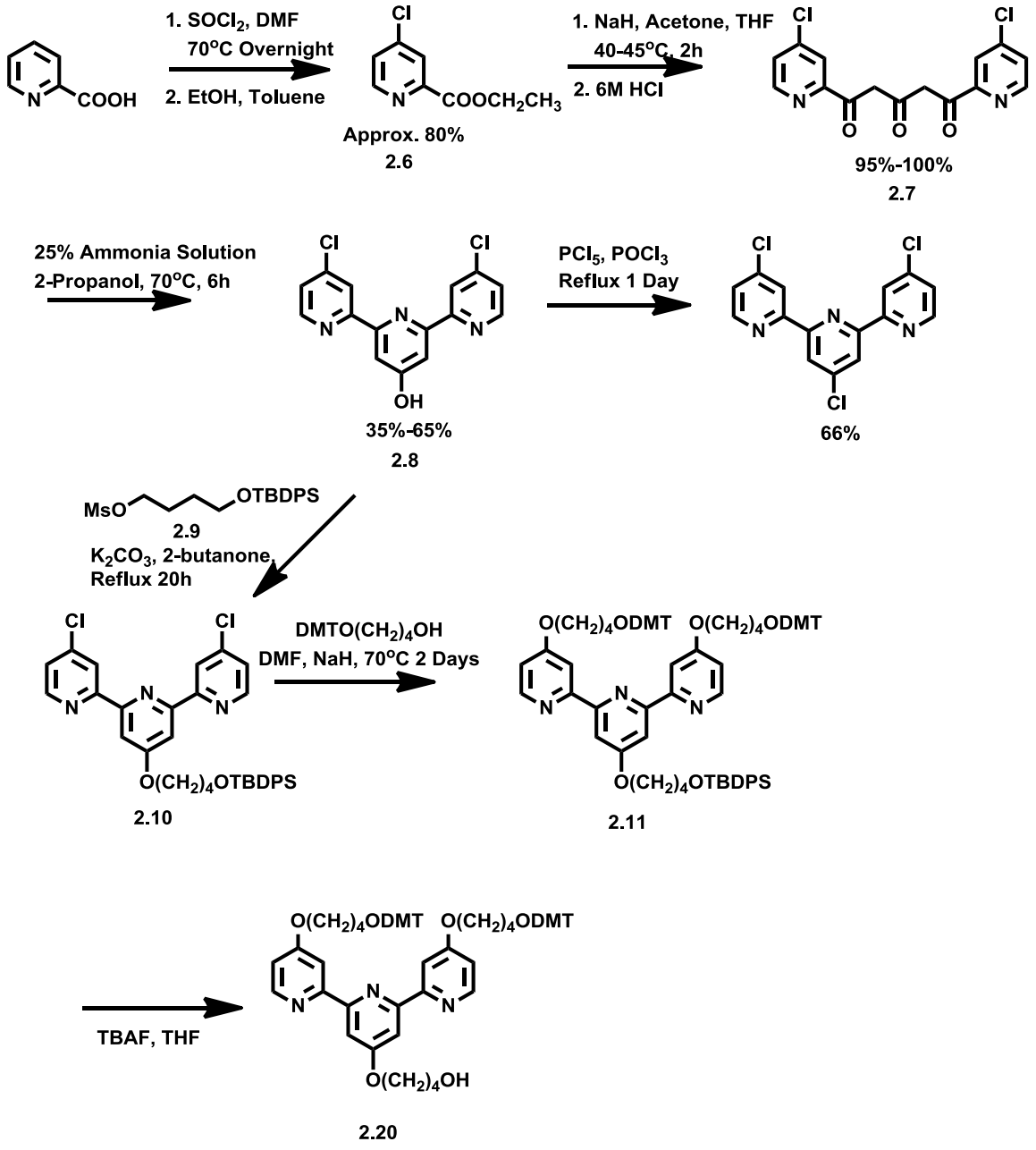

Scheme 2.1b. Terpyridine-linker formation based on new starting material-picolinic acid[5,24]

This route is the most straightforward one, but not the best. The ideal conditions for our DNA synthesis is that only one linker is deprotected while the other ones still have DMT attached. After coupling with the first DNA strand, the remaining two linkers are deprotected and

elongated. Another problem is that the starting material is expensive and the overall yield is very low due to the nitration step. We then came up with the other synthetic route[6], which could provide us the desired product with reduced cost. The starting material here is 2-picolinic acid, and after refluxing it with thionyl chloride, ethanol/toluene (1:1, (v/v)) was added to the mixture to generate a precipitate, which could be purified by extraction and column chromatography. The next step was the classical claisen condensation. We used sodium hydride as the base to remove the proton from acetone. The reaction went to completion after 2 hrs at 40^{o}C and neutralized by HCl. The product can be used without further purification. The 3rd step was ring closure which needed ammonia to form the central pyridine ring. Recrystallization was used to purify the product and that was the cause of a fluctuating yield. From compound **2.8**, we could make compound **2.3** which had three identical chlorines by chlorination, or we could couple the linker **2.9** with the terpyridine and add another two equivalents of linker **2.4** to provide our desired terpyiridine-linker complex **2.11**. Product **2.11** was then deprotected to yield **2.20** for further DNA coupling. The products were identified by MS and NMR.

2.2.3 Other related synthesis

In order to obtain terpyridine-DNA complexes with all the three arms having the same polarity, reverse phosphoramidites (3' DMT and 5' Phosphane) are necessary for the synthesis of the first oligonucleotide strand on the resin (instead of 3'-5' conventional synthesis, it elongates 5'-3'). Although the reverse dA, dG, dC and dT are commercially available, they are quite expensive due to the synthesis procedure (**Scheme 2.2**).

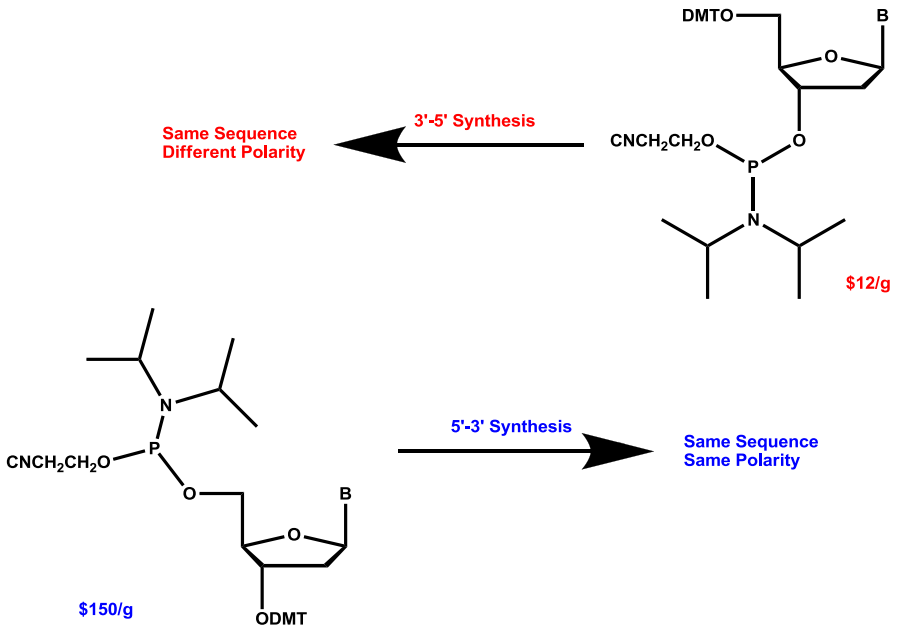

Scheme 2.2a. 3'-5' and 5'-3' syntheses

The syntheses of reverse phosphoramidites are shown below (**Scheme 2.2a)**. Instead of two step-syntheses for normal phosphoramidites, they are four step-syntheses for the reverse ones. Because there are free amino groups in dA, dC and dG, it is necessary to protect them before getting started. NH_2 group at C_6 of dA and the C_4 of dC are protected by benzoyl groups while the NH_2 at C_2 of dG is protected by an isbutyryl group. Then the 5' hydroxyls are protected by TBDMS followed by DMT protection on the 3' OH. Next step is to remove the TBDMS group and put the phosphoramidite on the 5' position. The final products are purified by precipitation and characterized by ^{31}P NMR.

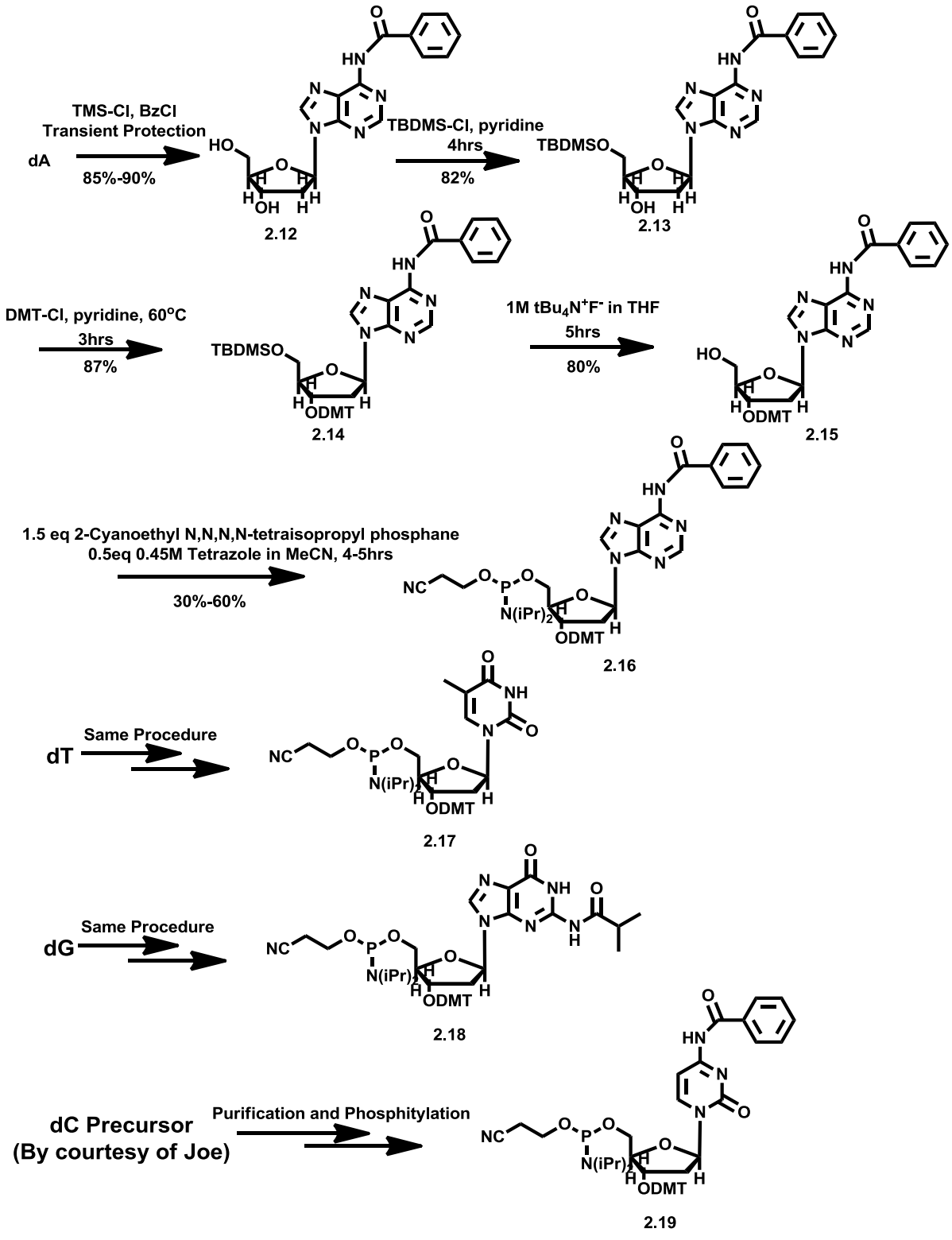

Scheme 2.2b. Syntheses of reverse phosphoramidites[25]

2.3. Conclusion

The terpyridine ligand is widely used in supramolecular systems. Schubert describes a number of synthetic routes for terpyridines with a single linker used in the supramolecular structures formation. Examples include metallosupramolecular polymers and dendrimer systems, multimetallic grid-tipe complexes and so on. In addition, terpyridine-DNA complex draws researchers' interest because of the self-assembly ability of DNA and ordered geometry provided by terpyridine. Kristen Stewart[7] in this lab made Ruthenium bis(terpyridine) tethering two DNA sequences in order to form a building block for the assembly of linear arrays. Hogyu[8] in Korea University reported the synthesis of the terpyridine derivative--a dimeric metal complex coupled with single strand DNA--can be used as an alternative to the Holliday junction. However, there are few reports of terpyridine with 3 alkyl linkers in the literature. It is probably because of the steric hindrance among the 3 pyridine rings in comparison with bipyridine. Another reason is that it is quite hard to purify terpyridine compounds on columns. They are very polar and easily to stick on the silica gel. As a result, our syntheses made terpyridine-metal-DNA octahedral geometry possible and might have profound applications.

2.4 Materials and Methods

2.4.1 Materials

Reagents are solvents were from Aldrich (St. Louis, MO), Molekula (Dorset, UK), Strem Chemicals (Newburyport, MA) and Lancaster (Windham, NH). ^{1}H and ^{31}P NMR spectra were obtained on 400MHz and 500MHz Varian multiprobe spectrometers. ESI and DART mass spectra were performed on Agilent LC-MS and JEOL DART-MS.

2.4.2 Methods: Synthesis of terpyridine **2.5**

Terpyridine N-oxide (2.1). 3g terpyridine was dissolved in 11mL acetic acid and heated with 9mL of 30% hydrogen peroxide in water for 2hrs at 80^{o}C. After adding another 9mL of hydrogen peroxide, the temperature increased to 90 ^{o}C and the mixture was heated for another 18hrs. Then the mixture was poured into 200mL acetone and stay for couple of hours. The precipitate was washed with acetone and filtrate with vacuum. The product was collected as white powder and the weight is 3.0-3.2g. ^{1}H NMR (400MHz, $CDCl_3$): δ 8.51-8.50 (d, 2H), δ 7.97-7.94 (d, 2H), δ 7.62-7.51 (dd, 2H), δ 7.29-7.22 (d, 2H).

4, 4', 4''-trinitro-terpyridine-N-oxide (2.2). 9mL Con. Sulfuric acid, 2.5mL fuming sulfuric acid and 4.5mL fuming nitric acid were added to 2.25g compound **2.1**. The mixture was heated

at 100 ^{o}C for 1h and then at 120 ^{o}C for 4hrs. A base trap was connected to the reflux condenser in order to absorb NO_2 and NO and move the reaction forward. The mixture was poured on 300mL ice water and neutralized by saturated sodium carbonate solution. The product was filtrated and recrystallized from pyridine/water (1.08g, 25%). ^{1}H NMR (400MHz, DMSO-d_6): δ 8.90-8.88 (s, 2H), δ 8.72-8.69 (d, 2H), δ 8.63-8.59 (d, 2H), δ 8.40-8.36 (m, 2H).

4, 4', 4''-trichloro-terpyridine (2.3). 480mg Compound **2.2** was added to a mixture of acetic acid (5.5mL) and acetyl chloride (3.6mL) at 60 ^{o}C for 2hrs. After neutralized with sodium bicarbonate, the precipitate (4, 4', 4''-trichloro-terpyridine-N-oxide, 300mg) was suspended in chloroform. PCl_3 was then added to the mixture and reflux for 1hr. The product came out after neutralization by NaOH with a beige color. It can be used directly at most times but some times need column purification (100% DCM to 2.5% MeOH in DCM). The final product weighs 200mg. ^{1}H NMR (400MHz, $CDCl_3$): δ 8.65-8.55 (m, 4H), δ 8.50 (s, 2H), δ 7.40 (dd, 2H).

1-trityloxy-1,4-butanediol (2.4). 3g 1,4-butanediol was dissolved in 15mL pyridine. 3.47g (0.4eq) DMTr-Cl was carefully added to the solution and the reaction went overnight. Then the solvent was removed by rotor-vap and the product was purified by silica gel (100% DCM to 1% MeOH in DCM with 0.5% TEA). The pure product is yellow sticky oil and can be dissolved in DMF for further coupling. ^{1}H NMR (400MHz, $CDCl_3$): δ 7.40-7.25 (m, 5H), δ 7.25-7.20 (m, 4H),

δ 6.96-6.93 (m, 4H), δ 4.40-4.33 (t, 1H), δ 3.75-3.70 (s, 6H), δ 3.38-3.33 (t, 2H), δ 2.98-2.90 (t, 2H), δ 1.60-1.40 (m, 4H).

4, 4', 4''-trilinker-terpyridine (2.5). 8eq of 1-trityloxy-1,4-butanediol (400mg) was dissolved in DMF with sodium hydride at 0^{o}C for 30 mins. Then 56mg compound **2.3** was added to the mixture and temperature was increased to 70 ^{o}C. The reaction lasted for 2 days. Crude product mixed with excessive linker was extracted and dried. At this moment, it is very hard to purify the mixture because of the polarity of terpyridine-linker complex. As an alternative way, I added 200 mg TBDMS-Cl to the mixture and dissolved it in DCM. In addition, TEA (1mL) and DMAP (20mg) were added to activate and accelerate the silyl bond formation reaction. Thus, the excess linker became 1-trityloxy-4-tert-butyldimethylsilyl-1,4-butanediol with a higher Rf. The desired product (180mg, 80%) was easily purified by column chromatography (100% DCM with 0.5% TEA to 2% MeOH in DCM with 0.5% TEA). ^{1}H NMR (400MHz, Acetone-d_6): δ 8.50-8.46 (d, 2H), δ 8.23-8.20 (d, 2H), δ 8.08 (s, 2H), δ 7.50-7.10, δ 6.90-6.80 (m, 39H), δ 6.95-6.92 (q, 2H), δ 4.28-4.16 (m, 6H), δ 3.75-3.65 (m, 18H), δ 3.20-3.10 (tt, 6H), δ 1.95-1.75 (m, 12H). ^{13}C NMR (100MHz, Acetone-d_6): δ 165.956, 158.552, 157.436, 156.930, 150.419, 145.553, 136.475, 136.393, 128.067, 127.620, 126.496, 112.909, 110.677, 107.276, 106.964, 85.750, 67.616, 62.705, 54.520, 26.267, 25.776. MS (ESI+): expected ($M+H^+$): 1404.64, observed: 1404.70.

2.4.3 Methods: Synthesis of terpyridine **2.20**

Ethyl 4-chloropicolinate (2.6). Mix DMF (5mL, 65mmol) with thionyl chloride (100mL, 1.3mol) at 40 ^{o}C. Add fine picolinic acid powder (50g, 406mmol) to the mixture in 10 equal portions over 30mins, while keeping the temperature between 37 and 42 ^{o}C. And then the temperature was raised to 70 ^{o}C over 2hrs (use base trap to absorb SO_2 and HCl), then kept it at 70 ^{o}C for 1 day. Volatiles were removed by rotor vap and toluene was added to the mixture (100mL). The suspension then was poured to an ethanol-toluene solution (1:1 (v/v), 120mL) cooled in an ice bath and kept for overnight. The precipitate was filtered and neutralized by 4M NaOH solution. Pure product (Appro. 35g) was obtained as oil after column separation. ^{1}H NMR (400MHz, $CDCl_3$): δ 8.70 (s, 1H), δ 8.20 (s, 1H), δ 7.52 (s, 1H), δ 4.58-4.40 (q, 2H), δ 1.58-1.40 (t, 3H).

1,5-bis-(4-chloro-pyridin-2-yl)-pentan-1,3,5-trione (2.7). Dissolve compound **2.6** (1g) with 0.14mL acetone in 4.1mL THF. The whole mixture was added to NaH (218mg)/THF(5.1mL) suspension within 2hrs at 40-45 ^{o}C. Then it was poured into 100mL water and added with 6M HCl to reach pH 7.0. The precipitate was filtered and used for next step without further purification. It (1g) was obtained as a yellow solid. ^{1}H NMR (400MHz, $CDCl_3$): δ 8.60-8.52 (d, 2H), δ 8.10-8.05 (s, 2H), δ 7.45-7.40 (d, 2H), δ 6.82-6.78 (s, 2H), 2.30-2.20 (s, 4H).

4'-hydroxyl-4,4''-chloro-terpyridine (2.8). 25% aqueous ammonia (3mL) was added to the compound **2.7** (1g) in 2-propanol (20mL). The mixture was heated to 70 ^{o}C for 6hrs. During this period additional ammonia solution (3×1mL) was cautiously added. The mixture was cooled, dried and filtered at 0 ^{o}C. The product weighs 350mg (40%) as a white solid. ^{1}H NMR (400MHz, DMSO-d_6): δ 11.20 (s, 1H), δ 8.70 (d, 2H), δ 8.60 (d, 2H), δ 7.90 (s, 2H), δ 7.62-7.60 (d, 2H).

4-(tert-butyldiphenylsilyloxy)-butyl methanesulfonate (2.9). 1.4-butanediol (1.01g, 11.2mmol) was stirred with TBDPSCl (3g, 11mmol) in pyridine for 3hrs. The product (2.11g, 6.43mmol, 60%) was purified by column (100%DCM with 0.1% TEA) and added with MsCl (0.733g, 6.43mmol) in DCM (10mL) and TEA (1mL) at 0 ^{o}C for 1hr. The product (2.1g, 80.8%) was extracted and purified by another column (100%DCM with 0.1% TEA). ^{1}H NMR (400MHz, $CDCl_3$): δ 7.67-7.62 (q, 4H), δ 7.45-7.35 (m, 6H), δ 4.26-4.20 (t, 2H), δ 3.73-3.65 (t, 2H), δ 2.95 (s, 3H), δ 1.90-1.85 (m, 2H), δ 1.70-1.62 (m, 2H). MS (ESI+): expected ($M+Na^+$): 429.16, observed: 429.5.

4'-(tert-butyldiphenylsilyloxy)-butyl,4,4''-chloro-terpyridine (2.10). Linker **2.9** (1g, 2.46mmol), compound 2.8 (0.8g, 2.52mmol) and K_2CO_3 (800mg) were dissolved in 2-butananol (10mL) and refluxed for 20hrs. The mixture then was extracted with Ethyl Acetate/water and purified by column (2% MeOH in DCM). The pure product is pale yellow crystal which weighs

1.2g (79%). ^{1}H NMR (400MHz, $CDCl_3$): δ 8.63-8.60 (s, 2H), δ 8.59-8.56 (d, 2H), δ 8.00 (s, 2H), δ 7.79-7.62 (d, 4H), δ 7.43-7.34 (m, 6H), δ 7.40 (d, 2H), δ 4.22-4.18 (t, 2H), δ 3.78-3.72 (t, 2H), δ 1.98-1.90 (m, 2H), δ 1.78-1.72 (m, 2H), δ 1.05-1.02 (s, 9H). ^{13}C NMR (100MHz, $CDCl_3$): δ 167.512, 157.452, 155.919, 149.988, 145.213, 135.545, 133.947, 129.570, 127.621, 124.034, 121.623, 108.326, 68.011, 63.444, 29.112, 26.855, 23.860, 19,123, 8.901. MS (ESI+): expected ($M+H^+$): 628.19, observed: 627.4.

4'-(tert-butyldiphenylsilyloxy)-butyl,4,4''-(trityloxy)-butyl-terpyridine (2.11) and 4'-butyl,4,4''-(trityloxy)-butyl-terpyridine (2.20). The first step is the same as making compound **2.5**. The second step is to remove TBDPS group by TBAF at room temperature in THF. Final product is pale yellow powder and is very hard to move on TLC (only showed orange color after sulfuric acid stain). ^{1}H NMR of compound **2.11** (400MHz, $CDCl_3$): δ 8.55-8.50 (d, 2H), δ 8.10 (s, 2H), δ 7.96 (d, 2H), δ 7.40-7.25 (m, 20H), δ 7.25-7.18 (m, 8H), δ 7.10 (d, 2H), δ 6.90-6.80 (m, 8H), δ 4.30-4.15 (m, 6H), δ 3.50 (t, 2H), δ 3.75-3.60 (m, 6H), δ 3.05-2.95 (m, 4H), δ 1.90-1.60 (m, 12H), δ 1.40-1.20 (m, 9H). ^{13}C NMR (400MHz, $CDCl_3$): N/A due to limited amount of the product. MALDI-TOF MS of compound **2.20**: expected: 1102.52, observed: 1102.52.

4, 4', 4''-trichloro-terpyridine (2.3). The same product as shown in scheme 1 can be obtained by replacing the middle hydroxyl group of compound **2.8** with chlorine. Pure compound **2.8** (1g,

3.1mmol) was added to PCl_5 (1.2g, 7.5mmol) in 10mL $POCl_3$ and the mixture was heated to be reflux for 1 day. Then it was carefully poured on ice and neutralized with aqueous NaOH solution with stirring overnight. Afterwards, the pink solid was extracted to chloroform and evaporate to dryness. The product is white solid and weighs 620mg (60%). ^{1}H NMR (400MHz, $CDCl_3$): δ 8.65-8.55 (m, 4H), δ 8.50 (s, 2H), δ 7.40 (dd, 2H).

2.4.4 Other terpyridine derivatives

Compound 2.12. Coevaporate dA (2.9g) with pyridine for 3 times. Add 7mL chlorotrimethylsilane to it at 0 ^{o}C and wait for 30 minutes. Then add 7mL Benzoyl Chloride to the mixture and remove it from ice bath. After sitting for 2hrs, the mixture was cooled down to 0 ^{o}C again and added with 20mL ice water. The new mixture was stirred for 15 minutes. 20mL Cont. Ammonia was then added to it and the mixture was concentrated to oil after 30 minutes. Add 50-100mL water to the oil and the product will go to the H_2O phase. The final product weighs 3.5g (86%) as white powder. ^{1}H NMR (400MHz, DMSO-d_6): δ 8.78-8.72 (s, 1H), δ 8.75-8.72 (s, 1H), δ 8.06-8.00 (m, 2H), δ 7.63-7.60 (m, 1H), δ 7.60-7.50 (m, 2H), δ 6.50-6.40 (m, 1H), δ 5.40-5.00 (2s, broad, 2H on –OH), δ 3.92-3.88 (m, 1H), δ 3.70-3.50 (m, 2H), δ 2.83-2.77 (m, 1H), δ 2.40-2.30 (m, 1H).

Compound 2.13. 2g of compound **2.12** stirred with 3g tert-butylchlorodimethylsilane in pyridine (100mL) for 3hrs at RT. The product (2.05g, 82%) was purified by column chromatography (7.5% MeOH in DCM). ^{1}H NMR (400MHz, DMSO-d_6): δ 8.78-8.74 (s, 1H), δ 8.60 (s, 1H), δ 8.06-8.00 (m, 2H), δ 7.63-7.60 (m, 1H), δ 7.58-7.50 (m, 2H), δ 6.50-6.40 (m, 1H), δ 4.45-4.40 (s, 1H on -NH), δ 3.92-3.88 (m, 1H), δ 3.70-3.62 (m, 2H), δ 2.83-2.77 (m, 1H), δ 2.40-2.30 (m, 1H), δ 0.80 (s, 1H).

Compound 2.15. Compund **2.13** (0.9g) was dissolved in 15mL pyridine. Trityl chloride (DMTrCl, 1.8g)) was added to the solution. The reaction lasted for 3hrs at 60 ^{o}C and the product (1.3g, 87%) was purified by extraction and column. The next step was to deprotect the 5' hydroxyl group by TBAF to provide compound 2.15 (0.9g, 80%). ^{1}H NMR (400MHz, $CDCl_3$): δ 8.95 (s, 1H), δ 8.05-8.00 (m, 2H), δ 7.60-7.20 (m, 9H), δ 6.90-6.80 (m, 4H), δ 6.40-6.36 (m, 1H), δ 5.78-5.70 (d, 1H), δ 4.63-4.60 (d, 1H), δ 4.06-4.02 (s, 1H), δ 3.80-3.75 (s, 6H), δ 3.40-3.25 (t, 1H), δ 2.80-2.65 (m, 1H), δ 1.80-1.65 (dd, 1H).

Compound 2.16. Add 1.5 eq 2-Cyanoethyl N,N,N,N-tetraisopropyl phosphane (0.2mL, 0.55mmol) to compound **2.15** (300mg, 0.456mmol) in acetonitrile. 0.98mL 0.45M Tetrazole (0.7eq) in acetonitrile solution was then added to the mixture in order to activate the reaction. After 4hrs, the reaction was quenched with MeOH and evaporated to dryness. The crude product

was dissolved in a minimum amount of DCM, and slowly titrated into 200mL stirring hexane. Pure product precipitated out and got filtered by vacuum filtration. The yield (30%-60%) did vary a lot due to the moisture in the air during the reaction. ^{1}H NMR (400MHz, $CDCl_3$): See Appendix for more information. ^{31}P-NMR (400MHz, $CDCl_3$): 150, 148 (2 diastomers).

Other reverse phosphoramidites (dG, dC, dT). The syntheses of those reverse phosphoramidites are very similar to the procedure for dA. The only differences are: 1. In transient protection step, we used isobutyryl group as the protecting group for dG. 2. dT has no amino groups on the base, so no protecting groups are necessary for dT. All the phosphoramidites had 150, 148 peaks on ^{31}P-NMR (please see appendix for more information).

Chapter 3: Synthesis of Three-Arm DNA-Terpyridine Conjugates

3.1 Introduction

A simple structure for an ordered 3D DNA lattice is based upon octahedron: Six DNA sequences oriented specifically around a central point. In very limited cases, more than one DNA strand has been tethered with an octahedral metal center. Previous work done in our lab involved the synthesis and analysis of a Ru-tris(bipyridine) complex with two DNA strands tethered to each bipyridine, its effect on duplex and triplex stability and its fluorescence properties[9]. Another example was the synthesis of Ru^{2+}-tris(bipyridine)-six DNA strands complexes for use towards the assembly of cubic lattices done by Kristen Stewart[10]. However, it was hard to form the desired product due to the degradation of DNA under high temperature when metal ions coordinate with bipyridine (**Scheme 3.1a**) and the difficulty of synthesizing five arms concurrently on the synthesizer (**Scheme 3.1b**). All of those undiscovered areas and problems made us think about using terpyridine. As a result, with the terpyridine-linker complexes on hand, we were able to proceed to the next step in making the six-armed center. The idea of syntheses is very simple: put either terpyridine/metal ion or terpyridine/DNA together and then add the third component afterwards.

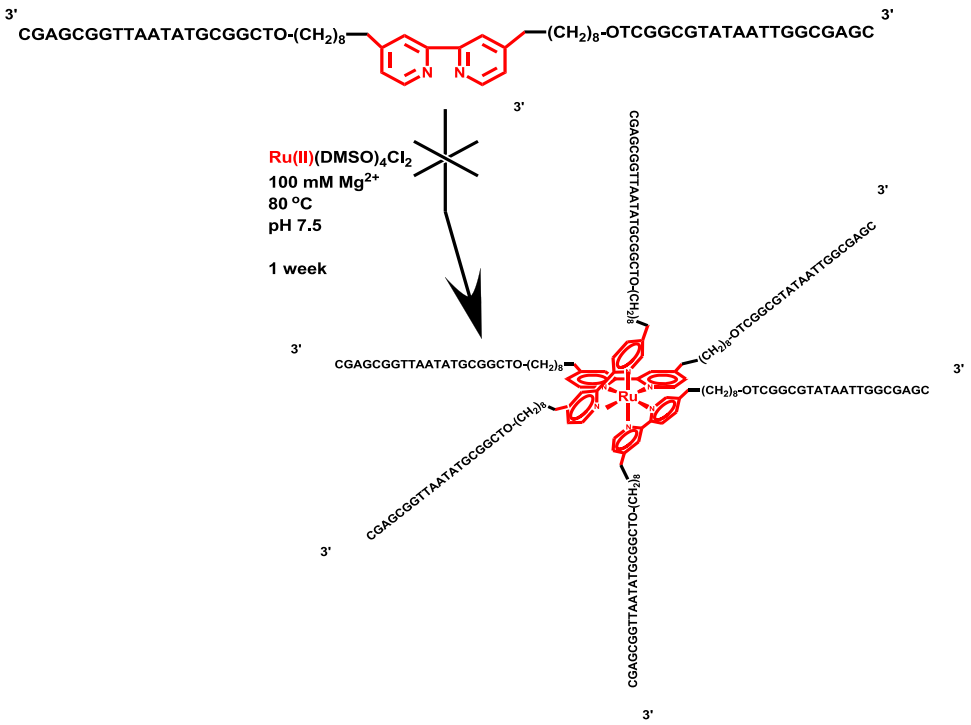

Scheme 3.1a. Previous study of metal-bipyridine-DNA chelation

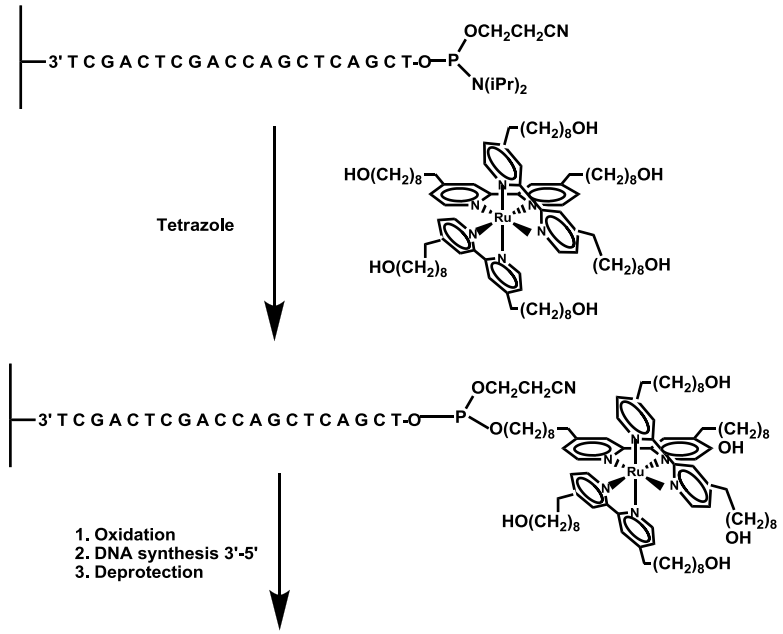

Scheme 3.1b. Strands elongation of metal-bipyridine-DNA complex

Our first attempt is to make terpyridine-metal conjugates. The result was promising because the color of terpyiridine compounds dramatically changed to red (with Ru^{2+}) or purple (with Fe^{2+}) that can be visualized naturally or UV-Vis spectroscopy. In addition, those colors stayed on the resin after the DNA synthesis suggesting the DNA-bis(terpyridine) coupling was successful. However, the disappearance of red/purple colors during the deprotection of DNA by treating with aqueous ammonia at 55 ^{o}C indicated that this method was not very successful. An alternative route of getting desired complex is to make DNA-terpyridine complex first (**Scheme 3.1c**) followed by metal coordination.

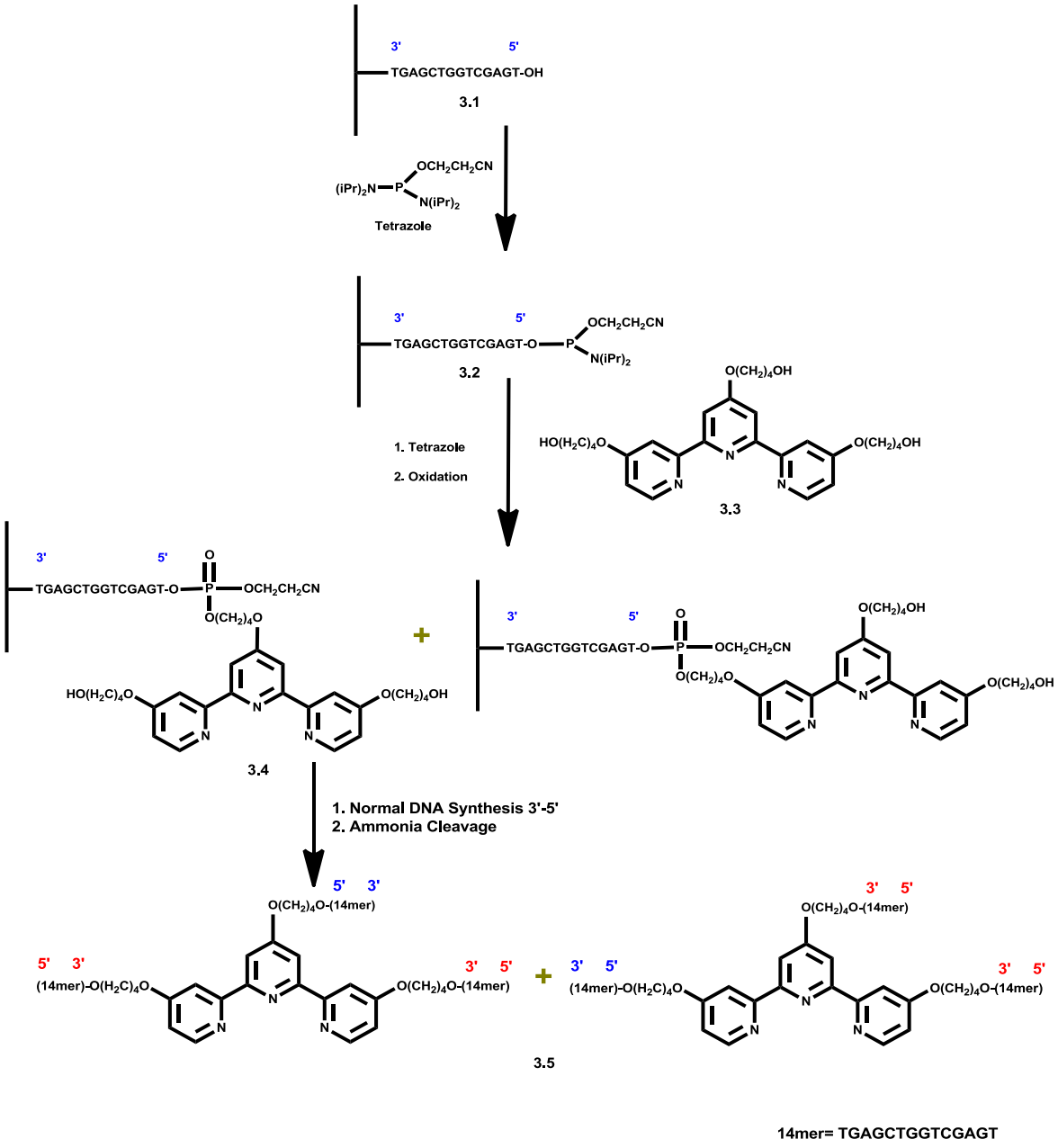

Scheme 3.1c. DNA synthesis and terpyridine coupling protocol

3.2 Results and Discussion

3.2.1 Reverse coupling protocol

Due to the difficulty of partial deprotection which allows only one free hydroxyl group exists on the terpyridine-linker complex, we had to come up with the reverse coupling protocol. This method requires four steps (**Scheme 3.1c**): 1. The synthesis of first strand on 1000Å CPG (Controlled Pore Glass); 2. 5'-OH phosphitylation; 3. Coupling of DNA and terpyridine; 4. Sequence elongation from terpyridine. It was noticeable that the coupling between terpyridine and support-bound oligonucleotide could randomly provide two products with three different arms if normal phosphoramidites were used for the first strand synthesis. However, there was no such problem since all DNA arms in the terpyridine metal center were of the same sequence and polarity if reverse phophoramidites were used for the first strand synthesis.

3.2.2 DNA synthesis, elongation and purification

The ideal products of our DNA syntheses are symmetric conjugates with three identical arms. In order to prepare them, it was necessary to initiate DNA synthesis using a 5'-bound nucleoside and elongate the strand in the 5' to 3' direction using 5'-cyanoethyl, 3'-DMT nucleoside phosphoramidites. After incorporation of terpyridine complex, synthesis was continued in the 3'-5' direction using conventional phosphoramidites. Pure desired product was made by using commercial reverse phosphoramidites as well as laboratory synthesized ones, but the yield was

not good due to the ultra sensitive nature of the reverse phosphoramidites toward humidity. It decomposed even under -20^{o}C. In order to get more DNA-terpyridine complex and lead the following metal coordination test, it is better to use 3'-CE phosphoramidite instead of the expensive 5'-CE ones and if that provides us decent amount of DNA-terpyridine-metal complex, then the synthesis could move back to the symmetric conjugates.

All DNA syntheses were performed on an ABI-394 DNA synthesizer. In order to decrease the possibility of lowing the yield while keeping the sequences fairly flexible, 14mers were used as the standard DNA for further studies. At the end of last nucleotide coupling cycle, the hydroxyl group at the 5'-termini was deprotected and covalently bonded with 2-Cyanoethyl N,N,N,N-tetraisopropyl phosphane to provide the resin-bound phosphoramidite. Terpyridine-DNA coupling was done manually and a further elongation was performed by running a customized cycle for the first nucleotide and normal 2 min coupling time for the rest of the sequence. The crude product was then soaked in aqueous ammonia for full deprotection and then purified by reverse phase HPLC. Final pure DNA-terpyridine complex was collected after gel separation for further hybridization and metal chelation study.

3.2.3 Gel electrophoresis study

Gel electrophoresis is one of the leading techniques used for the separation of DNA, RNA and protein/peptide molecules. There are usually two types of gels: Polyacrylamide Gel Electrophoresis (PAGE) and Agarose Gel. For DNA purification, PAGE is most commonly used to separate relatively short sequences (2-80mer) while Agarose is used for longer sequences (80-200mer). In order to analyze our terpyridine-3×14mer complex, 20% polyacrylamide gels were prepared for electrophoresis. The desired conjugates were supposed to run slower than a single strand 42mer oligonucleotide. And the truncated sequences should be either 14mer or 28mer. Pictures in the following showed gel separation results of both "reverse DNA-terpyridine complex" (**Figure 3.2a**) and normal DNA-terpyridine complex (**Figure 3.2b**).

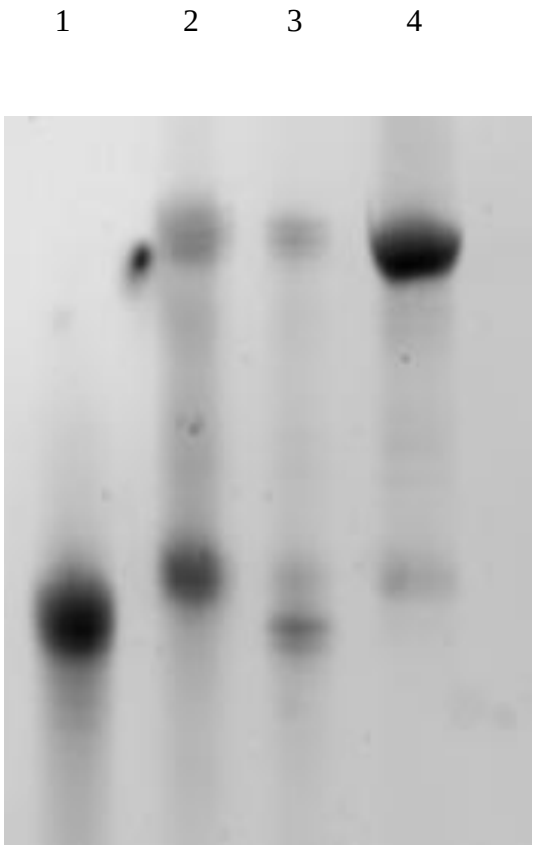

Figure 3.2a. Gel Electrophoresis of symmetric DNA-terpyridine complex
Lane 1: 28mer standard
Lane 2-4: Peaks 3-5 from HPLC

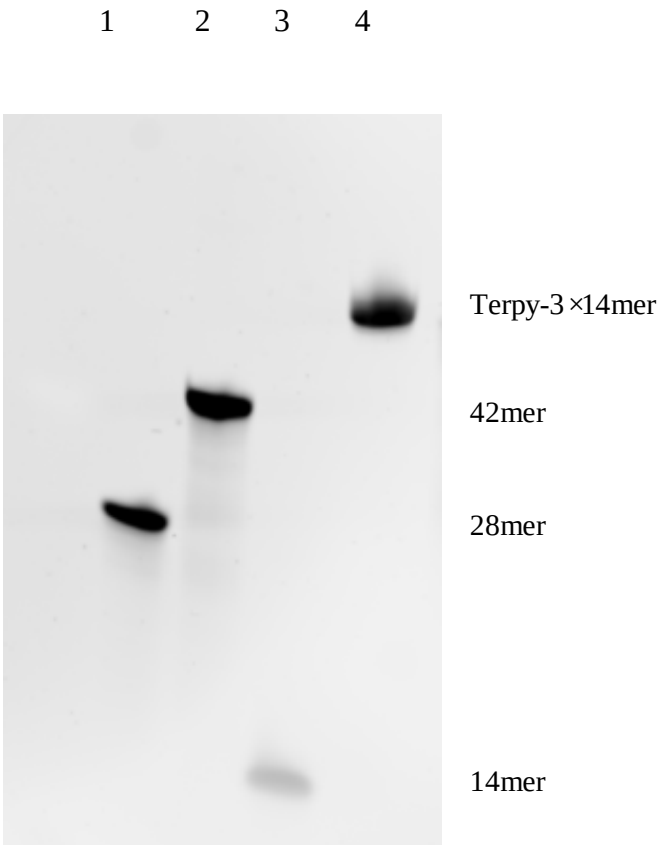

Figure 3.2b. Gel Electrophoresis of asymmetric DNA-terpyridine complex
Lane 1-3: Pure 28mer, 42mer and 14mer correspondingly. Lane 4: Pure synthetic terpy-3×14mer complex

The result of reverse oligonucleotide-terpyridine synthesis varied a lot. Two out of five times were successful. The yield after the first elongation step was 25% calculated by the absorption of DMT cation V.S. 3.6μmol starting material. The product was then purified by gel electrophoresis and stored at -20 ^{o}C with a total amount of 0.13μmol (3.6%). However, the complex decomposed

gradually and could not be seen on the gel after 4 months. An analytical HPLC plot proved that there were two peaks instead of one in the product solution. It was thought that the product obtained from gel purification had some impurity which could affect the stability of pure complex in solution. As a result, the whole synthesis and purification should be optimized. For the purpose of saving time and money, we turned to use traditional 3'-CE phosphoramidites. Once the procedure became clear, syntheses would be performed with 5'-CE phosphoramidites for the generation of conjugates of uniform polarity.

The synthesis of the first strand, coupling and elongation by using 3'-CE phosphoramidites were carried out in a more cautious manner in order to avoid side reactions. The HPLC program for the purification was also optimized to give a better separation. The gel result is shown in **Figure 3.2b**. The first three lanes represent the standards: a 28mer, a 42mer and a 14mer and the last lane is the terpyridine-3×14mer. It is clear that due to the larger size of branched DNA-terpyridine complex, the compound moves slower than the single 42mer strand which has the same number of nucleotides.

3.2.4 Yield improvement strategies

The synthesis of terpyridine-3×14mer complex did not have a worry-free one step procedure. The nature of the reverse coupling protocol requires four steps—first strand synthesis, phosphitylation, terpyridine coupling and strands elongation. Truncated sequences were mostly generated from failed phosphitylation and coupling steps (**Scheme 3.2a**). It is obvious that moisture in the air is the biggest problem for those off-synthesizer reactions. More importantly, once the resin based single-strand DNA is phosphitylated, it becomes the limiting reagent. In other words, if there is any moisture that quenches the DNA-bound phosphoramidite, the synthesis is not going to be successful.

In order to get the best result, both column and beads were dried on high vacuum for over-night. All the solvents and reagents for the manual coupling were fresh and used immediately. Since it was inevitable to remove the column off after each synthesis, drying was necessary before each manual coupling process. In addition, it was also very important to wash the beads with ultra dry ACN and dry it by Argon while plugging the column back to the synthesizer.

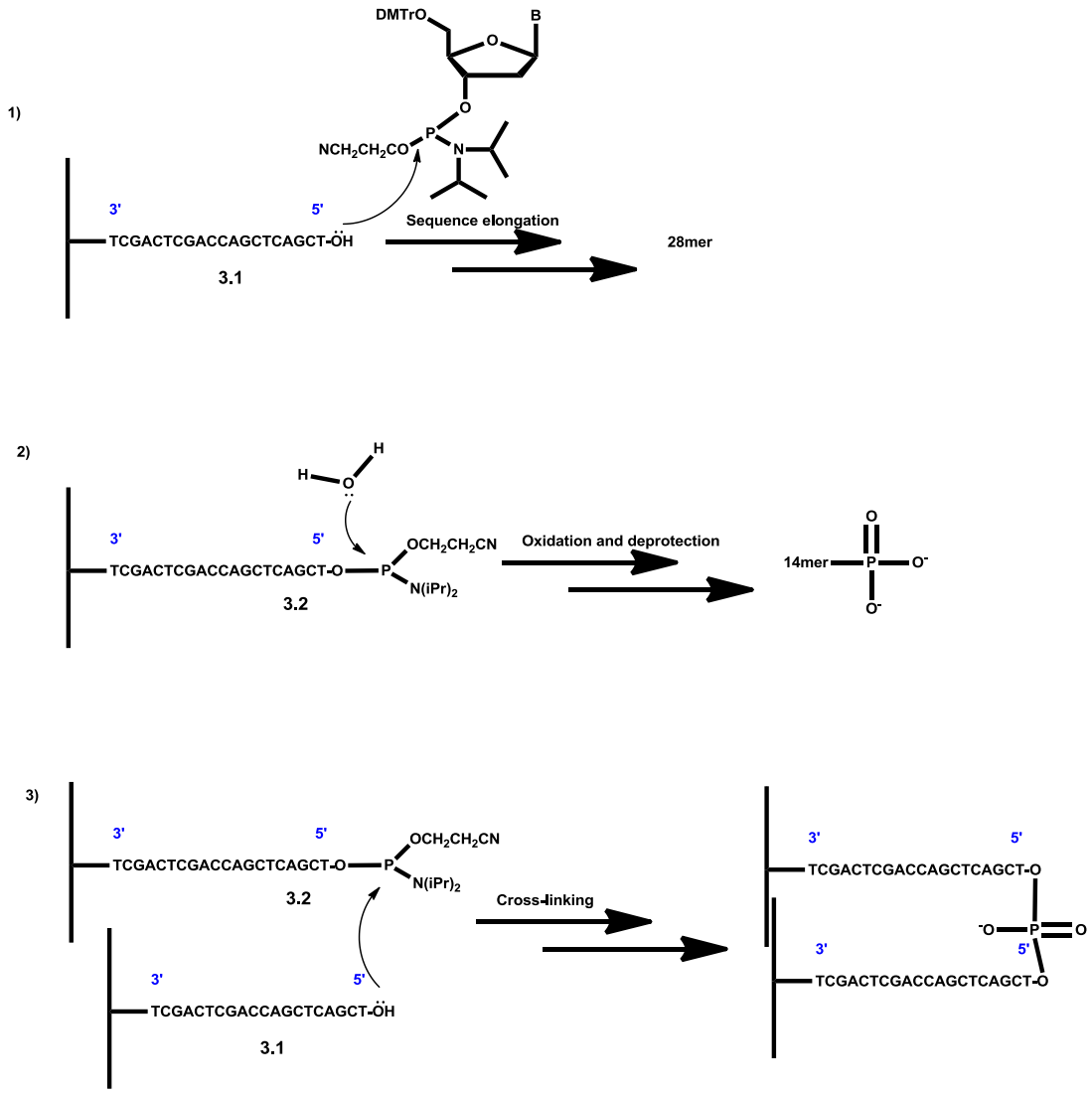

Scheme 3.2a. Multiple possibilities of forming non-terpyridine-DNA complex

In addition to water prevention, a capping step was added after the phosphitylation (**Scheme 3.2b**) to avoid unwanted elongation. Free hydroxyls at the 5' termini of the first strand were capped by acetyl group by using an automatic program on the synthesizer. As a result, those truncated sequences did not have DMTr groups on the 5'-OH termini so that they came off fast from the reverse phase HPLC.

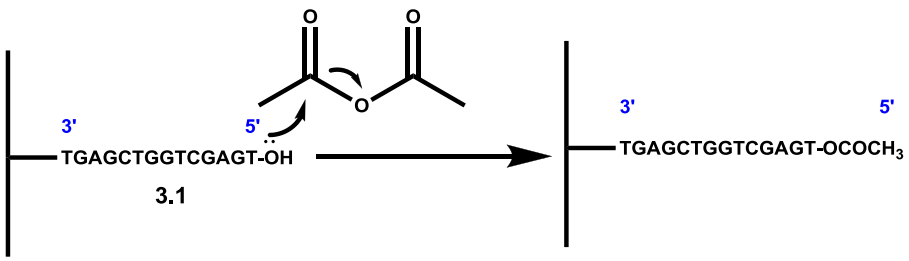

Scheme 3.2b. Capping of unreacted first sequence

Another reason for the low yield at the beginning of our DNA synthesis was that the coupling cycle for the first elongation was too short (5 seconds injection and 15mins coupling). The best way to improve this procedure was to modify the synthesis cycle. The coupling cycle was set to be performed two times more and in each one the waiting time was changed from 2 min to 30 min.

The yield increased dramatically from less than 1% to 6.8% because of those modifications. Finally a plausible amount of terpyiridine-DNA complex was synthesized for further characterization.

3.2.5 Other related DNA synthesis

Complexes that had three "ACTCGACCAGCTCA" DNA arms were also synthesized using the same strategy. A single-stranded DNA 14mer that had the same sequence was also synthesized

with an average yield of 80%. They were both prepared for further hybridization study which will be covered in detail in next chapter.

3.3 Conclusion

The synthesis of terpyridine-linker complex tethering three DNA arms has proven to be quite challenging. Not only did the complicated procedure of reverse coupling protocol make it difficult, but also both the known and unknown factors such as humidity and intermolecular interactions lead to low yield of our desired product. The best way to conduct DNA synthesis on terpyridine is to have a terpyridine with two linkers protected by DMTr and one linker with a reactive phosphoramidite. Thus, normal DNA synthesis can be performed by using normal and the special phosphoramidites with little difficulty. In other words, once compound **2.11** becomes phosphoramidite, the syntheses of either terpyridine-DNA complex with same polarity or terpyiridine-DNA complex with different polarity could be much easier.

3.4 Materials and Methods

3.4.1 Materials

Oligonucleotides were synthesized on an Applied Biosystems 394 DNA/RNA synthesizer (Forster City, CA). DNA synthesis grade acetonitrile and dichloromethane was purchased from Fisher Scientific (Fair Lawn, NJ). DNA synthesis reagents, 3' –cyanoethyl (CE) phosphoramidites, 5'-CE phosphoramidites, 3' -1000Å controlled pore glass (CPG) and 5' -1000Å CPG were obtained from Glen Research (Sterling, VA).

High performance liquid chromatography was done on a Waters 600E Multisolvent Delivery system equipped with a Waters 2487 dual wavelength absorbance detector (Milford, MA). Purification was performed on a 10cm long, 4.6mm diameter column containing POROS Oligo R3 reverse phase support purchased from Applied Biosystems (Framingham, MA). Analytical HPLC was performed on a 4.6×250mm self-packed column containing spherical ODS-Hypersil C18 support from Varian (Walnut Creek, CA). HPLC grade acetonitrile was also obtained from Fisher Scientific.

Concentration of samples was determined using UV-Vis measurements obtained on a Beckman DU640B spectrometer (Fullerton, CA). Reverse phase chromatography was performed by using GE G10 and G25 column containing cross-linked dextran (Picasaway, NJ). Acrylamide and bisacrylamide were from ICN (Aurora, OH). Polyacrylamide Gel Electrophoresis (PAGE) apparatus was from Hoefer Scientific (San Francisco, CA). Ethidium bromide was obtained from

Sigma (St. Louis, MO), 28mer and 42mer DNA single strand standard was purchased from IDT (Coralville, IA). Imaging of PAGE was conducted on a BioRad Molecular Imager FX system equipped with Quantity One software.

3.4.2 Methods: DNA synthesis

The initial 14mer DNA sequence was synthesized on a 3.6μmol scale on 1000Å CPG in the conventional manner. 500Å CPG did not work well because our conjugates are much larger than single strand DNA. Either 5'-CE phosphoramidites or 3'-CE phosphoramidites were used as monomer. Synthesis was performed trityl (DMTr) off. The product was then dried under vacuum and then kept in Argon for further coupling.

3.4.3 Methods: DNA-terpyridine coupling, DNA strands extension and purification

The terpyridine-linker complex was then introduced by using a reverse coupling technique[11 12]. 200μL 1M 2-(cyanoethyl)-tetraisopropylphosphoramidite in acetonitrile was drawn into a 1mL plastic syringe with a Luer fitting. 200μL 0.45M tetrazole activator solution was drawn into a second syringe. The syringes were attached to the ends of the DNA synthesis column and the

solutions mixed. The column was placed on a shaker platform and phosphitylation was allowed to occur for 4 hours. After the shaking process, the column was immediately washed on the synthesizer and purged with argon. A capping step was performed on the synthesizer with a longer injection time (30secs) and longer waiting time (2mins) to enforce a complete coupling process. Then a solution of 25mg of complex 2.5 in 150μL acetonitrile was drawn into one syringe and 150μL 0.45M tetrazole activator solution was drawn into a second syringe. These were attached after washing the column briefly on the synthesizer by flushing with acetonitrile and reverse flushing with argon. The solutions were mixed and coupling was allowed to proceed for 18 hours followed by oxidation on the synthesizer. It was noticeable that capping was not performed since all of the hydroxyl groups on the complex were left unprotected and thus would result in synthesis termination. The first elongation step was performed by using a unique cycle—three coupling process with 30mins waiting time in each. After the coupling was done, normal 2mins cycle was then applied to the synthesis of the rest of the sequences.

Following deprotection by using aqueous ammonia solution at 55^{o}C for over night, conjugates were purified on a POROS 4.6mm×100mm column packed with Oligo R3 reverse phase support with a flow rate of 3mL/min in 50mM TEAA buffer (pH=7.0) and an acetonitrile gradient (buffer A (5%) for 3mins, then 0% B to 30% B (70%) over 17mins, followed by 30% B to 70%

B for 15mins, then 10mins to reach 100% B). The terminal DMTr was removed by reaction in 80% acetic acid for 30mins at 0^{o}C and samples were desalted on G10 column.

3.4.4 Denaturing Gel electrophoresis analysis

Conjugates were further purified and characterized by denaturing PAGE (15%, 19:1 acrylamide: bisacrylamide). 12.5mL 40% acrylamide solution, 5mL 10×TBE (pH=8.3) buffer, 23g Urea were mixed together with water and heated to get a 50mL 15% gel solution. After cooling down the solution, 300μL 10% Ammonium persulfate solution (APS) was added to the mixture followed by 25μL of Tetramethylethylenediamine (TEMED). The gel solution was then injected into the space between two glass plates and became a 1mm thick film. It was necessary to prerun the electrophoresis for 1hr at 16W and then compounds mixed glycerol were loaded into the gel wells. The running time depended on the average size of the compounds as well as the Voltage. Analytical gel was stained by EB and visualized by imager and then discarded right after use. For semi-prepare gels, the bands should be seen under UV. Bands corresponding to the desired products were excised and recovered by extraction with 0.5M Ammonium Acetate. The compound then was desalted and lyophilized to dryness. The purity of the conjugates was confirmed by PAGE analysis and the quantity was determined by UV-Vis spectroscopy.

Chapter 4: Hybridizations Study of DNA-Terpyridine Complex and Metal Coordination

4.1 Introduction

Monomer building blocks containing multiple single-stranded DNA sequences could play an important role in the self-assembly of larger matrices. The goal of the project was to synthesize a metal centered DNA conjugate with six tethered DNA sequences and octahedral geometry by using solid phase DNA synthesis methods. With the terpyridine-DNA complexes on hand, both of the characterization of terpyridine-metal coordination and the hybridization ability test of DNA arms with their complementary sequences were performed. Once the synthesis of the DNA-terpyridine-metal conjugate was accomplished, hybridization studies would be performed in order to determine the ability of these conjugates to hybridize into higher ordered structures.

Metal complexes of 2,2':6',2''-terpyridine and its derivatives have been known for over sixty years. The tridentate ligand was initially used for the colorimetric determination of metal ions[13]. The unique nature of d-π^* back donation made terpyridine a transition metal ion detector with excellent binding affinity. Besides the extensive use of terpyridine by inorganic chemists, more recently, these compounds have become a significant part of a wide range of new applications such as photosensitizers for solar-energy conversion schemes, environmental sensors, building block of supramolecular conjugates and DNA metallointercalators[14]. Kristen Stewart in

Mclaughlin's lab had synthesized ruthenium bis(terpyiridine) tethering two DNA sequences that served as a building block for the assembly of linear arrays[15]. In addition, she also synthesized six-arm DNA-bipyridine-ruthenium building blocks by the reverse coupling protocol. However, the yield was too low to be seen on non-radioactive gels and also most of the product was trapped in the gel well, which means a large degree of aggregation existed. As a result, it is very challenging to make the metal chelated DNA-terpyridine complex due to strong charge-charge repulsion among those DNA arms. All attempts were used to get the desired metal-terpyridine-DNA complex including using different transition metals, different temperature/time control and pH adjustment.

4.2 Results and Discussion

4.2.1 DNA-terpyridine(-Metal) complex hybridization study by native gel electrophoresis

Multiple bands corresponding to conjugates with different numbers of arms can be observed after PAGE. Analysis of the hybridization products of the conjugates plus varying ratios of complementary native 14mer was performed by nondenaturing PAGE and visualized by ethidium bromide staining. The analysis of the hybridization products for conjugate **3.6** (**Scheme 4.2a**) is shown in **Figure 4.2a**.

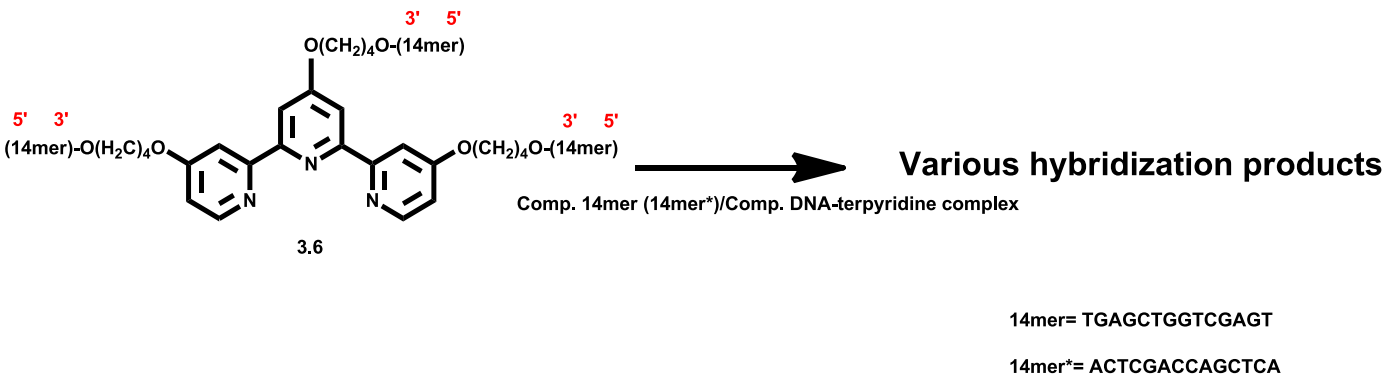

Scheme. 4.2a. Hybridization of terpyridine-DNA (same polarity) complex with its complementary sequences 14mer*

It was obvious that from the structure of terpyridine-DNA complex, the number of hybridization events should correlate with the number of arms present on each conjugate. Therefore, for the three-arm DNA-terpyridine conjugate, three hybridization events should be observed. The pronounced increase in apparent length of the conjugates with increasing duplex character may be explained by the fact that, with increasing duplex character, the conjugates become less flexible. As the conjugates become more rigid, a greater overall reduction in mobility through the get pores is observed. Lane 10 was the standard compound **3.6** and Lane 5-8 showed a stepwise hybridization process by adding different equivalent of complementary 14mers. In addition, the formation of high molecular weight assemblies occurred (Lane 4) as indicated the presence of the material that did not migrate from the gel well. Furthermore, it was noticeable that there were bands running much slower than the standard in Lane 1-3 which represented higher molecular

weight complex. This compound indicated the formation of Ru-bis(terpyridine) complex, but further hybridization tests are necessary for final characterization. There were still a great amount of compound **3.6** existed in those lanes, which means the metal-terpyridine coupling was not complete even performed over night at 40^{o}C.

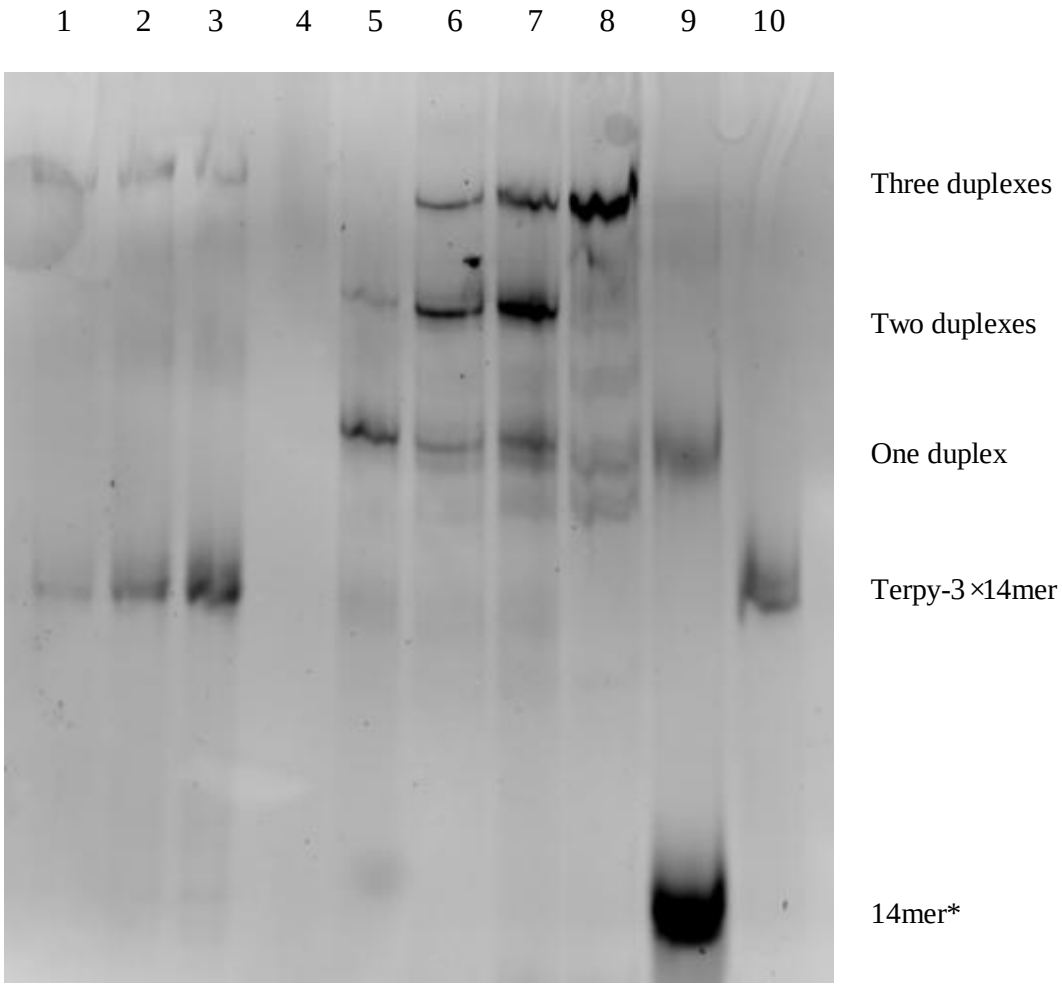

Figure 4.2a. Native gel study of terpyridine-DNA complex (**symmetric**) hybridization and metal chelation. Lane 1-3: Terpy-3×14mer : Ru^{2+}=2:1 with terpyridine concentrations 10μM, 20μM, 40μM respectively; Lane 4: Terpy-3×14mer : complementary terpy-3×14mer=1:1; Lane 5-8: Terpy-3×14mer : complementary 14bp standard (14mer*)=1:10, 1:3, 1:2 and 1:1, respectively; Lane 9: Complementary 14bp standard (14mer*); Lane 10: Terpy-3×14mer. Hybridizations were performed in 89mM TB + 1mM $MgCl_2$ buffer.

Smearing was a big problem for the symmetric terpyridine-DNA complex. Hybridization tests for asymmetric terpyridin-DNA complex (**Scheme 4.2b**) provided a better picture with a higher resolution and purer spots (**Figure 4.2b**).

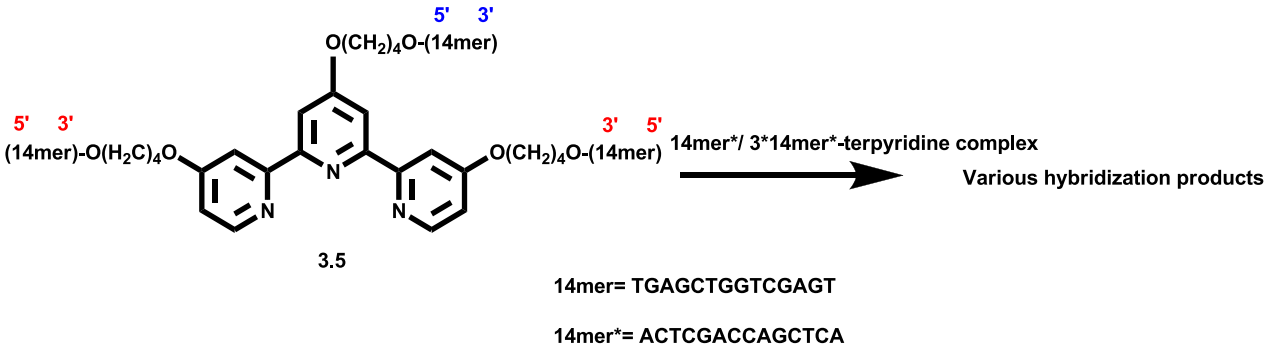

Scheme. 4.2b. Hybridization of terpyridine-DNA (different polarity) complex with its complementary sequences 14mer*

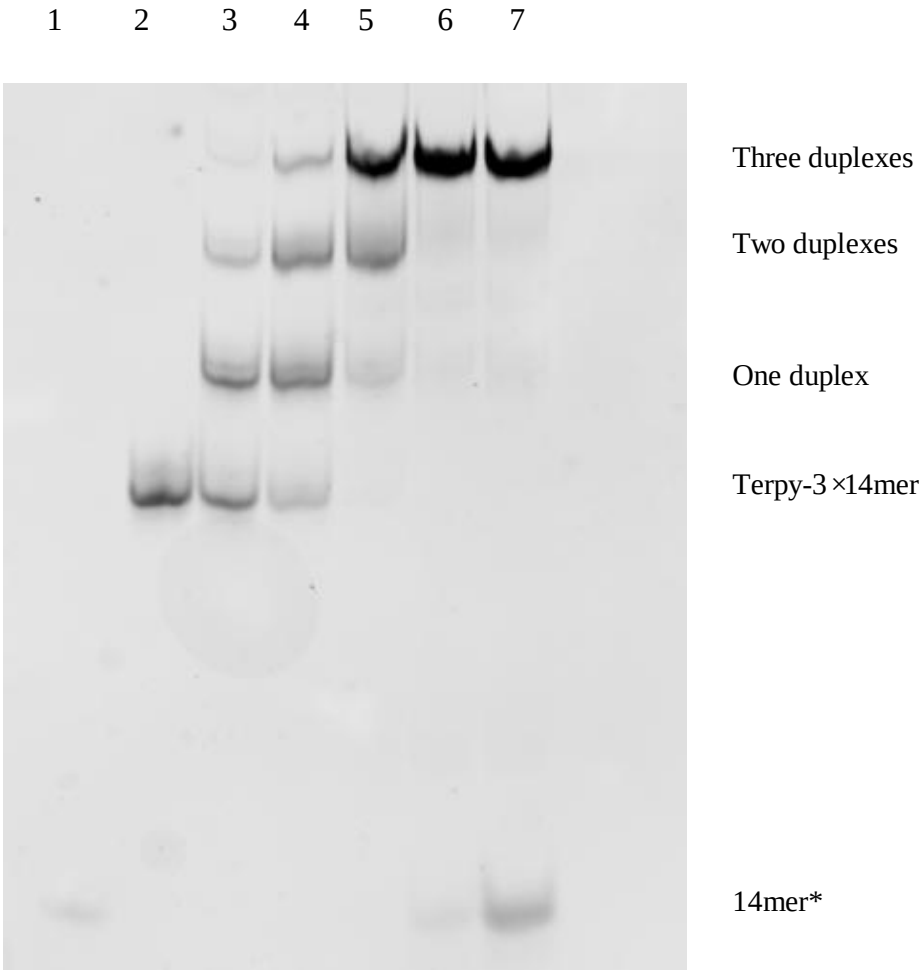

Figure 4.2b. Native gel study of terpyridine-DNA complex (**asymmetric**) hybridization and metal chelation. (from left to right) Lane 1: Complementary 14bp standard (14mer*); Lane 2: Terpy-3×14mer standard; Lane 3-7: Terpy-3×14mer : complementary 14bp standard (14mer*)=1:0.5, 1:1, 1:2, 1:3 and 1:6, respectively. Hybridizations were performed in 89mM TB + 1mM $MgCl_2$ buffer.

The ability to shift the entire initial complex to band 6 and 7 indicated that all conjugate samples contain three arms. In addition to confirming the number of DNA arms present in each of the

conjugates, this analysis showed that hybridization occurs cleanly and that intermediate structures (i.e. structures with partial arms) were not formed.

Fe^{2+} was used to coordinate with the terpyridine due to its high binding affinity (Log K_1=7.1, Log K_2=13.8) in our DNA-terpyridine-metal complex formation process. It was proved by our previous research that overnight heating was necessary for terpyridine-Ru^{2+} coordination but not for terpyridine-Fe^{2+}. The Iron (II) coordination products are shown in **Figure 4.2c**. In our experiments, both terpyridine-Fe^{2+} and DNA-terpyridine-Fe^{2+} mixtures were heated at 50^{o}C for only 30mins. UV-Vis spectra showed the linear increase of d-π* back donation absorption at 551-554nm for terpyridine-Fe^{2+} when concentration of both $FeCl_2$ and terpyridine solution increased (**Figure 4.2d**). Meanwhile, the absorption at 554nm for DNA-terpyridine-Fe^{2+} complex perfectly fitted in the linear plot (**Table 4.1**). This result confirmed that a coordination complex exists upon mixing Fe^{2+} and DNA tethered ligands.

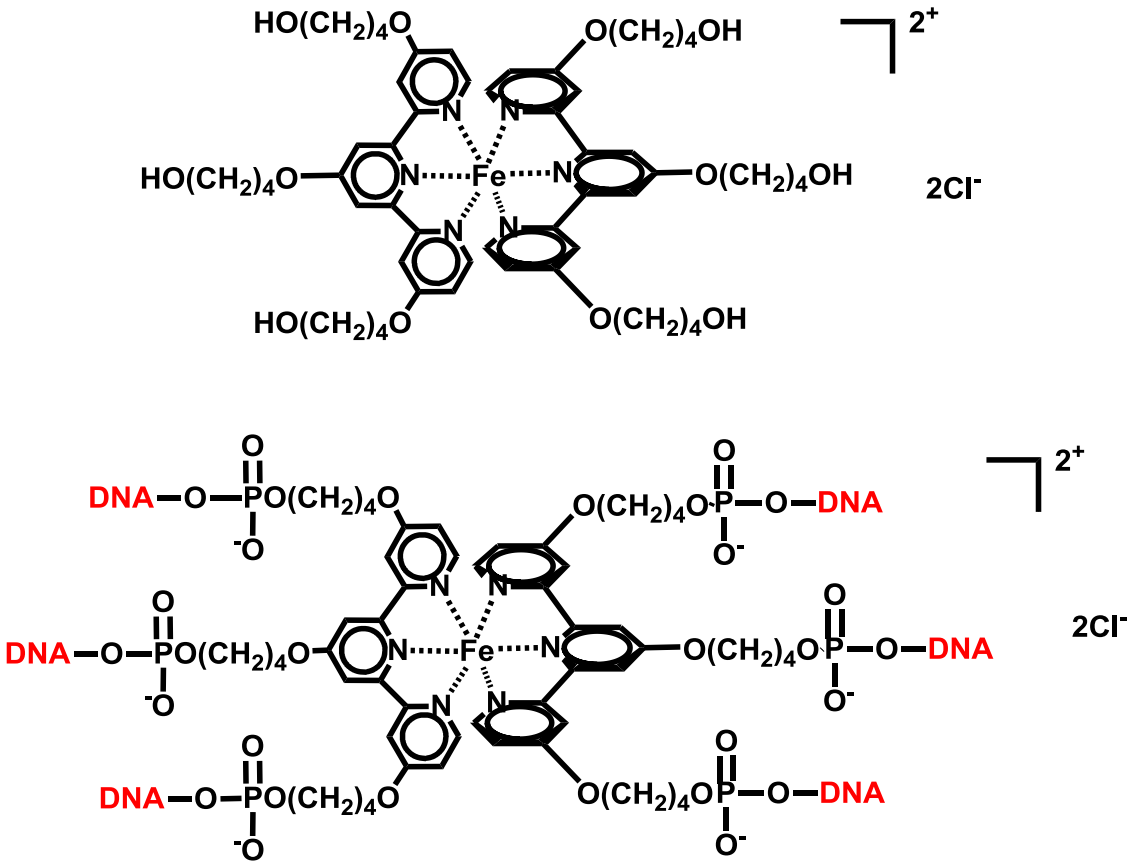

Figure 4.2c. Above: Fe^{2+}-terpyridine ligands complex; Below: Fe^{2+}-terpyridine-DNA complex

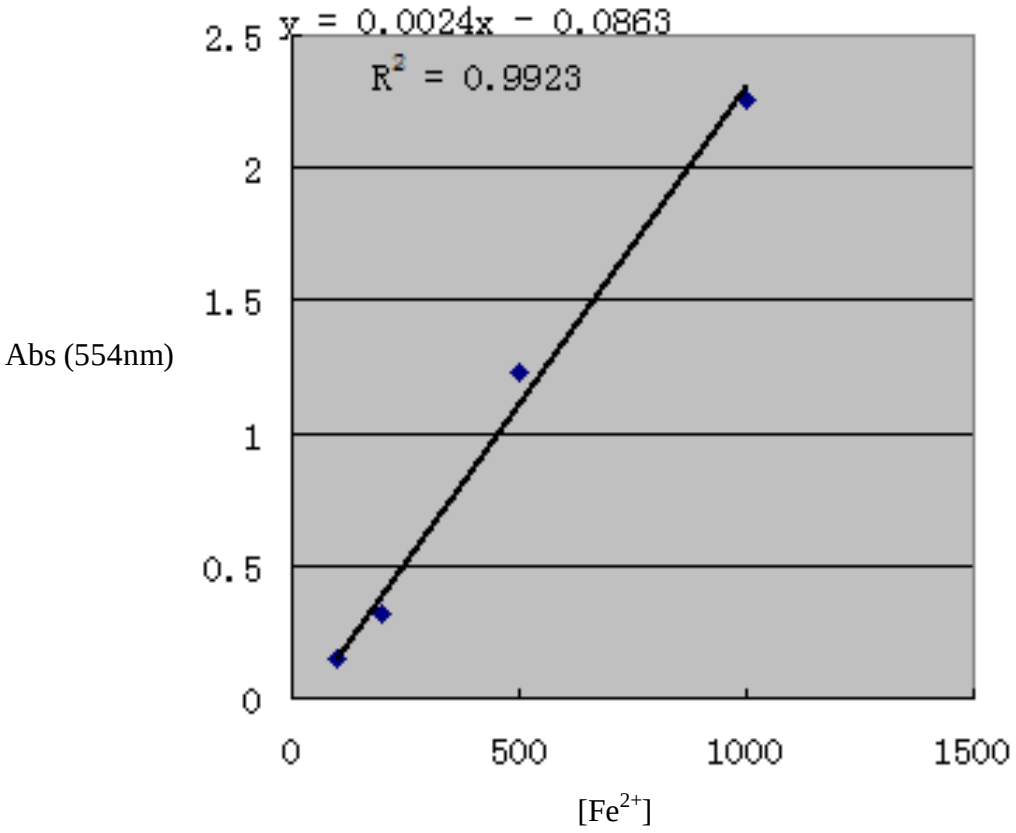

Figure 4.2d. Linear increase of UV absorption at 554nm for terpyridine-Fe^{2+} complex at different concentrations. X-axis—[Fe^{2+}] (μM); Y-axis--Abs

Ligands and metal source	Abs (554nm)
Terpyridine-linkers (Compound 3.3): 1mM $FeCl_2$: 0.5mM	2.26
Terpyridine-linkers (Compound 3.3): 0.5mM $FeCl_2$: 0.25mM	1.23
Terpyridine-linkers (Compound 3.3): 0.2mM $FeCl_2$: 0.1mM	0.3242
Terpyridine-linkers (Compound 3.3): 0.1mM $FeCl_2$: 0.05mM	0.1502
Terpyridine-linkers-DNA (Compound 3.6): 0.077mM $FeCl_2$: 0.039mM	0.1158

Table 4.1. UV-Vis absorption of Ligand-Metal complex

However, native gel electrophoresis did not provide very positive information. It was hard to visualize bands that represented larger complexes on the gel. Moreover, relatively long

incubation times at 50°C made the bands diminish on the gels. We deduce that the coordination product is not very stable at 50°C and under basic gel buffer conditions (pH=8.3). One of the reasons for this problem is charge-charge repulsion among the six DNA arms. Another possible reason is that Fe^{2+} ions intend to become $Fe(OH)_2$, $Fe(OH)_3$, FeO or Fe_2O_3 in basic aqueous conditions. Further investigation was necessary and due to the limit amount our terpyridine-DNA complex, radio-labeled compounds were used for gel electrophoresis.

4.2.2 DNA-terpyridine(-Metal) complex hybridization study by radio labeling

Ethidium Bromide is widely used as a fluorescent tag staining DNA in PAGE gels. When exposed to ultraviolet light, it will fluoresce with an orange color, intensifying almost 20-fold after binding to DNA. It provides a good way of visualizing DNA under UV with a fairly small amount of compound. However, it is not ideal to consume our precious product on gels extensively due to the multi-step organic synthesis lost, non-100% yield on the synthesizer and low coupling yield for DNA-terpyiridine-linker complexes. We then turned to use radio-labeling PAGE (**Scheme 4.1**) which only requires nM scale instead of μM of DNA.

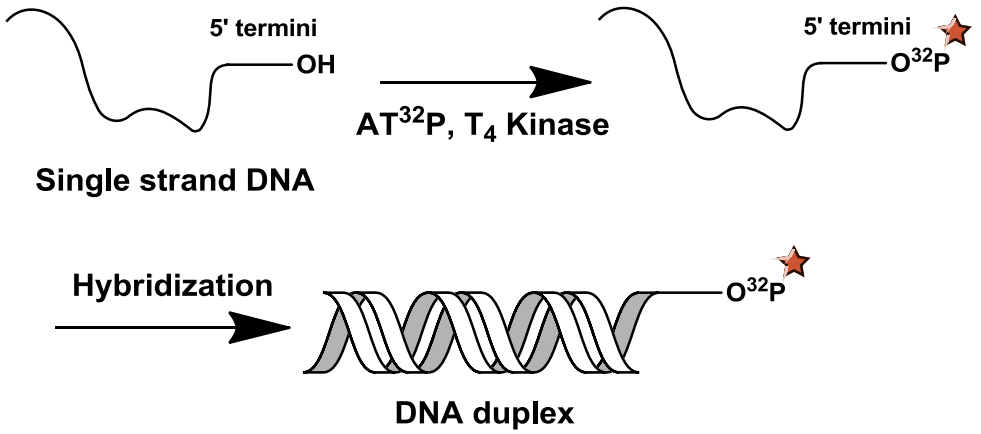

Scheme 4.1. The use of radio-labeling technique in DNA determination

There are two ways of visualizing the gel by radio labeling. One is to label the terpyiridine-DNA complex (**Figure 4.3a**), and the other is to label the complementary 14mer (**Figure 4.3b**). It was obvious that both gel results showed stepwise band shift due to the three arms nature of the hybridized terpyiridine-DNA complexes. In addition, in the labeled 14mer* hybridization test, a half equivalent of $FeCl_2$ was added to samples with high salt concentration buffer in order to test the terpyridine-DNA complex-metal coordination. However, no higher molecular weight bands were found on the gel. Meanwhile, another experiment was performed with lower pH for both samples and gel running buffers. Fresh $FeCl_2$ solution was made with a pH of 5.2. The DNA-terpyridine complex was dissolved in 0.1M NaH_2PO_4 and 0.1M $MgCl_2$ solution (pH=5.0). The PAGE was run in 1×TB buffer (pH=7.0) which was neutralized by HCl. The gel (**Figure 4.3c)**

indicated that there was indeed a shift on Lane 3 which represented the existence of Iron (II)-bis(terpyridine) complex. Higher bands shown on Lane 9 and Lane 10 also indicated the existence of Ru (II)-bis(terpyridine) and it was even more obvious that the last two lanes had bands in the gel well with great darkness. This sign suggested that there were hybridized Ru (II)-bis(terpyridine) in the mixture. However, this gel looked not perfect and some of the spots were smeared and could not be seen clearly on screen. The reason could be either long time run (12hrs) or the change of buffer's pH. Further investigation is necessary for getting better gel results.

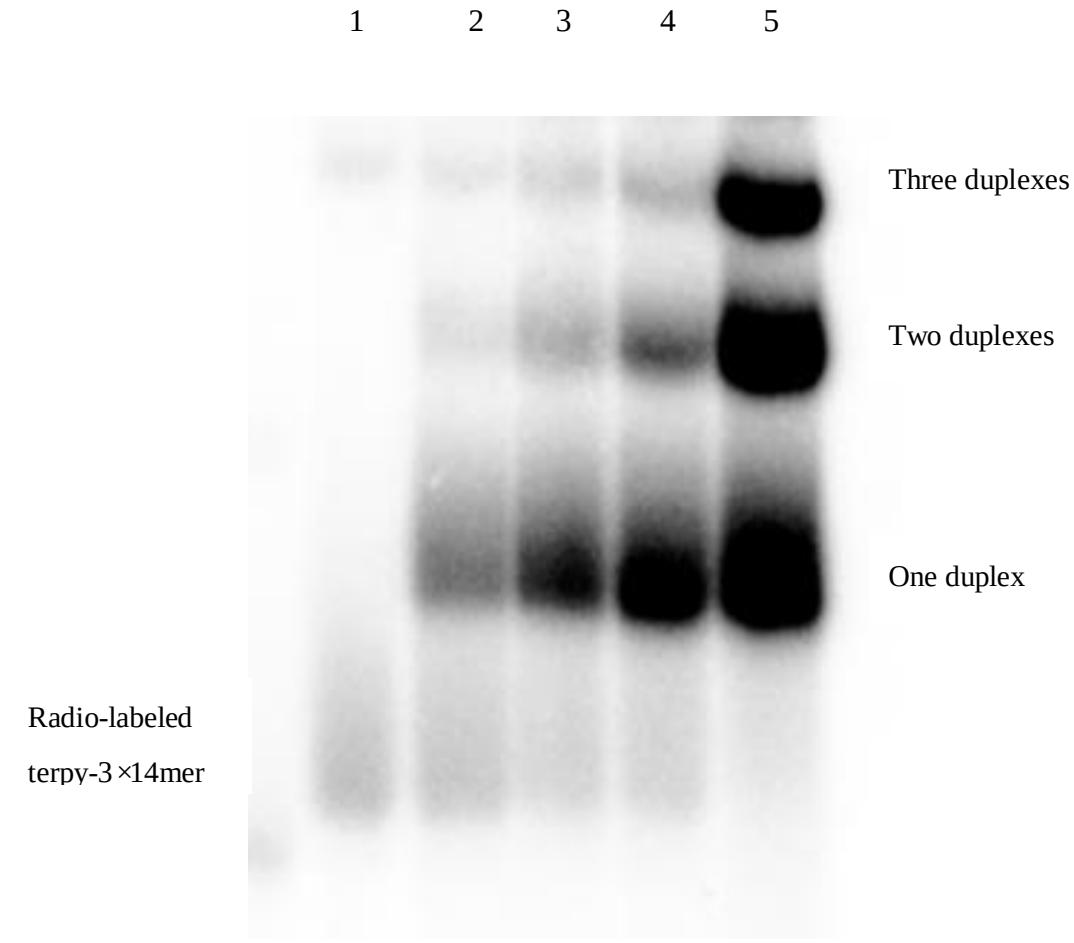

Figure 4.3a. Hybridization of **Compound 3.5** to its complementary 14bp standard (14mer*). Analysis was performed by 15% nondenaturing PAGE 19:1 crosslinking. **Compound 3.6** was radio-labeled by [γ-^{32}P] ATP at its 5' –OH position. Lane 1: Radio-labeled Terpyridine-DNA standard; Lane 2-5: Radio-labeled terpyridine-DNA complex : 14mer*=1:0.5, 1:1, 1:2 and 1:3, respectively.

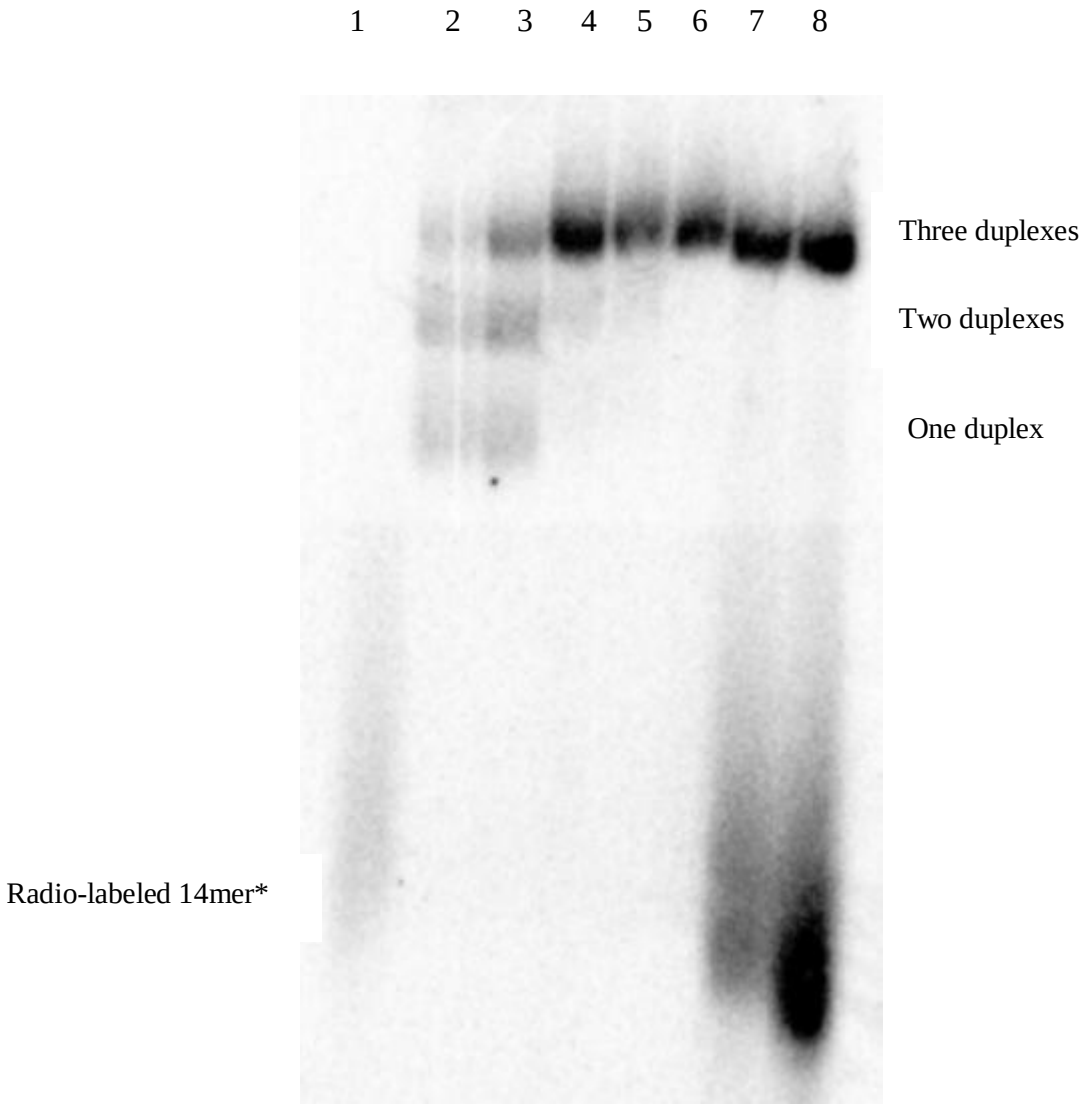

Figure 4.3b. Hybridization of **Compound 3.5** to its complementary 14bp standard (14mer*). Analysis was performed by 15% nondenaturing PAGE 19:1 crosslinking. 14mer* was radio-labeled by [γ-^{32}P] ATP at its 5' –OH position. 0.5 eq of **$FeCl_2$** was added to all samples for metal coordination test. Lane 1: Radio-labeled 14mer*; Lane 2-8: Terpyridine-DNA complex : radio-labeled 14mer*=1:1, 1:2, 1:3, 1:4, 1:5, 1:6 and 1:10, respectively.

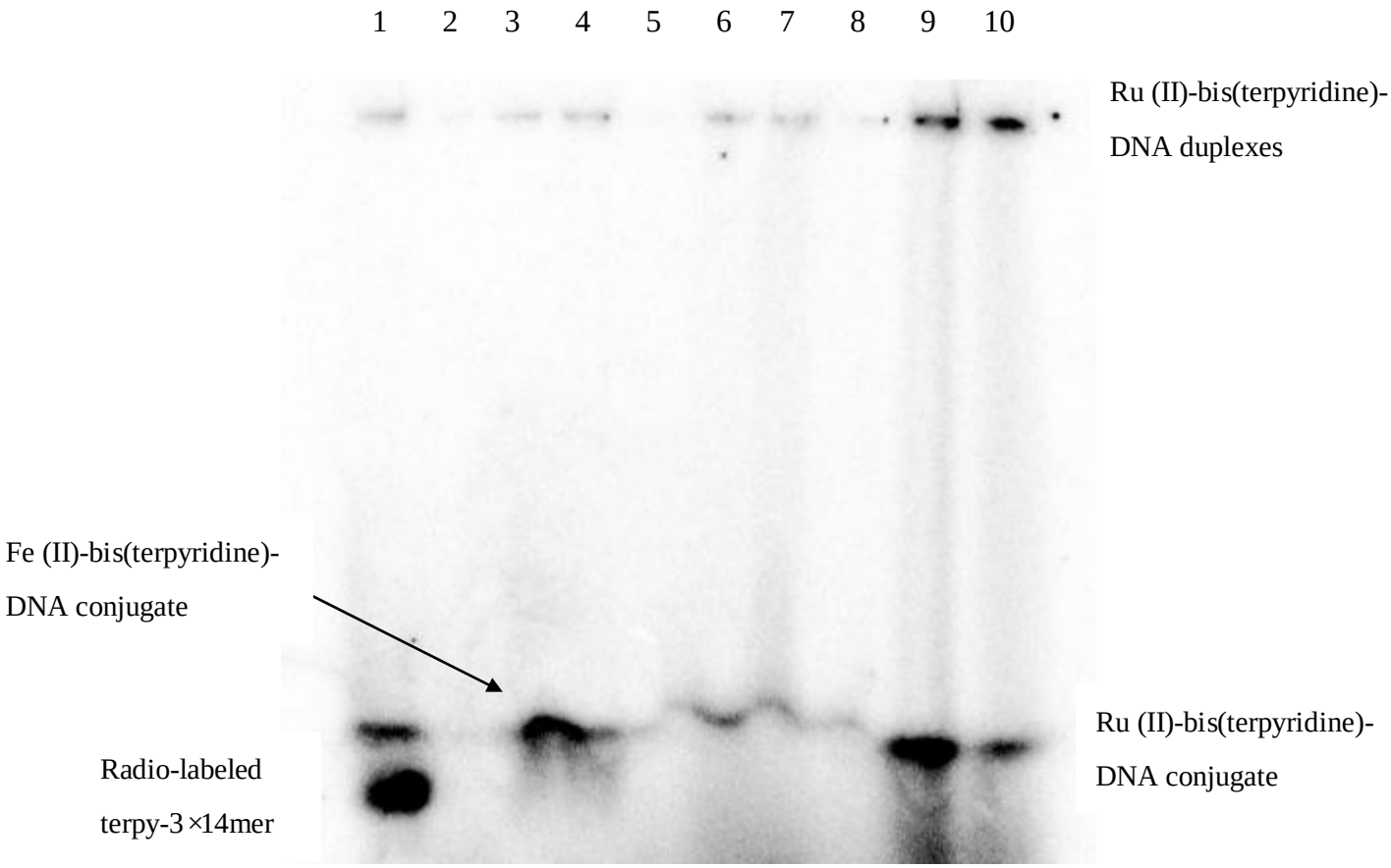

Figure 4.3b. Metal-ligand chelation test. Analysis was performed by 10% nondenaturing PAGE 19:1 crosslinking. Both **Compound 3.5** and complementary 14bp standard (14mer*) were radio-labeled by [γ-^{32}P] ATP at their 5' –OH positions. Lane 1: Radio-labeled Terpyridine-DNA standard; Lane 2: Radio-labeled 14mer*; Lane 3: Radio-labeled Terpyridine-DNA complex : $FeCl_2$=1:0.5; Lane 4: Radio-labeled Terpyridine-DNA complex : $Ru(DMSO)_4Cl_2$=1:0.5; Lane 5-7: Radio-labeled Terpyridine-DNA complex : $FeCl_2$: Radio-labeled 14mer*=1:0.5:1, 1:0.5:3 and 1:0.5:6, respectively; Lane 8-10: Radio-labeled Terpyridine-DNA complex : $Ru(DMSO)_4Cl_2$: Radio-labeled 14mer*=1:0.5:1, 1:0.5:3 and 1:0.5:6, respectively.

4.3 Conclusion

The hybridization of terpyridine-DNA complexes tethering with the complementary sequence was successful. Different PAGE methods were used to prove the existence of three tethered DNA arms. In addition, UV-Vis spectra provided strong evidence of Fe (II)-bis(terpyridine) conjugate formation. However, the gel analysis was just partially successful. Among many possibilities of not seeing our desired bands on the gel, pH was confirmed to be a primary factor of affecting gel results. Further work will still be necessary to optimize the characterization of these conjugates including pH adjustment, coupling temperature control and other visualizing tools. Furthermore, the hybridization test results obtained at this time have offered a number of insights into the synthesis of six-arm metal complex-DNA conjugates. First, to select the right metal ion is very important. The dielectric ion should have a high binding ability for terpyiridine as well as a fairly good stability in water solution. Second, an increase in rigidity of the conjugate might help the coordination because charge-charge repulsion could be reduced in such a rigid geometry. Third, a terpyridine with shorter sequences (for example, 4mer) is easier to be synthesized and can be used as a primary tool for detecting metal-terpyridine-DNA coordination.

4.4 Future Work

The unique structure and self-recognition properties of DNA can be applied to generate self-assembling DNA nanostrucutres for specific shapes. The short term goal of this project is to make a metal centered DNA conjugate with six tethered DNA arms and octahedral geometry utilizing solid phase synthesis methods. Instead of using reverse coupling protocol, phosphitylated compound **2.20** could be used as other normal phosphoramidites on the synthesizer and the synthesis will be conducted with little difficulty. In addition, pH dependent metal coordination and hybridization experiments need to be continued in order to find the best way of forming the six-arms conjugate. Once the procedure is clear, reverse phosphoramidites could be applied to the synthesis of symmetric DNA-terpyridine complexes. Our long term goal is to investigate other possible ways of building up DNA 3D structures. One possibility is to use DNA "origami" method which could serve as platforms to arrange oligonucleotides/DNA with high precision and specificity[15,16]. This "one pot" procedure enables the formation of arbitrary shapes that are 10-100nm in diameter by using numerous short DNA strands to direct the folding of a long DNA single strand with the help of computer programs. This technique was originally performed to generate 2D DNA nanostructure and recently Ebbe S. Andersen et al. extended it into three dimensions. Meanwhile, other assembly strategies could also be considered to build complicated 3D DNA nanostructures[17-23].

4.5 Materials and Methods

4.5.1 Materials

All chemical reagents are solvents were from Aldrich (St. Louis, MO). Acrylamide and bisacrylamide were from ICN (Aurora, OH). Polyacrylamide Gel Electrophoresis (PAGE) apparatus was from Hoefer Scientific (San Francisco, CA). $AT^{32}P$, T_4 Kinase, T_4 Kinase buffer and BSA were from New England Biolabs (Ipswich, MA), 28mer and 42mer DNA single strand standard was purchased from IDT (Coralville, IA). Imaging of PAGE was conducted on a BioRad Molecular Imager FX system equipped with Quantity One software.

4.5.2 Methods: Hybridization experiments and gel development procedure

For the hybridization studies, each sample was prepared by adding the required amount of DNA-terpyridine complex and its complementary strand to an eppendorf tube, then being dried by spin vac. Buffers adding to the residue varied, from 1×TB-100mM $MgCl_2$ (pH=8.3) to 0.1M NaH_2PO_4 + 0.1M $MgCl_2$ solution (pH=5.0). Samples were heated for 2 mins at 95^oC and cooled gradually to RT. After cooling, 30% glycerol which was 40% of the volume in each eppendorf (normally 4μL) was added to all samples. Final mixtures were loaded on to 19:1 cross-linked 10%-15% non-denaturing gels and were developed using a 1×TB-100mM $MgCl_2$ buffer system

at 250V for 6-8 hours. Gels running in pH=6.5 buffer had a slower shift due to the partially neutralization of negative charges on DNA, so the time extended to 10-12 hours. Hybridization events were visualized by ethidium bromide staining.

[γ-^{32}P] ATP was used as the radio-active source for the radio-labeling experiments. The DNA-terpyridine complex/14mer* was diluted to 10 μmol/L as stock solution. 2 μL 10 ×T_4 buffer, 15 μL H_2O, 2 μL stock solution, 1 μL T_4 kinase and 0.4 μL AT^{32}P were added to an eppendorf and incubated at 37^{o}C dry bath for 1hour. After cooling down the sample, extra AT ^{32}P was filtered off and the product was spinned to dryness. Another 20 μL of DI water was then added to the eppendorf to make sure the final concentration is 1 μmol/L. This radio-labeled compound was then mixed with complementary sequences or metals for further gel electrophoresis.

Refereneces:

2) Ulrich S. Schubert, Harald Hofmeier and George R. Newkome, *Modern Terpyridine Chemistry*, Wiley-VCH Verlag GmbH & Co. KGaA, Weinheim

3) F.H. Case, *J. Org. Chem.* **1962**, *27*, 640-641.

4) T. Wieprecht et al., *Journal of Molecular Catalysis A: Chemical* **2003**, *203* 113-128.

6) Jin Seok Choi, Chang Won Kang, Kisung Jung,Jung Woon Yang, Yang-Gyun Kim, and Hogyu Han, *JACS* **2004**, *125*, 8606-8607.

7) Wiederholt, K.; McLaughlin, L.W. *Nucleic Acids Res.* **1999**, *27*, 2487-2493.

8) Kristen M. Stewart, Javier Rojo, and Larry W. McLaughlin, *Angew. Chem.* **2004**, *116*, 5932-5935.

10) Gianolio, D.A.; Segismundo, J.M.; Mclaughlin, L.W. *Nucleic Acids Res.* **2000**, *28*, 2128-2134.

9), 11) Rajur, S.B.; Robles, J; Wiederholt, K.; Kuimelis, R.W.; Mclaughlin, L.W. *J.Org. Chem.*, **1997**, *62*, 523-529.

12) Sarah E. Hobert, Jessica T. Carney, Scott D. Cummings, *Inorganica Chimica Acta*, **2001**, *318*, 89-96.

13) E.C. Constable, *Adv. Inorg. Chem. Rad. Chem.* **1986**, *30*, 69.

1), 5), 14) Kristen M. Stewart and Larry W. Mclaughlin, *Chem. Commun.* **2003**, 2934-2935.

15) Andersen ES, Dong M, Nielsen MM, Jahn K, Subramani R, Mamdouh W, Golas MM, Sander B, Stark H, Oliveira CL, Pedersen JS, Birkedal V, Besenbacher F, Gothelf KV, Kjems J., *Nature.* **2009**, *459(7243):*73-6.

16) P.W.K. Rothemund, "Folding DNA to create nanoscale shapes and patterns" *Nature* **2006**, *(440)* 297–302.

17) Chen, J. H. & Seeman, N. C. Synthesis from DNA of a molecule with the connectivity of a cube. *Nature* **1991**, *350*, 631–633.

18) Shih, W. M., Quispe, J. D. & Joyce, G. F. A 1.7-kilobase single-stranded DNA that folds into a nanoscale octahedron. *Nature* **2004**, *427*, 618–621.

19) Goodman, R. P. et al. Rapid chiral assembly of rigid DNA building blocks for molecular nanofabrication. *Science* **2005**, *310*, 1661–1665.

20) Douglas, S. M., Chou, J. J. & Shih, W. M. DNA-nanotube-induced alignment of

membrane proteins for NMR structure determination. *Proc. Natl. Acad. Sci. USA,* **2007**, *104*, 6644–6648.

21) Andersen, F. F. et al. Assembly and structural analysis of a covalently closed nanoscale DNA cage. *Nucleic Acids Res.* **2008**, *36*, 1113–1119.

22) Yang, H. & Sleiman, H. F. Templated synthesis of highly stable, electroactive, and dynamic metal-DNA branched junctions. *Angew. Chem. Int. Ed.* **2008**, *47*, 2443–2446.

23) He, Y. et al. Hierarchical self-assembly of DNA into symmetric supramolecular polyhedra. *Nature* **2008**, *452*, 198–201.

24) Katsuyuki Nakashima, Sanae Okamoto, Masakazu Sono and Motoo Tori *Molecules* **2004**, *9,* 541-549.

25) Michael J. Gait *Oligonucleotide synthesis-a practical approach* **1990**, 25-33.

Appendix

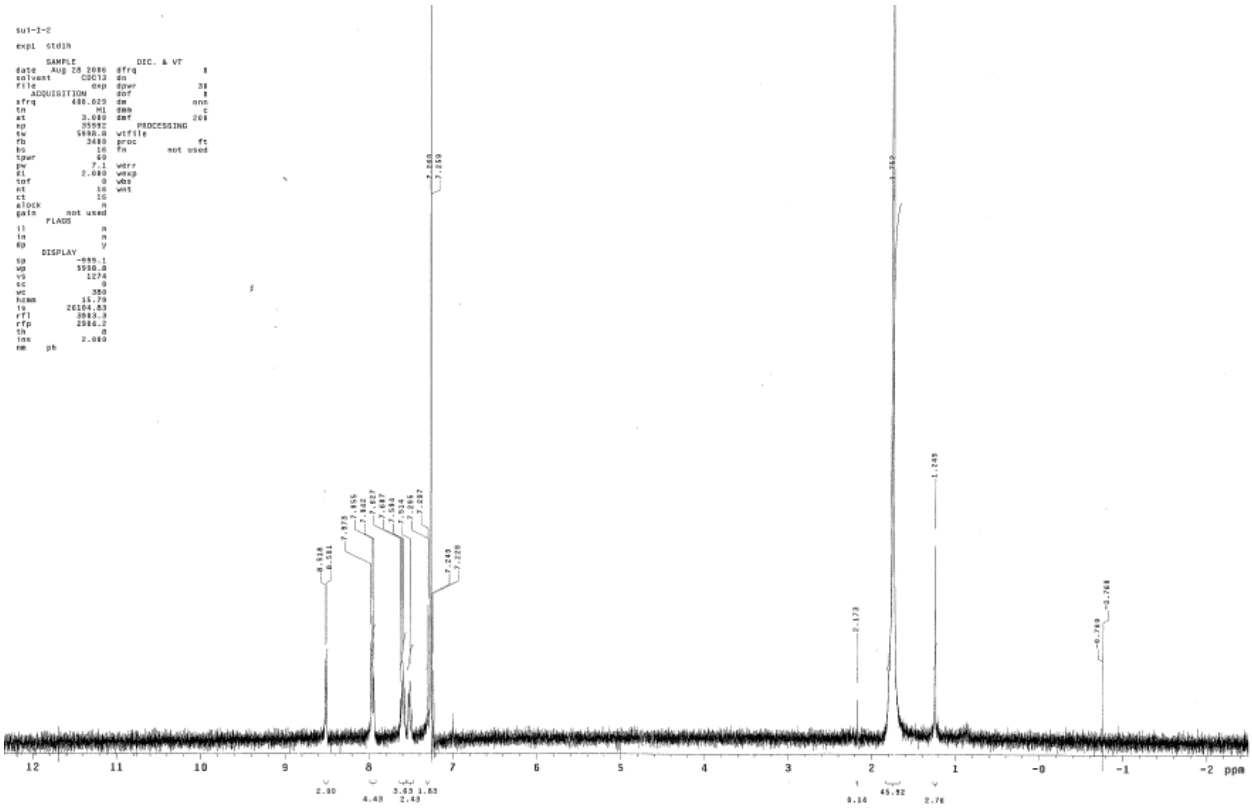

Figure A2.1. ^{1}H NMR of compound 2.1

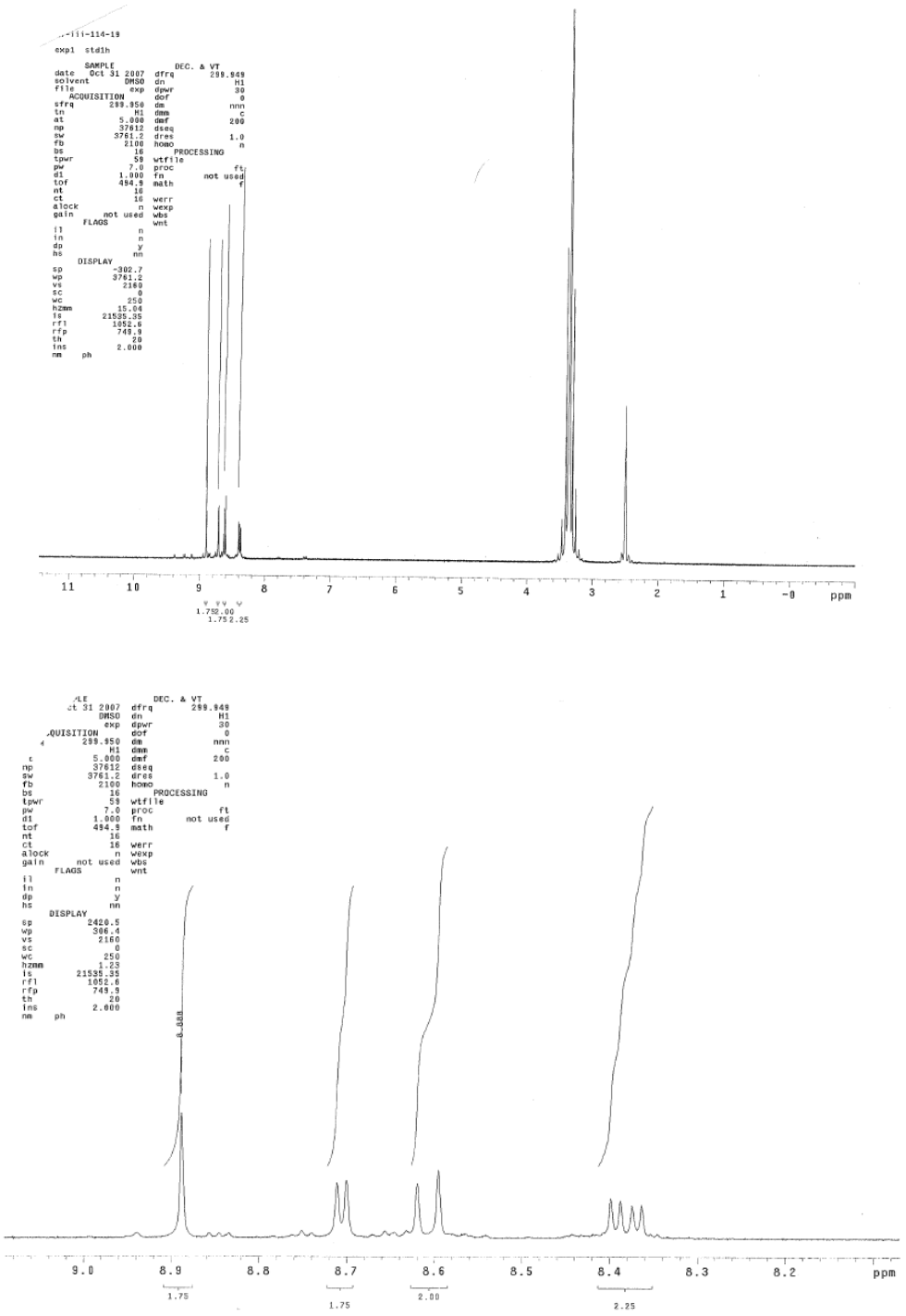

Figure A2.2. ^{1}H NMR of compound 2.2

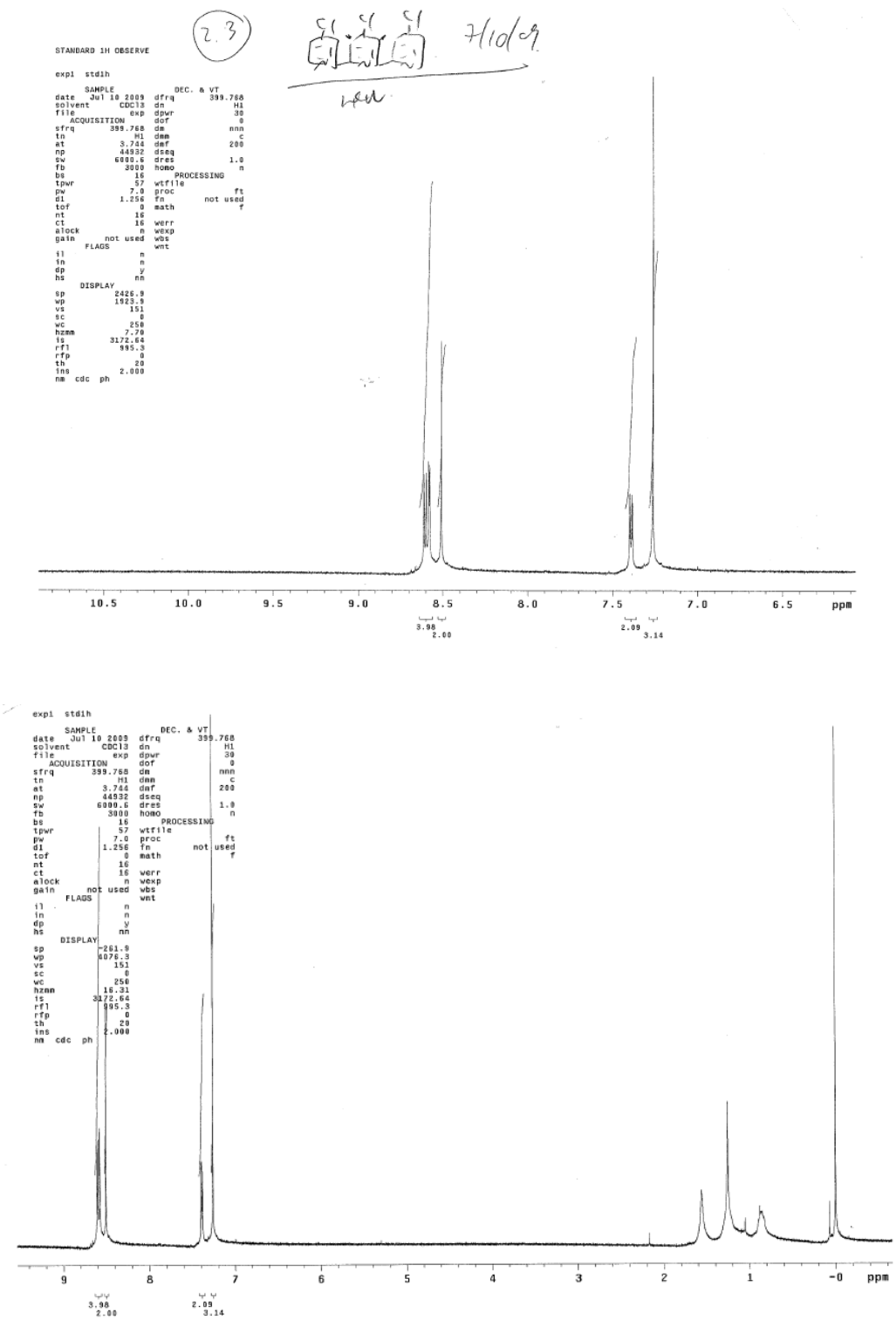

Figure A2.3. ^{1}H NMR of compound 2.3

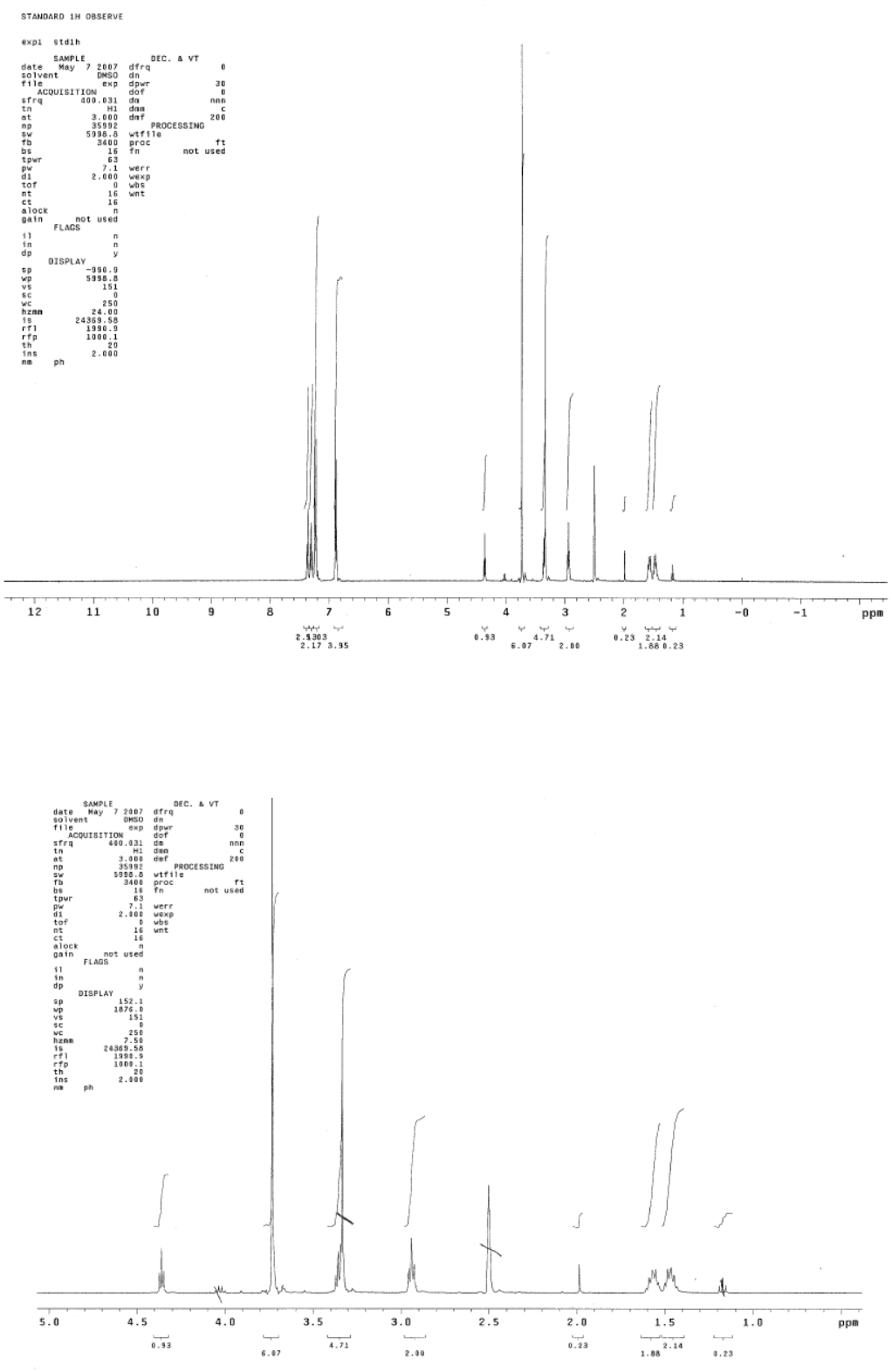

Figure A2.4. ^{1}H NMR of compound 2.4

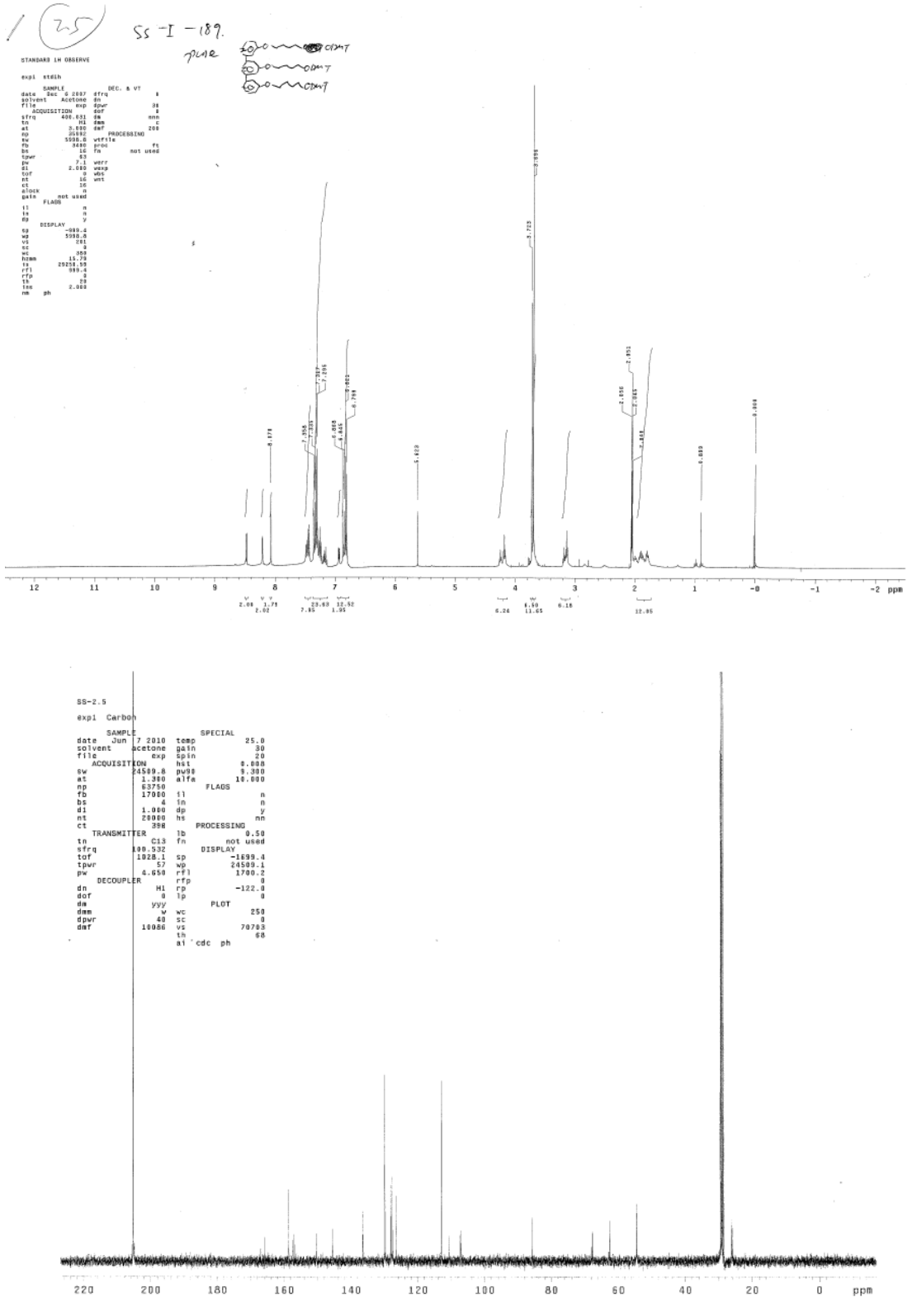

Figure A2.5a. ^{1}H and ^{13}C NMR of compound 2.5

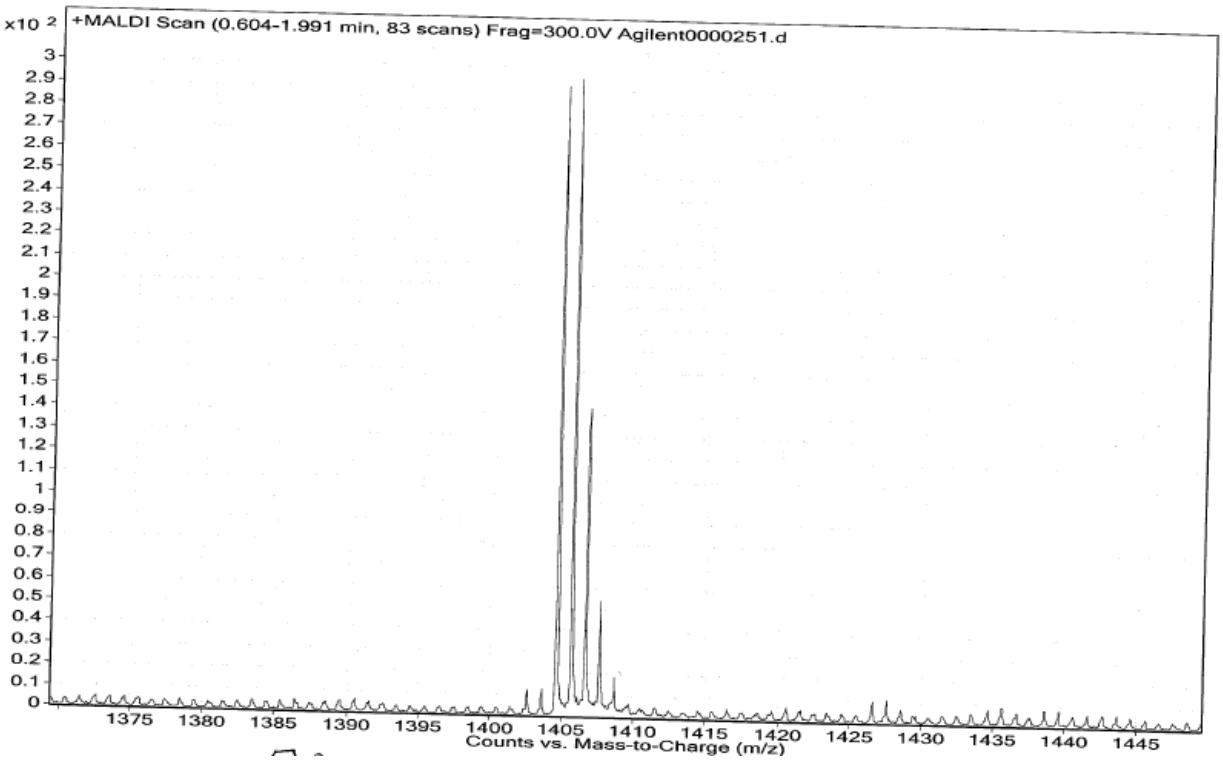

Figure A2.5b. MALDI-TOF MS of compound 2.5

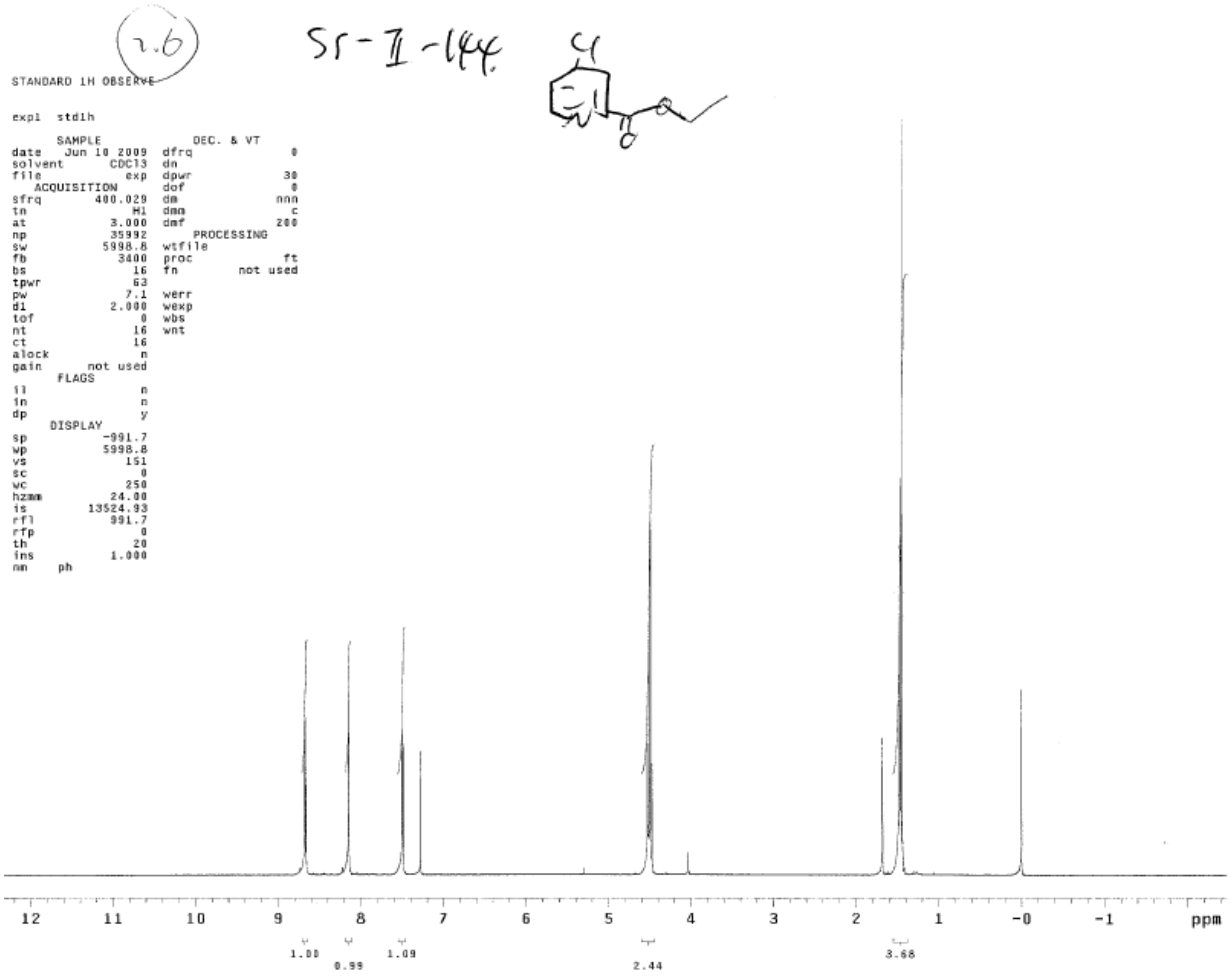

Figure A2.6. ^{1}H NMR of compound 2.6

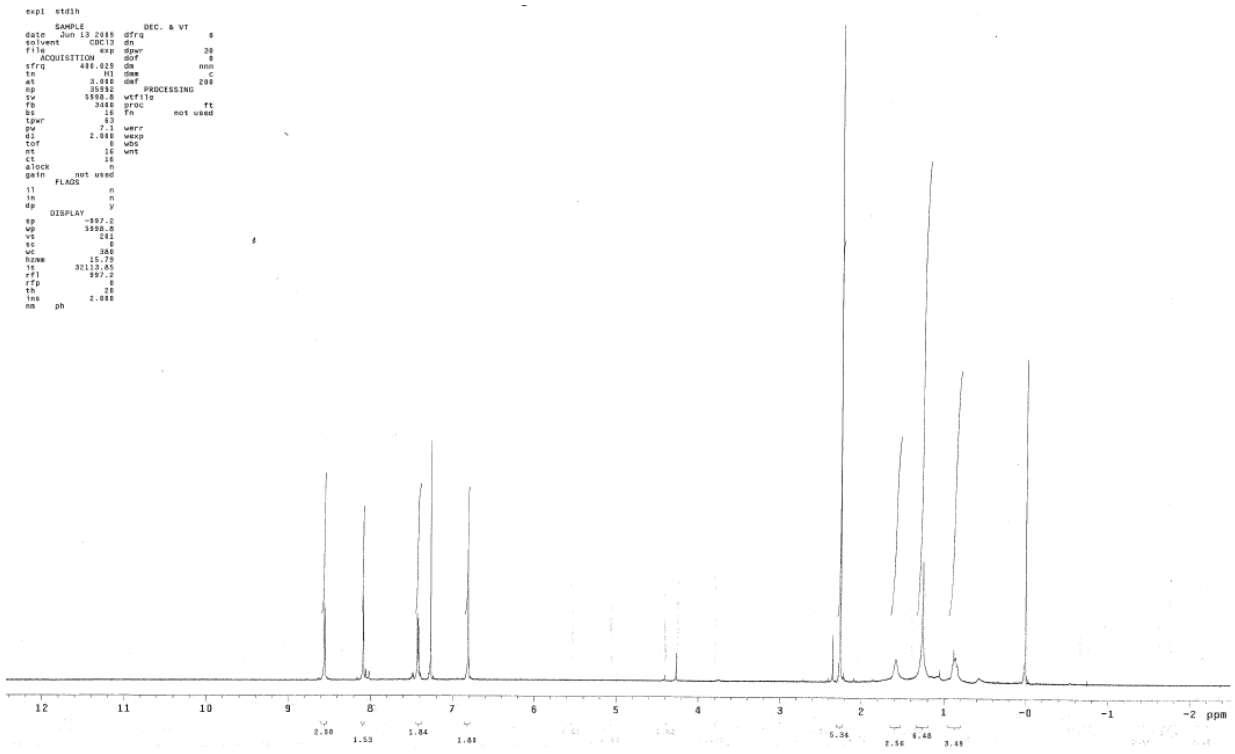

Figure A2.7. ^{1}H NMR of compound 2.7

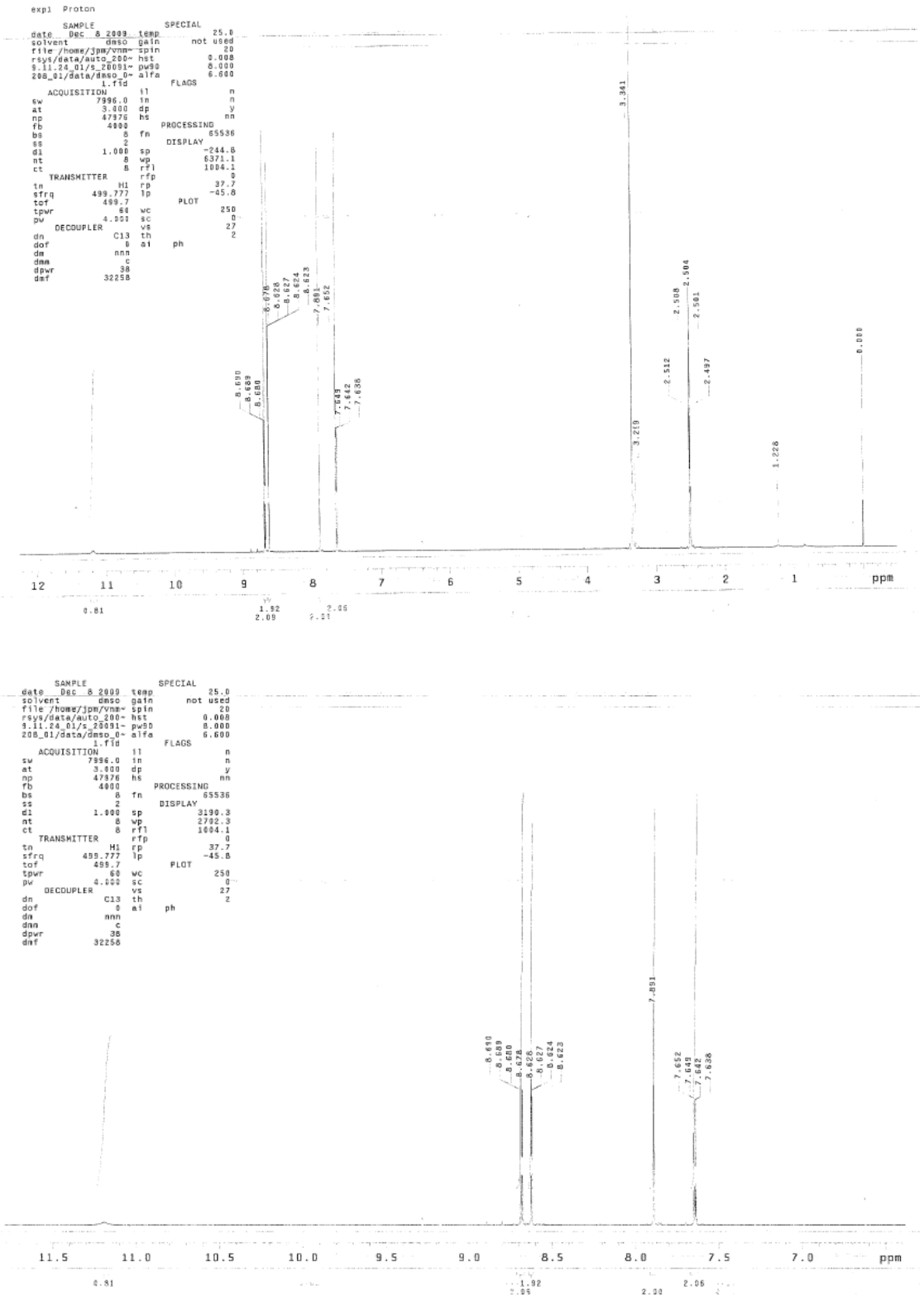

Figure A2.8. ^{1}H NMR of compound 2.8

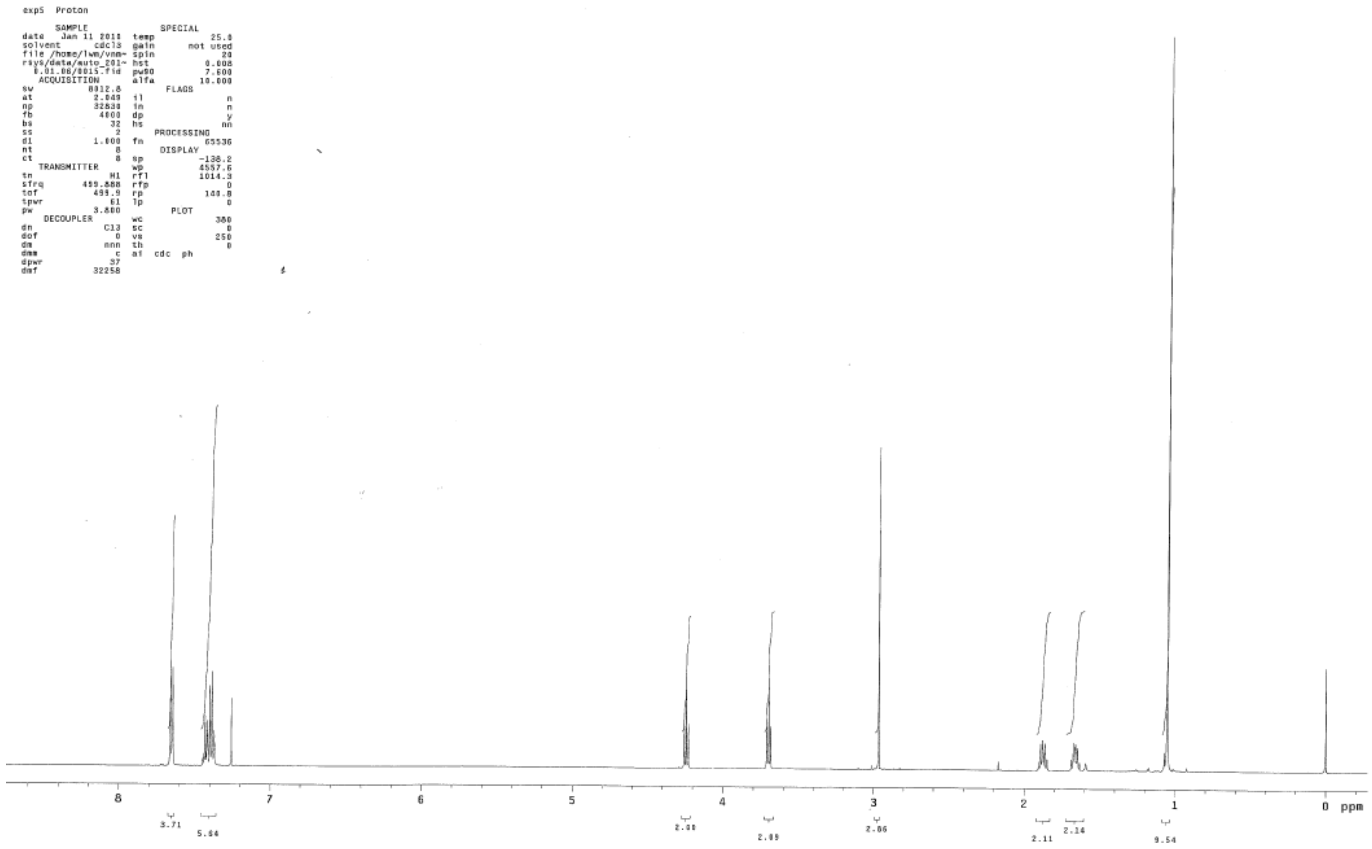

Figure A2.9. ^{1}H NMR of compound 2.9

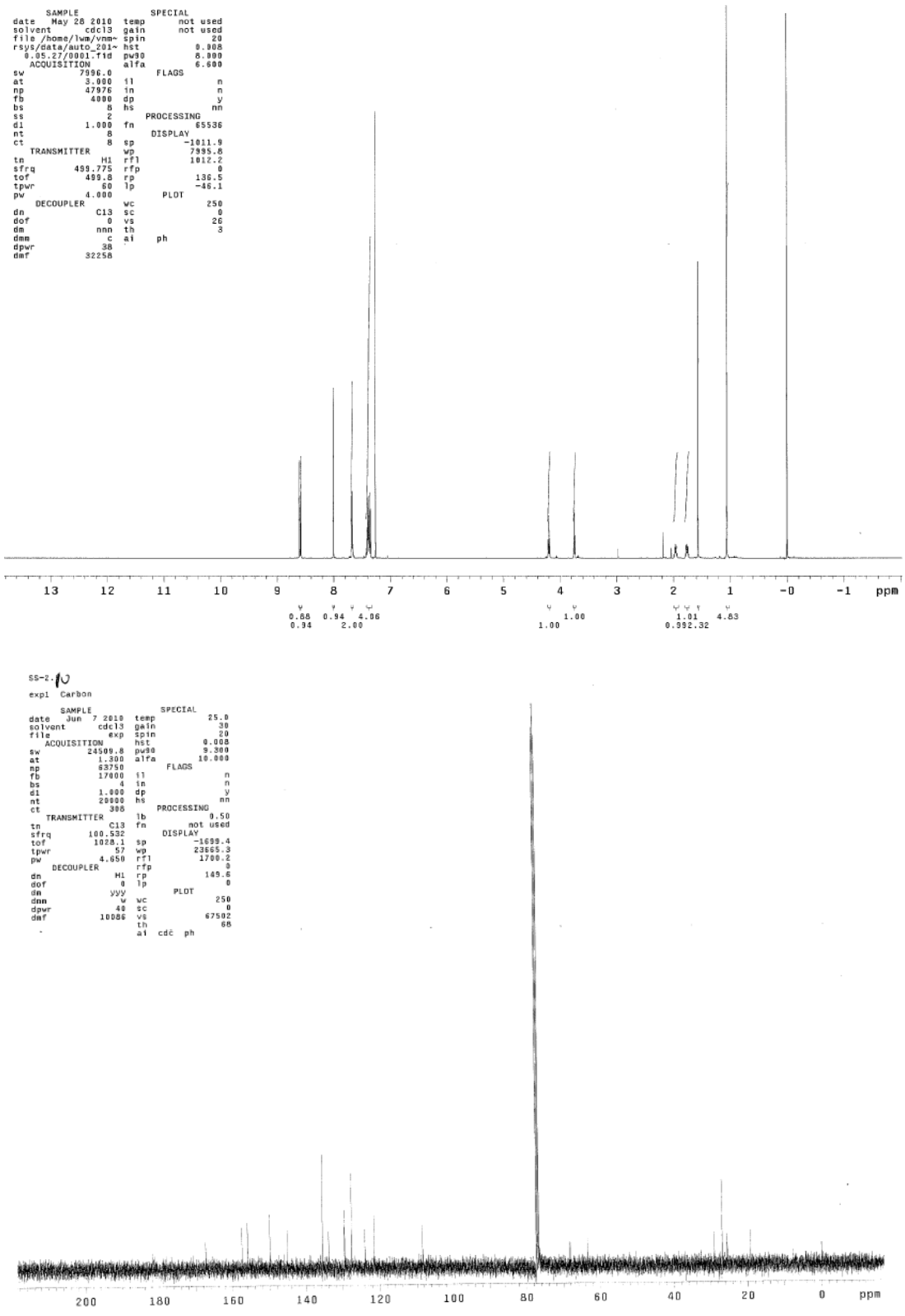

Figure A2.10a. ^{1}H and ^{13}C NMR of compound 2.10

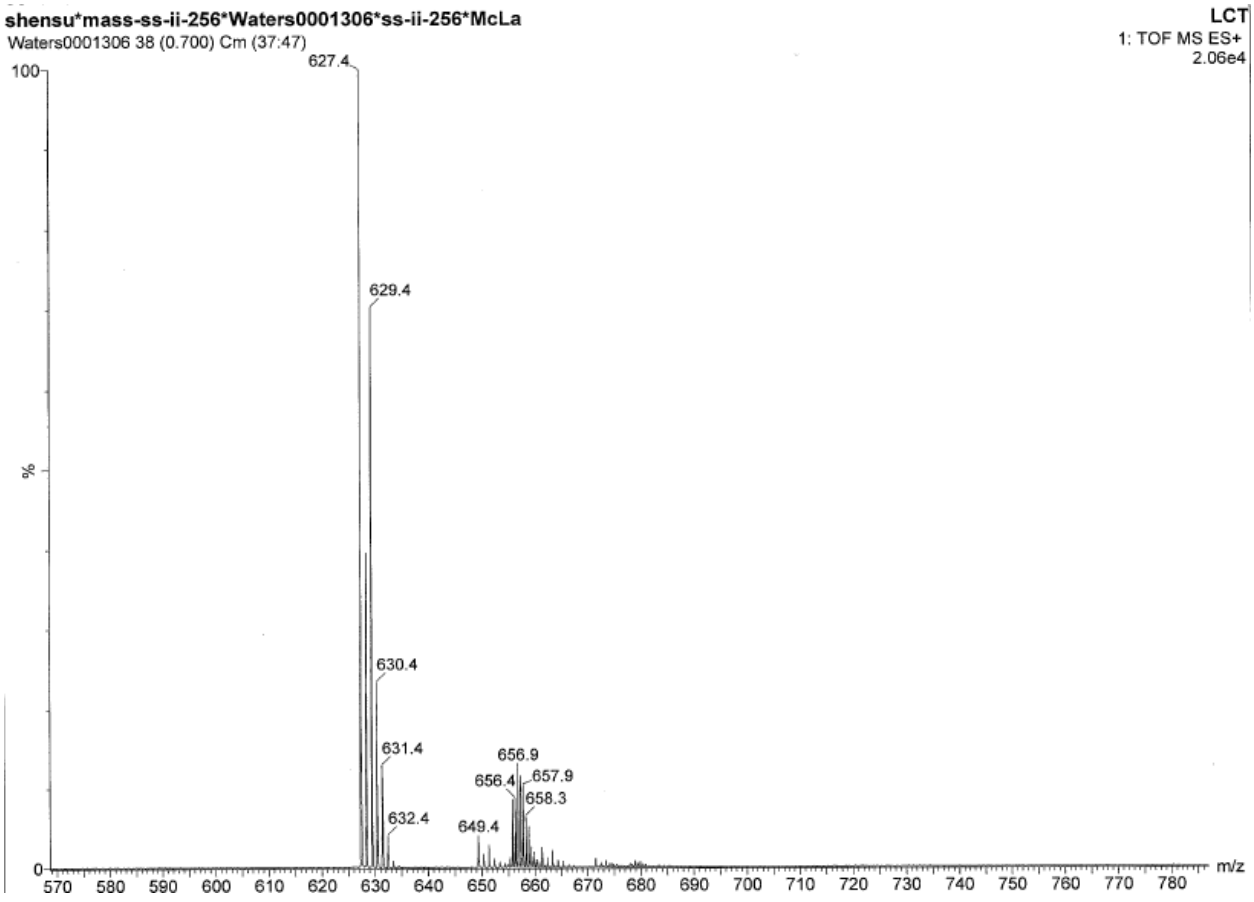

Figure A2.10b. ESI MS of compound 2.10

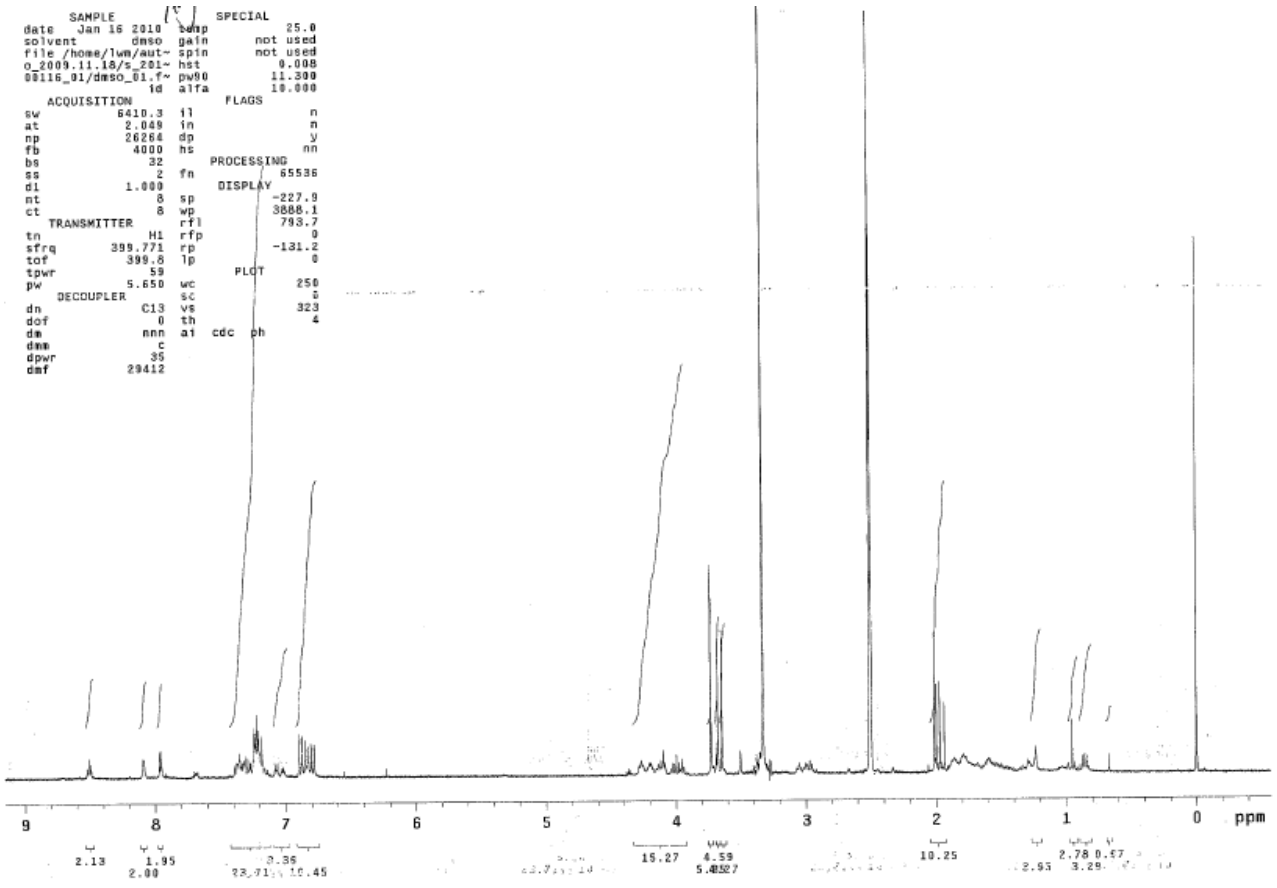

Figure A2.11. ^{1}H NMR of compound 2.11

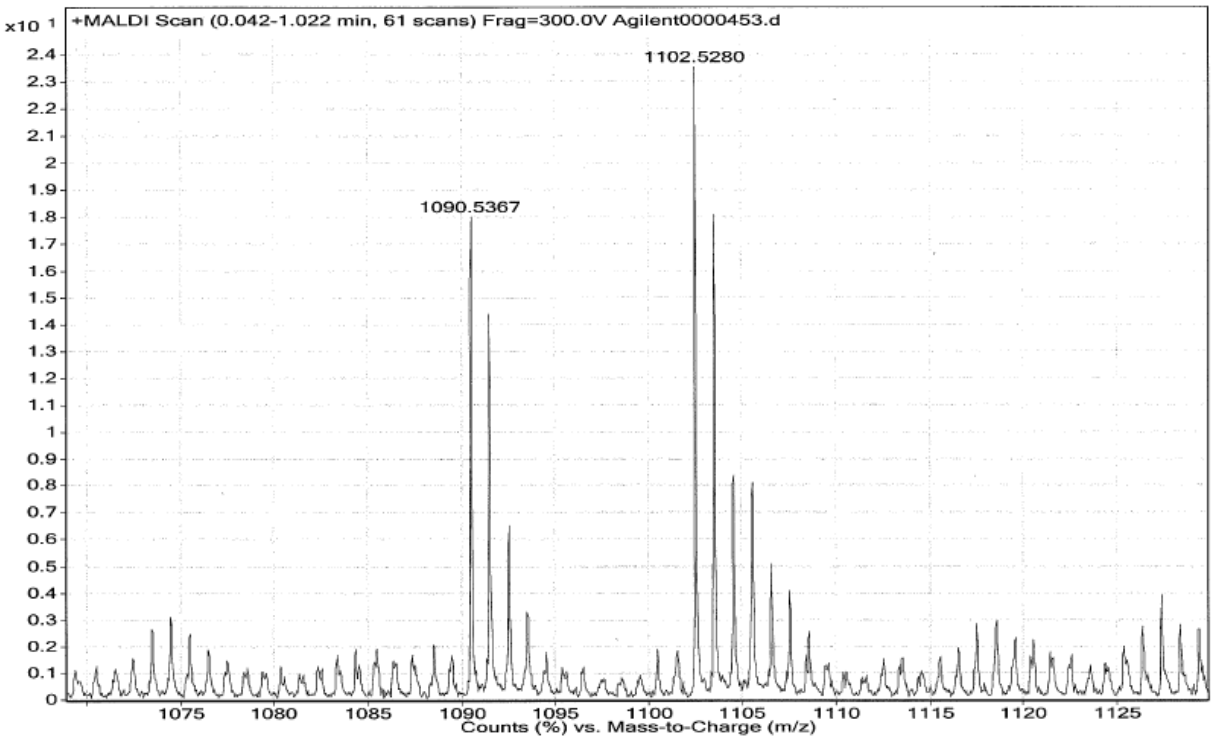

Figure A2.11b. MALDI-TOF MS of compound 2.20

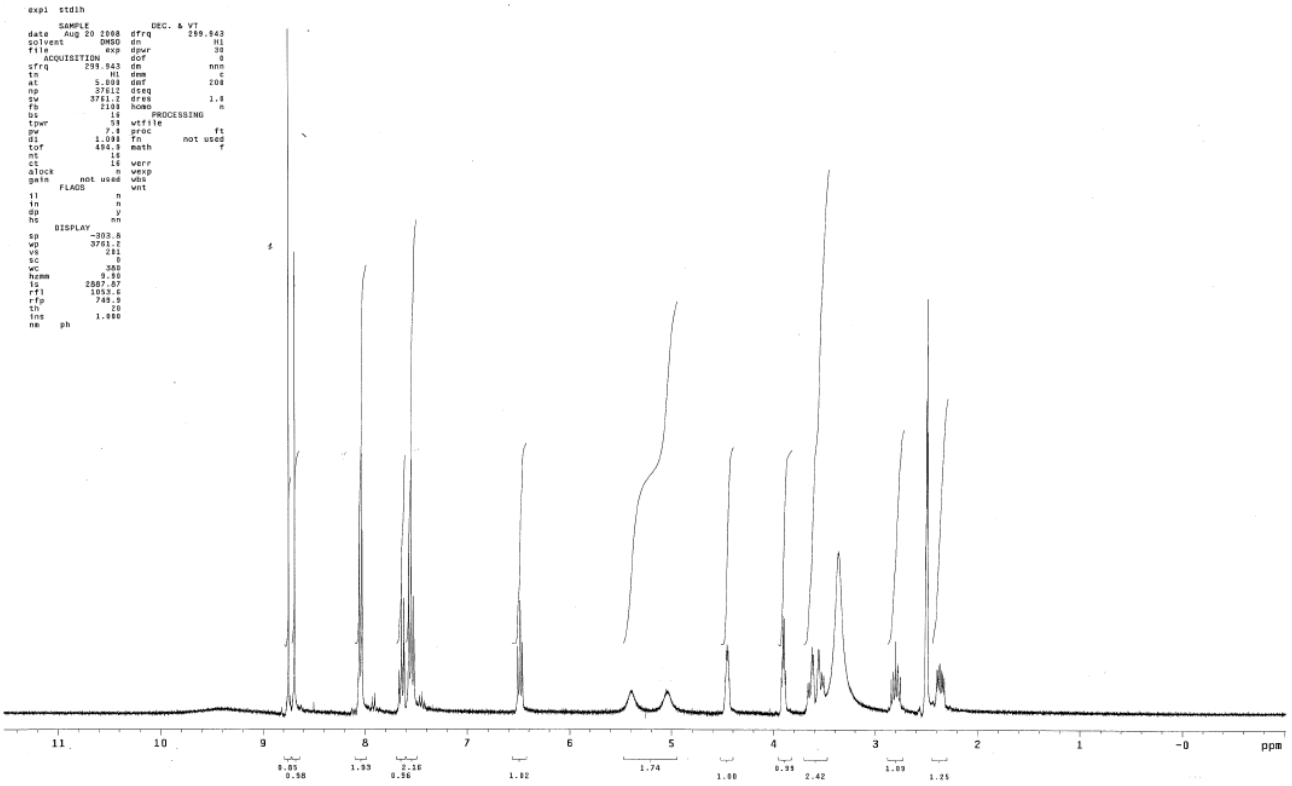

Figure A2.12. ^{1}H NMR of compound 2.12

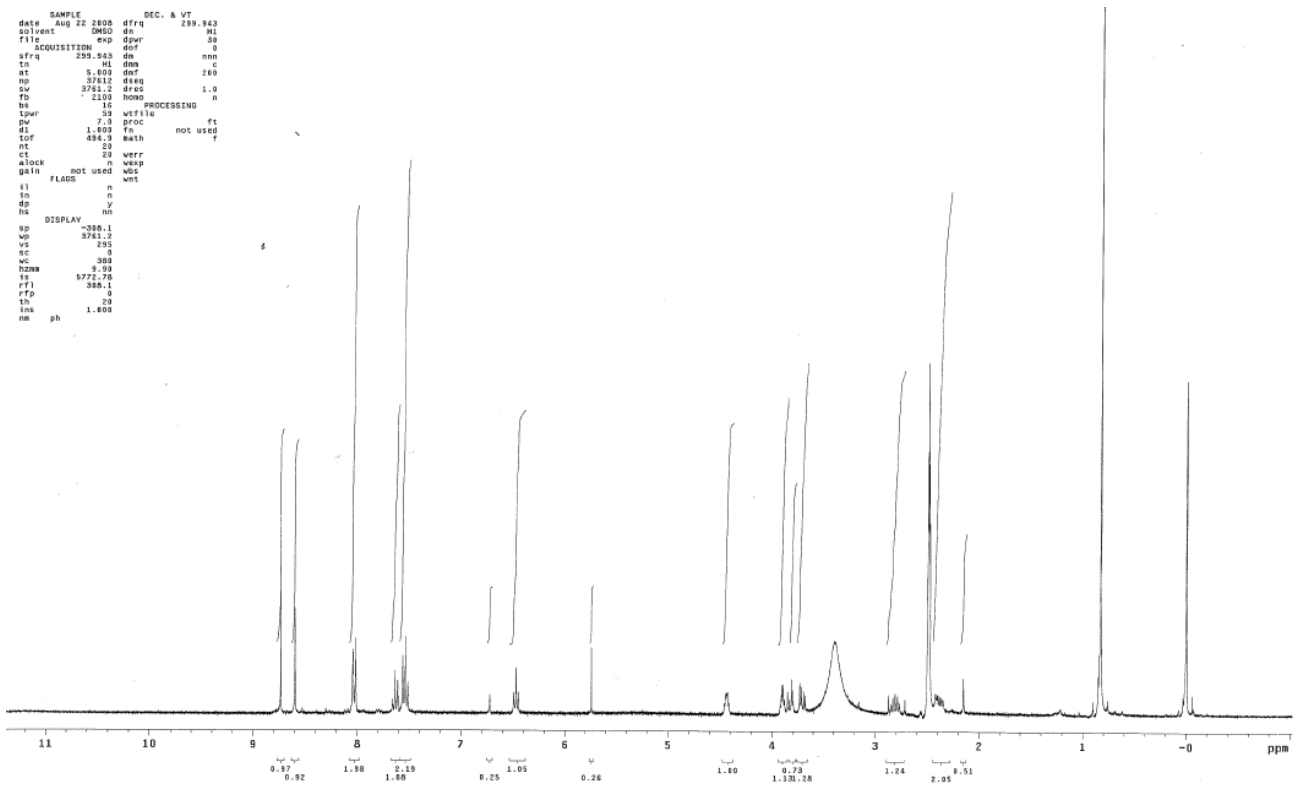

Figure A2.13. ^{1}H NMR of compound 2.13

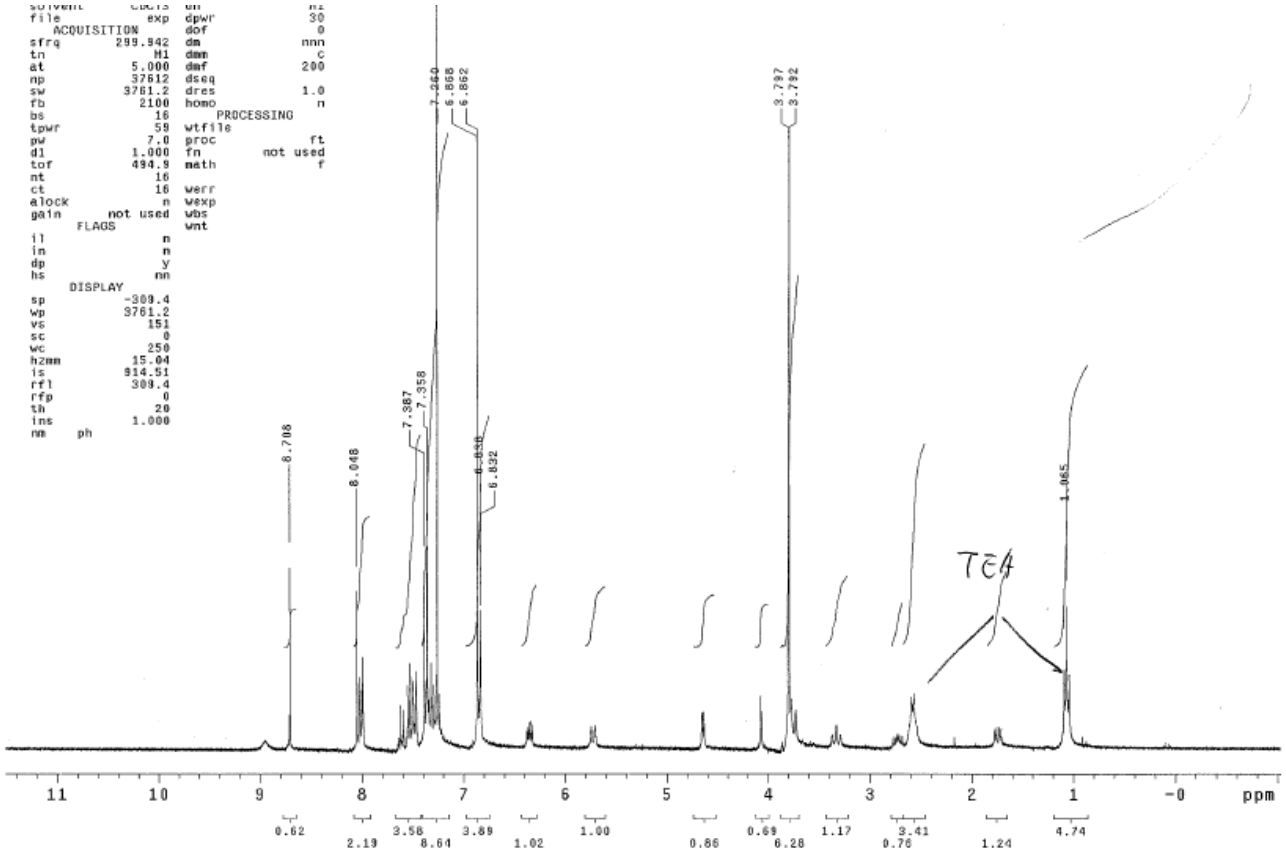

Figure A2.15. ^{1}H NMR of compound 2.15

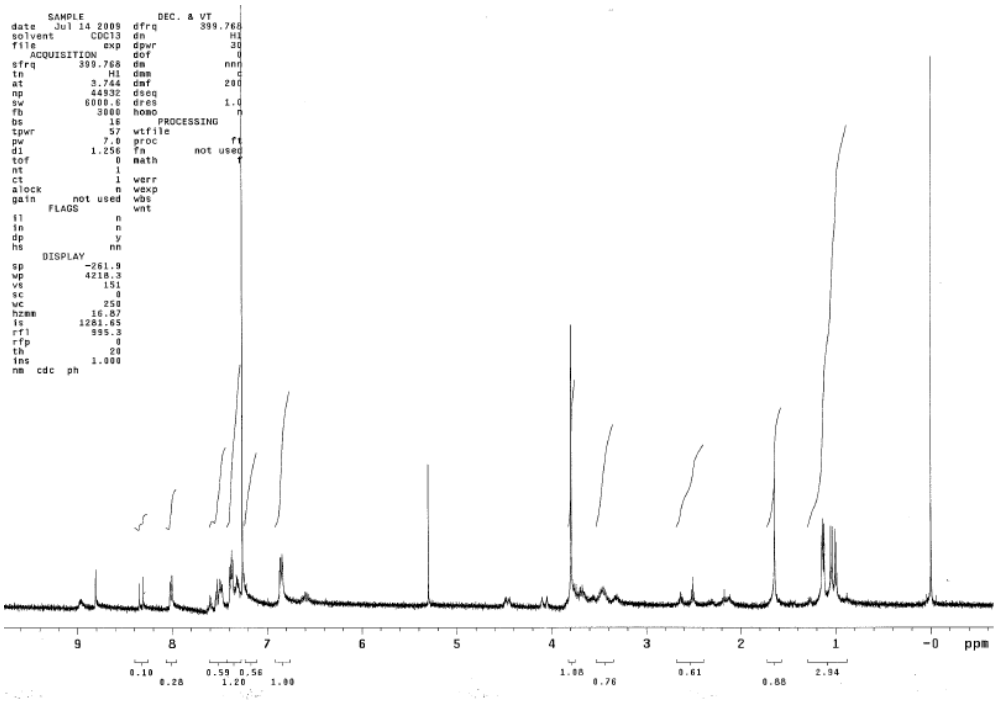
SAMPLE
date Jul 14 2009
solvent CDCl3
file exp
ACQUISITION
sfrq 399.768
tn H1
at 3.744
np 44932
sw 6008.6
fb 3868
bs 16
tpwr 57
pw 7.0
d1 1.256
tof 0
nt 1
ct 1
alock n
gain not used
FLAGS
il n
in n
dp y
hs nn
DISPLAY
sp -261.9
wp 4218.3
vs 151
sc 0
wc 250
hzmm 16.87
is 1281.65
rfl 995.3
rfp 0
th 29
ins 1.000
nm cdc ph
DEC. & VT
dfrq 399.768
dn H1
dpwr 30
dof 0
dm nnn
dmm c
dmf 280
dseq
dres 1.0
homo n
PROCESSING
wtfile
proc ft
fn not used
math f
werr
wexp
wbs
wnt
9
8
7
6
5
4
3
2
1
-0
ppm
0.10
0.28
0.59
0.56
1.20
1.00
1.85
0.76
0.61
0.88
2.94

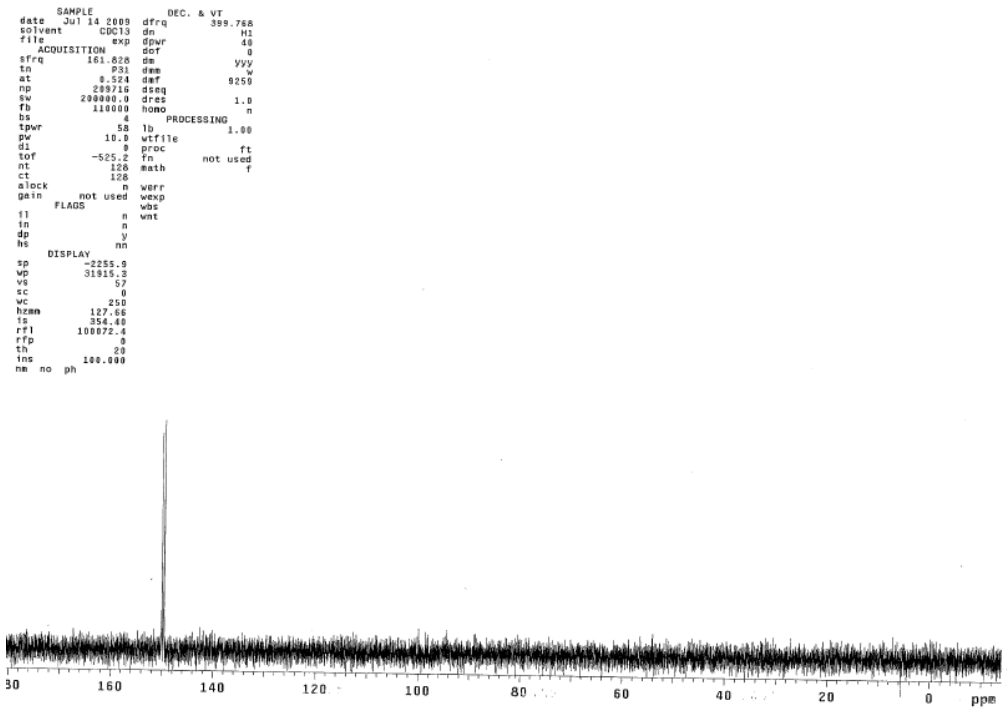

Figure A2.16. ^{1}H and ^{31}P NMR of compound 2.16

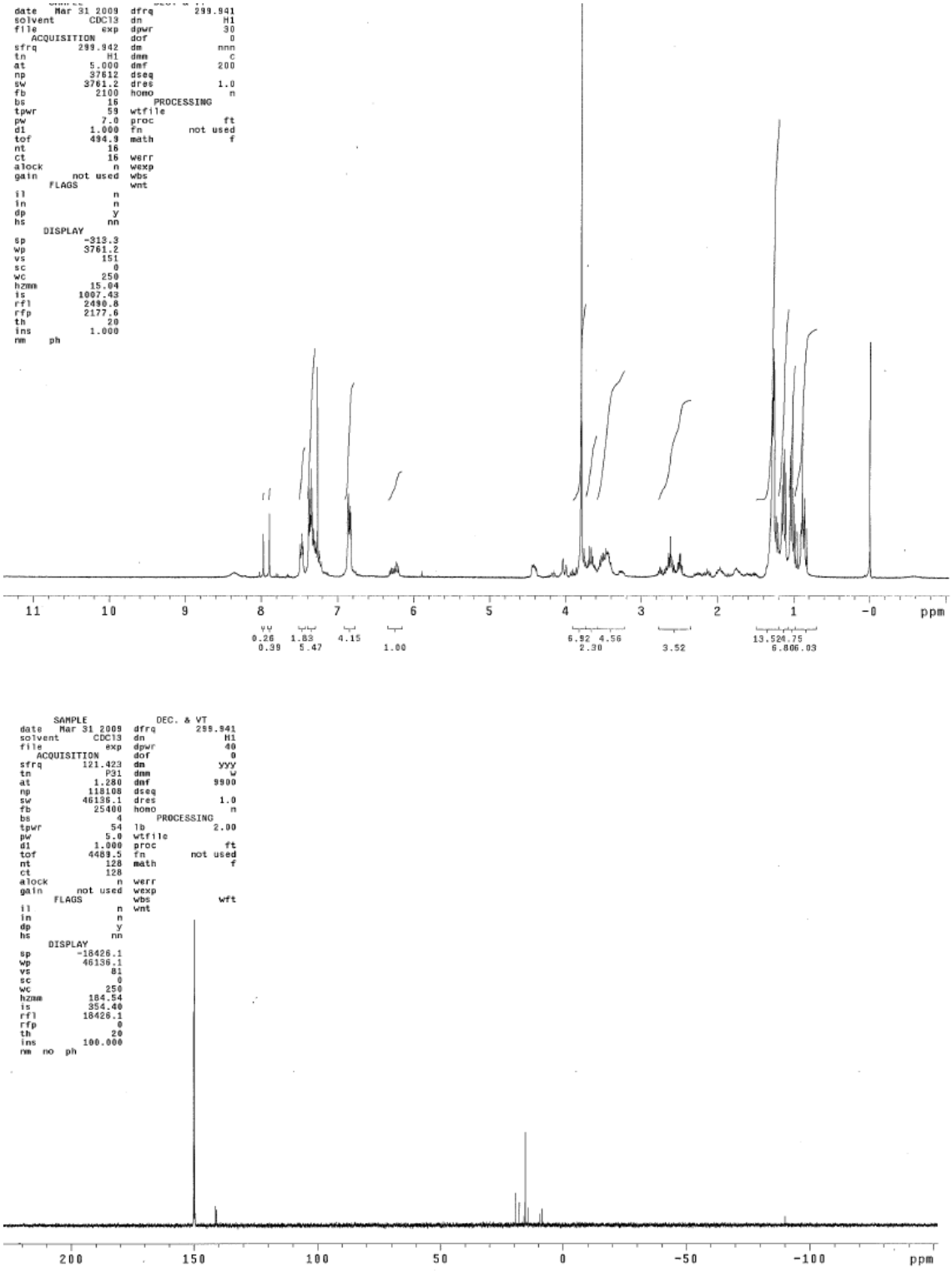

Figure A2.17. ^{1}H and ^{31}P NMR of reverse dG

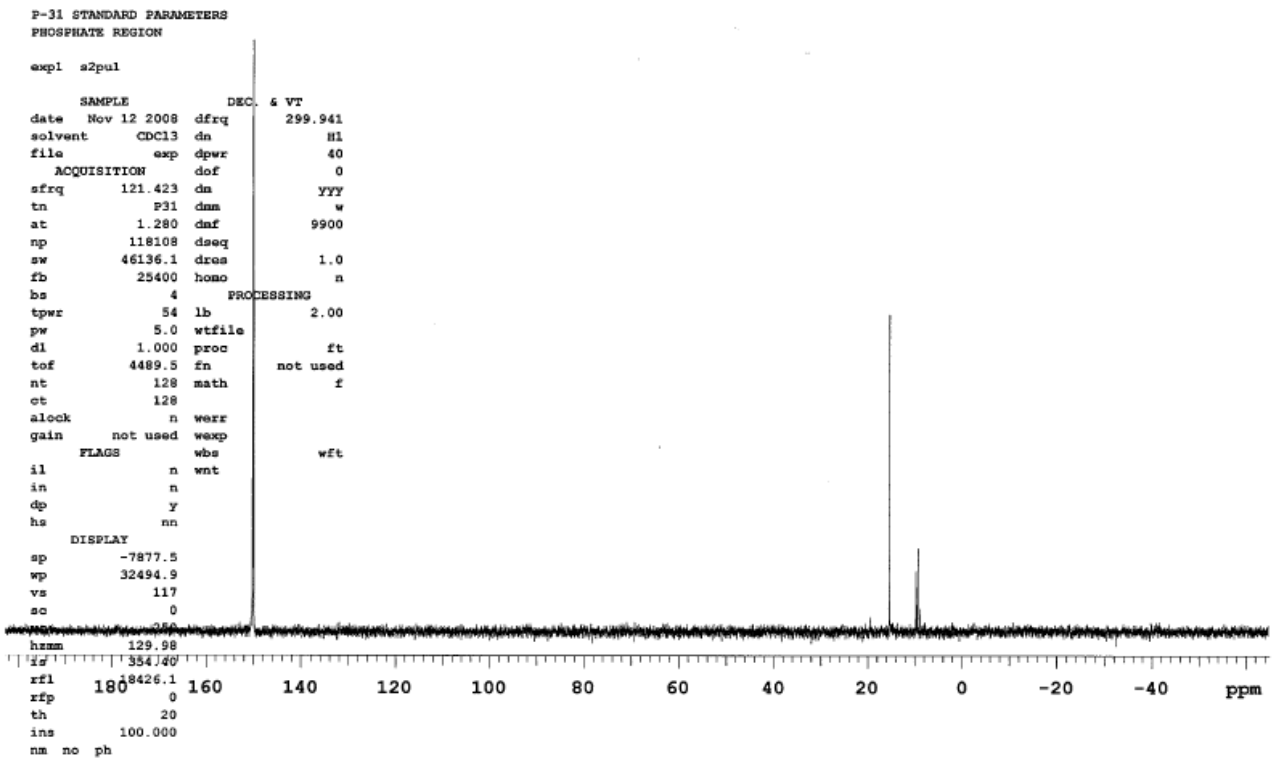

Figure A2.18. ^{31}P NMR of reverse dC

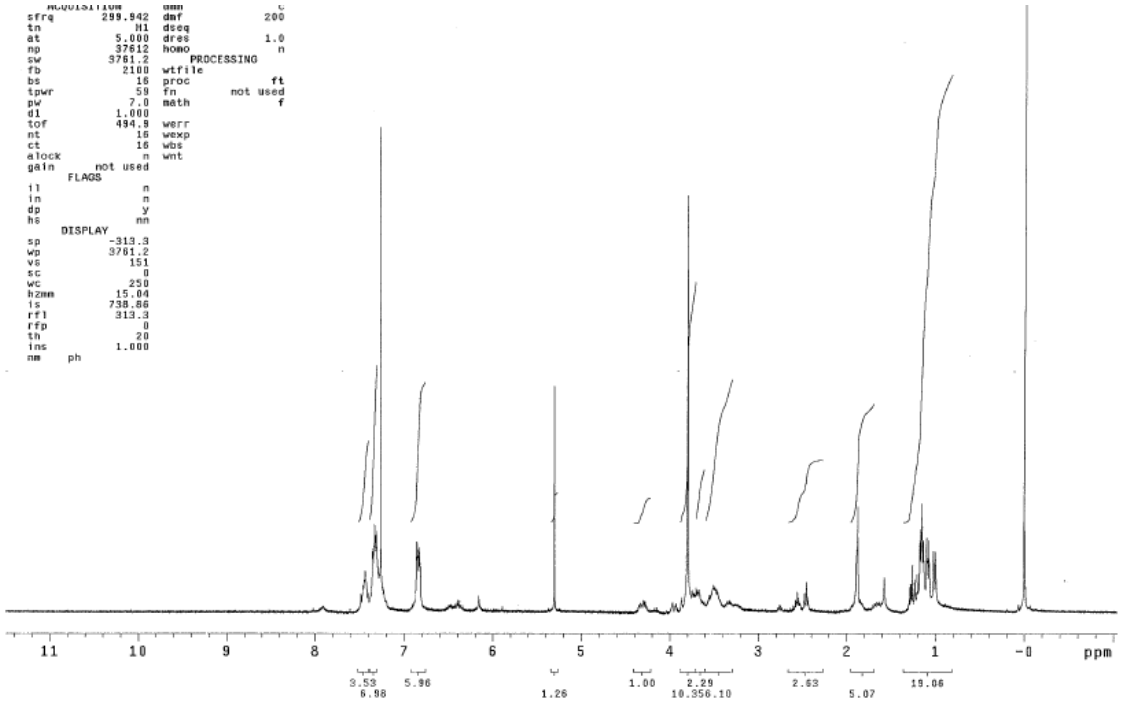

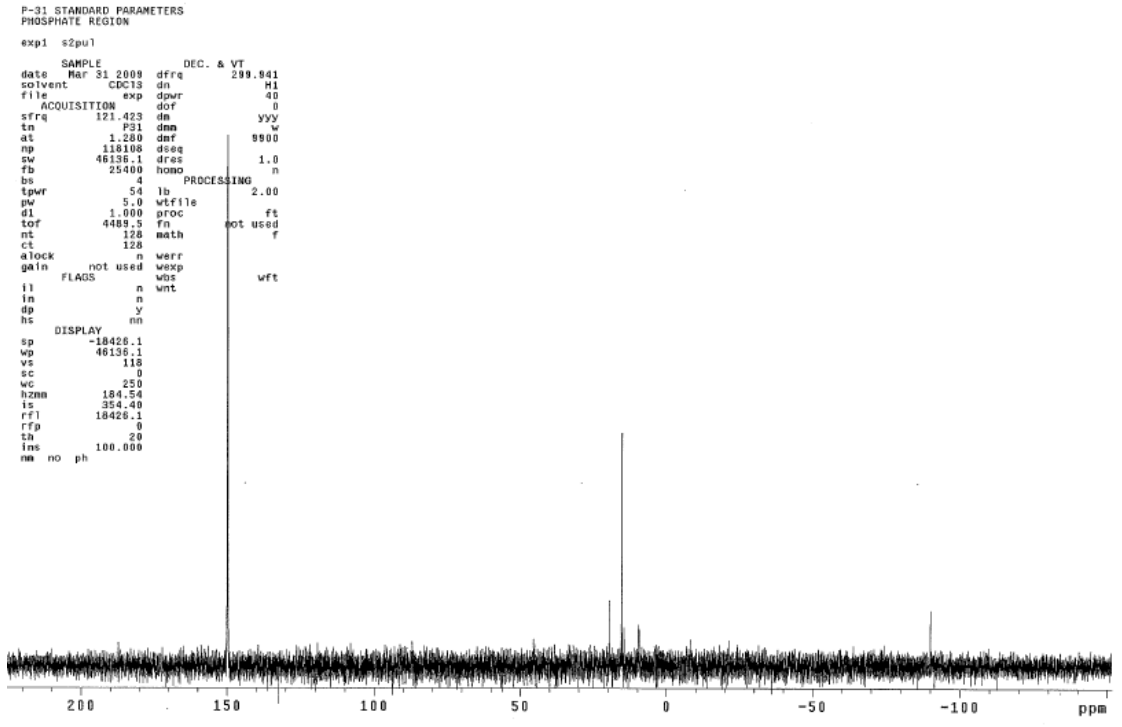

Figure A2.19. ^{1}H and ^{31}P NMR of reverse dT